12-2013

Assessment of the Predictive Reliability of a SWAT Flow Model and the Evaluation of Runoff Generation and BMP effectiveness in a Shale-Gas Impacted Watershed Using a Modeling Approach

Kwasi Asante
University of Arkansas, Fayetteville

Assessment of the Predictive Reliability of a SWAT Flow Model and the Evaluation of Runoff Generation and BMP Effectiveness in a Shale-Gas Impacted Watershed Using a Modeling Approach

Assessment of the Predictive Reliability of a SWAT Flow Model and the Evaluation of Runoff Generation and BMP Effectiveness in a Shale-Gas Impacted Watershed Using a Modeling Approach

A dissertation submitted in partial fulfillment
of the requirements for the degree of
Doctor of Philosophy in Environmental Dynamics

by

Kwasi Asante
Kwame Nkrumah University of Science and Technology
Bachelor of Science in Geodetic Engineering, 2007
University of Arkansas
Master of Arts in Geography, 2009

December 2013
University of Arkansas

This dissertation is approved for recommendation to the Graduate Council.

_____	_____
Dr. Jackson D. Cothren Dissertation Director	Dr. John V. Brahana Committee Member
_____	_____
Dr. Ralph K. Davis Committee Member	Dr. Greg Thoma Committee Member

ABSTRACT

In order to ensure a harmonious harness of shale-gas resources while ensuring minimal damage to the environment, it is imperative that studies to conduct to inform various aspects of managing the environment. This includes the development of reliable hydrologic models to inform in decisions concerning water and the environment.

The first objective of this study was to evaluate the predictive reliability of the Soil and Water Assessment Tool (SWAT) model based on respective methods of LULC data classification and data type spatial resolution. Results showed that the high-resolution data classified with object-oriented image method does not provide any significant advantage in terms of the model's flow predictive reliability. The second goal focused on an application of the object-oriented image analysis technique for change detection related to shale-gas infrastructure and subsequently evaluates the impact of shale-gas infrastructure on stream-flow in the South Fork of the Little Red River (SFLRR). Results showed that since the upsurge in shale-gas related activities in the Fayetteville Shale Play (between 2006 and 2010), shale-gas related infrastructure in the SFLRR have increased by 78% corresponding to a differential increase on storm water flow by approximately 10% over a projected period of simulation. The last objective deals with the evaluation of BMP effectiveness in a shale-gas watershed using a modeling approach. Three BMPs identified to control flow were introduced and simulated for a simulation (2000 to 2009) and projected (2010 to 2020) periods. The differences in the flow output at the watershed outlet for each BMP scenario were derived by comparing baseline and respective BMP scenarios. Results indicate that the BMPs have an average effectiveness of approximately 80% in reducing storm water flow attributable to shale-gas.

ACKNOWLEDGEMENT

I would like to express my profound gratitude to my parents for all the sacrifices, support and encouragement throughout my academic life. Special thanks to my uncles Dr. Stephen Asiedu-Asante and Mr. Seth Frimpong-Asante for their immense help in raising me.

My appreciation also goes to my esteemed academic advisor Dr. Jackson Cothren for the direction, counsel and encouragements throughout my graduate education. Also my gratitude goes to my committee members; Dr. Brahana, Dr. Davis and Dr. Thoma for their invaluable corrections and direction throughout this study. My special gratitude goes to Dr. Mansoor D. Leh for his invaluable numerous corrections and pieces of advice. Lastly I acknowledge my best friends, Kobla Nanewortor and Christopher Angel, my brothers, Enoch Snr and Jnr, Nana Dei and Kwasi Larbi and my precious in-laws Dr. and Mrs. Albright for your varied support and encouragement.

DEDICATION

I especially dedicate this dissertation to my dearest uncle Seth Frimpong-Asante (who lost his life a year ago); you will always be an irreplaceable figure in my life no matter what. Also I dedicate this study to my uncle Dr. Stephen Asiedu-Asante for instilling in me the spirit of hard work and determination. I also specially dedicate this dissertation to my very supportive wife Bethney Asante for all the encouragement and unqualified support.

TABLE OF CONTENTS

CHAPTER 1: INTRODUCTION

1.0 Problem Definition

Unconventional natural-gas resources, particularly shale-gas, have seen major changes in exploration and development in the conterminous United States in recent years (Figure 1). Using hydraulic fracturing and horizontal drilling, energy companies have begun exploration and development of this resource with resultant changes in the land-use land-cover (LULC). These changes ultimately affect important factors such as the hydrologic regime of the watersheds in which their activities occur.

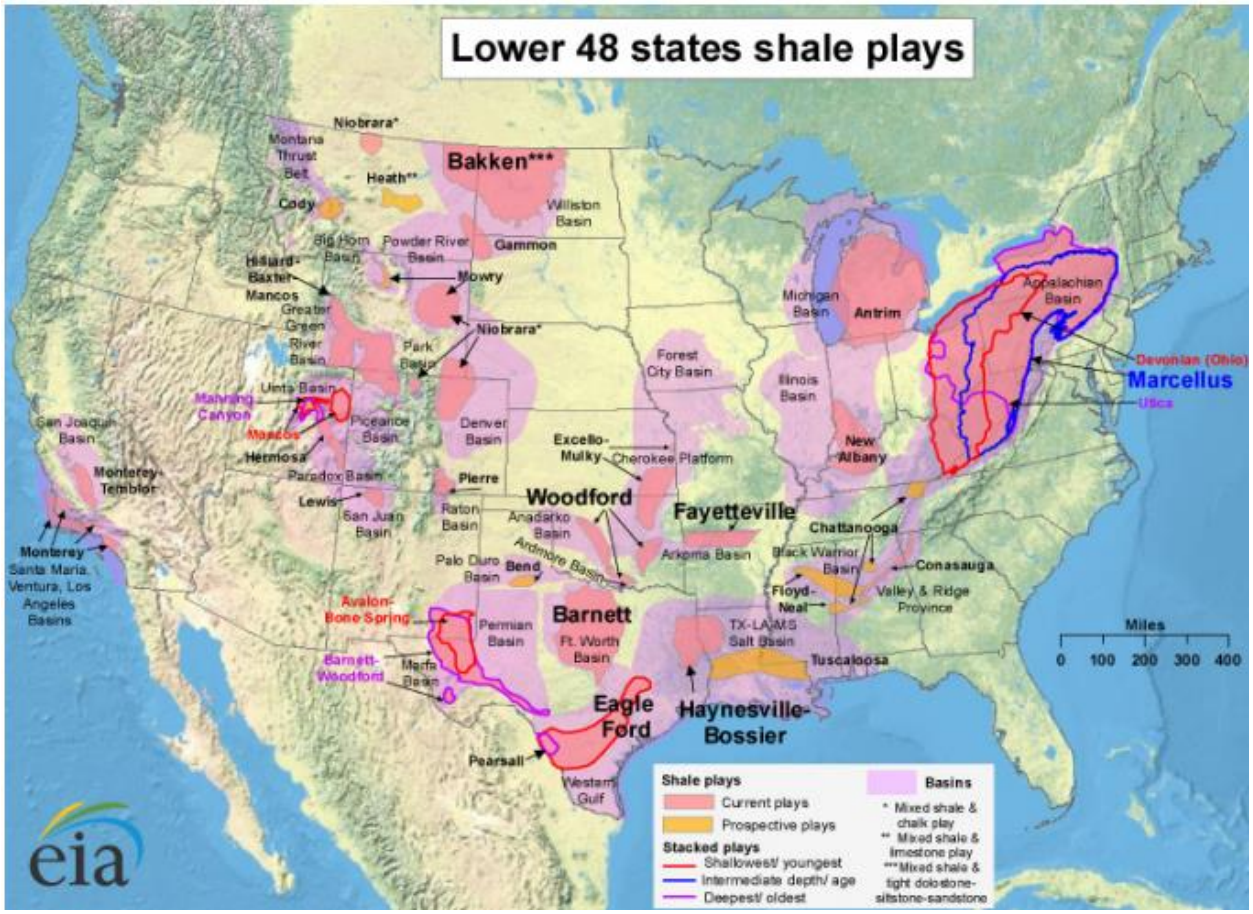

Figure 1: Major shale deposits and significant shale plays in the conterminous U.S. (as of May, 2011). Source: Energy Information Administration

This dissertation investigates shale-gas related infrastructure changes, the impact on land-use land-cover change and the subsequent potential impact on surface-runoff generation. Geographic Information Science (GIS) and hydrologic modeling using the Soil and Water Assessment Tool (SWAT) (Arnold et al., 1998) are used to evaluate environmental impacts specifically related to LULC change and the resultant generation of storm-water runoff as the resultant of LULC changes. The prediction accuracy of hydrologic models such as SWAT has been shown to depend on the input LULC data. This data is typically created using moderate-resolution (30 m) satellite imagery and an assortment of maximum-likelihood classification techniques. The availability of low-cost United States Department of Agriculture National Agricultural Imagery Program (USDA-NAIP) aerial imagery data of significantly higher resolution (1 m and 2 m) and the emergence of object-based land-cover classification methods, have the potential to produce land-use land-cover maps of significantly higher accuracy. This presents a significant advantage in the choice of data for both spatial and hydrologic analyses.

However, research on the effect of high resolution LULC input data on various SWAT model outputs show that higher resolution data do not always produce hydrologic models of better prediction ability. These mixed results arise in part due to the fact that the traditional pixel-based image classification methods are designed for moderate-resolution satellite imagery and are not well suited to deal with the high spectral and spatial variances inherent in high-resolution imagery. A more modern computer-vision-based method known as the object-oriented imagery analysis (OOIA) technique has seen extensive use in small-scale studies. This method involves an important first step known as image segmentation; which is based on the hierarchical aggregation of pixels into objects and the subsequent classification of these objects using the

high degree of variation inherent in the spectral, shape, context, texture etc. of the respective objects and at some scale of pixel (Baatz and Schape, 2000).

Albeit a combination of OOIA and the availability of low-cost aerial imagery present a potential increase in LULC classification accuracy, no study can be located that employs these two advantages in quantifying the relative change in infrastructure related to shale-gas activities and their impact on the overall LULC change of the watersheds in which they occur. The ability to readily and accurately produce and quantify land-cover changes impacted by shale-gas activities in comparison to other urban infrastructure will greatly serve in decision-making and policy formulation. Furthermore, a previous study (Bosch et al., 2004), has compared the differential effect of high or low-resolution LULC data on SWAT outputs. However, there is little research on the impact of classification methods and how the accuracy with which these methods can be used to correctly extract land-use data related to local LULC changes affects SWAT runoff model predictive reliability. What is lacking is a study that quantifies model predictive reliability based on a defined level of uncertainty for SWAT models calibrated for runoff with high-resolution LULC data derived with object-oriented image classification and of low-resolution imagery derived with pixel-based maximum-likelihood method.

The oil and gas industry though exempt from the provisions of the National Pollutant Discharge Elimination System (NPDES), under the Clean Water Act (CWA) the regulatory concern is with the Endangered Species Act (ESA) particularly with reference to such predominantly forested areas such as the Upper Little Red River watershed of north-central Arkansas. Their activities could have potential adverse impacts due to the generation of storm-water carrying sediment discharged into receiving downstream waters bodies. This has the impact of increasing turbidity, total suspended solids and reduction in the levels of oxygen for aquatic life. Any such impact

considered to be detrimental to species listed under the ESA could result in infractions of the law. In this sense, albeit the ESA does not directly regulate the oil and gas industry, there are possible applications of the law when the industrial activities are deemed as infractions of the law.

This has led to trends where although not required under any regulatory framework, some shale-gas operators and pipeline companies have taken the initiative to implement storm-water and erosion control Best Management Practices. However, the Oil Pollution Act (OPA) of 1990, which controls oil and gas activities in Arkansas, does not explicitly define BMPs or BMP guidelines, particularly for storm-water management in oil and gas industrial watersheds. However it is known that knowledge about the effectiveness of BMPs can be studied with hydrologic model. In this sense SWAT model has been applied to evaluate various erosion and sedimentation BMP scenarios and quantify agricultural conservation practices in both large and relatively small watersheds (Betrie et al., 2011; Arabi et al., 2007). However, the model has not been applied in any feasibility study meant to evaluate the effectiveness of BMPs implemented in a shale-gas activity setting to mitigate threats in terms of storm-water runoff posed by shale-gas activities. This study explores this unexamined area and evaluates the feasibility of implementing BMPs designed for storm-water management in a shale-gas related construction watershed.

1.1 Motivation

Natural-gas from unconventional sources such as shale is increasingly becoming the fuel of choice especially as public awareness of the need to become energy-independent gains pervasive acceptance. The United States has substantial reserves of this resource. 2012 proved reserves for the entire United States is estimated to be about 273 trillion cubic feet (Tcf) (Gruenspecht, 2012). This has spurred a significant increase in exploration and production activities throughout the country. Concurrent with these activities, public concern about related environmental problems has intensified and stakeholders have sought meaningful answers to allay the fears of the disparate groups.

The ability to readily detect and quantify changes in the LULC resulting from activities of the shale-gas industry will serve to inform policy and management practices aimed at curbing the impacts on the hydrology of the affected watersheds. A quantification of the relative acreage and changes in infrastructure in the respective shale-gas plays is essential to aide decisions in the issuance of permits, environmental assessment, hydrologic studies and most importantly an inventory of infrastructure arising from shale-gas exploration and production. This body of knowledge could be used in LULC change predictive models with particular emphasis on shale-gas related developments. A comparison with other infrastructure change such as urban developments will convey a better understanding of the relative impact of the shale-gas related activities on the overall land-cover change of a watershed.

LULC data at different spatial resolutions have also been shown to affect hydrologic model outputs (Wegehenkel et al., 2006). Combined with high-resolution (1 m) National Agricultural Imagery Program (NAIP), object-oriented image analysis (OOIA) known to produce land-use data of higher classification accuracy than pixel-based methods (Platt and Rapoza, 2008;

Willhauk, 2000). The availability of inexpensive yet readily available aerial imagery such as NAIP data offers the opportunity of applying aerial imagery for the study of the impact of shale-gas activities on hydrologic resources. This presents a cost-effective alternative to the conventional and expensive-to-obtain satellite imagery data. The evaluation of hydrologic model predictive reliability resulting from input LULC data of classified with object-based and pixel-based methods have the advantage of providing critical information in the performance of cost-benefit analyses regarding the choice of method of classification and data resolution for a particular application.

The controlling processes in the hydrology of a watershed have been shown to be scale dependent (Seyfried and Wilcox, 1995). The ability to quantify processes at varying spatial resolutions is expected to provide enhanced understanding of the key processes and controls in a watershed and inform the choice of management options that are available. The ability to assess the effectiveness of management practices with hydrologic modeling also offers stakeholders with a cost-effective means of BMP choice and evaluation in the watershed. This inevitably translates into the integration of key environmental concerns in effectively determining and mitigating impacts of shale-gas exploration and production activities. Lastly, the ability to apply the SWAT model in such an industrial environment answers questions on the feasibility of using a primarily agricultural-based distributed hydrologic model in studying non-agricultural related applications. This may subsequently enhance the range of applicability of the model.

1.2 Research Questions

Traditional pixel-based image classification methods designed for moderate-resolution images are not well-suited to deal with the spatial and spectral variances inherent in high-resolution images. Pixel-based classification essentially identifies the class of each pixel by comparing the spectral value of individual pixels with sampled training classes and assigns the pixel to a specific class based on a specific classification algorithm (Lillesand et al., 2004). The object-oriented image classification technique developed from computer-vision research has been variously applied to high-resolution images and has been found to produce classified images of better accuracy than pixel-based methods (Whiteside and Waqar, 2005). OOIA incorporates a multi-scale segmentation approach that groups pixels into homogenous image objects based on defined shape, texture, spatial and spectral characteristics of the pixels (Baatz et al., 2001). This approach results in discrete regions that are spectrally and spatially homogenous and allows for the identification of object features at specific scales of segmentation. Homogeneity in this regard refers to the fact that the spectral variance within an object is less than the spectral variance between objects (Laliberte et al., 2004). The segmented image objects can then be classified by using either the nearest-neighbor classifier or membership function classifier based on fuzzy-logic combined with user supplied knowledge.

Platt and Rapoza (2008) made a comparison of the traditional pixel-based classification using maximum-likelihood and object-oriented image classification paradigm embedded in eCognition software. They showed that a combination of the segmentation process, nearest-neighbor classifier and expert knowledge yielded improved accuracy over a pixel-based approach. Accuracy assessment is subsequently used to assess the uncertainty associated with a particular classified image. A key research question in this regard is to determine what level of statistical

significance is attainable with the detected change of shale-gas infrastructure. Also in comparison to other infrastructure change, an answer to the above research question may provide an indication of the level of significance the relative changes in infrastructure (as detected from high-resolution NAIP imagery using the object-oriented image analysis technique) impact the overall land-use land-cover change.

Shale-gas exploration and production invariably contributes to changes in the land-cover regime of a watershed. This ultimately has the potential to impact the hydrology of the watershed as well. Wegehenkel et al. (2006) found that a two percent increase (2.9% to 4.9%) in the developed land class of a watershed resulted in 70% increase in the surface runoff predictions in their hydrologic modeling exercise. Therefore, to better represent the prevailing complexities in a system, it is imperative that the classification method captures as accurately as possible the prevailing LULC conditions in the landscape. Similarly, the ability of a hydrologic model to represent and predict changes in hydrology of a watershed is achieved through calibration. Model calibration as a procedure essentially relies on the assumption that the observation data are error-free (Moriasi et al., 2007). With this assumption, a model is calibrated by comparing repeated simulations with the observations until a "best-fit" parameter set has been found. Calibration ultimately relies on the accuracy of model input data.

The question to be answered concerning this section of the research is whether high-resolution LULC input data derived with OOIA provides a SWAT runoff model of better predictive ability than a lower-resolution LULC input data produced with the pixel-based maximum-likelihood technique. Furthermore, it is imperative to also determine the level of predictive accuracy that is associated with the combinations of method of production (pixel-based or OOIA) and image resolution (1 m or 30 m) on the so-derived SWAT runoff models. And lastly, to determine the

feasibility of a primarily agricultural-based model such as SWAT in applications for BMP implementation in a shale-gas environment.

1.3 Research Objectives

The overall goal of the research is to quantify spatial and hydrologic effects of shale-gas exploration and production on the environment. The specific objectives of the research include;

1. To evaluate the predictive reliability of a calibrated SWAT stream-flow model set-up with high-resolution (1 m) NAIP LULC data classified with object-oriented image analysis technique and low-resolution (28.5 m) LULC data classified with pixel-based maximum likelihood method.
2. To quantify the overall LULC change relative to shale-gas related infrastructure from 2006 and 2010 using NAIP aerial imagery classified with Object-oriented image analysis and assess their contribution to the generation of the storm-water runoff and stream-flow in the most active (in terms of shale gas activities) 10-digit HUC sub-watershed of the Little Red River watershed.
3. Employ a modeling approach to evaluate the effectiveness of the implementation of storm-water BMPs in mitigating runoff generation identified in a high shale-gas activity watershed.

1.4 Research Hypotheses

Based on the objectives as outlined above the research hypotheses are broadly categorized as follows:

Hypothesis 1: High-resolution LULC data obtained through OOIA yields a SWAT runoff model of higher predictive ability than the same model created with a low-resolution LULC data derived through pixel-based maximum-likelihood classification.

Hypothesis 2: Shale-gas related activities have a significant effect on land-cover change from 2006 to 2010 in the South-Fork of the Little Red River watershed.

Hypothesis 3: The SWAT model can be used to guide the choice and evaluate effectiveness of BMPs meant to control storm water runoff in the South Fork of the Little Red River watershed.

1.5 Study Significance

The ability to quantify processes at varying spatial resolutions is expected to provide enhanced understanding of the key processes and controls in the study watershed and inform the choice of management options that are available. Also, the ability to assess the effectiveness of management practices with hydrologic modeling also offers stakeholders with a cost-effective means of BMP choice and evaluation.

To date (2012), no study can be located that evaluates the impact of shale-gas related infrastructure on the overall LULC change in the Fayetteville Shale play in north-central Arkansas. The United States Department of Agriculture Farm Service Agency (USDA-FSA) administers "leaf-on" aerial image collection on a regular basis. This readily available NAIP data, when combined with efficient image classification methods has the potential to produce LULC data of improved accuracy. Therefore, using high-resolution (1 m) USDA NAIP data

from 2006 and 2010 and OOIA, changes in land-cover related to shale-gas infrastructure in the South Fork of the Little Red River watershed are quantified and assessed. This gives a significant advantage over traditional pixel-based image classification methods designed for low-resolution satellite images. Pixel-based methods are not well-suited to deal with the spatial and spectral variances inherent in high-resolution images.

The object-oriented image classification technique developed from computer-vision studies has been variously applied to high-resolution images and has been found to produce classified images of higher accuracy than pixel-based methods (Whiteside and Waqar, 2005). OOIA incorporates a multi-scale segmentation approach that groups pixels into homogenous image objects based on defined shape, texture, spatial and spectral characteristics of the pixels (Baatz et al., 2001). The resultant classified image has been shown to be of much better accuracy than the pixel-based method carried out on low-resolution imagery (Platt and Rapoza, 2008). LULC data so obtained has the potential to improve hydrologic model outputs. However, it not clear whether the combination of OOIA with high-resolution necessarily translates into better hydrologic model predictive reliability. This study addresses land-use land-cover change as detected from high and low-resolution imagery and the corresponding impacts on storm water flow in the South Fork of the Little Red River watershed of north-central Arkansas.

References

Arabi M, Frankenberger J R, Engel B A, and Arnold JG, 2007. Representation of Agricultural Conservation Practices with SWAT. Hydrological Processes. doi:10.1002/hyp.

Arnold J G, Srinivasan R, Muttiah R S and Williams J R, 1998. Large Area Hydrologic Modeling and Assessment Part I: Model Development. Journal of The American Water Resources Association 34 (1): 73–89.

Baatz M, Heynen M, Hofmann P, Lingenfelder I, Martthias Mimier, Amo Schape, Michaela Weber M, and Willhauck G, 2001. eCognition User Guide 2.0 : Object Oriented Image Analysis. Munich, Germany: Definiens Imaging GmbH.

Baatz M, and Schape A, 2000. Multiresolution Segmentation : an Optimization Approach for High Quality Multi-scale Image Segmentation. Ed. J Strobl, T Blaschke, and G Greisebener. Journal of Photogrammetry and Remote Sensing 58 (3-4): 12–23. http://www.mendeley.com/research/multiresolution-segmentation-an-optimization-approach-for-high-quality-multiscale-image-segmentation/.

Betrie G D, Mohamed Y A, van Griensven A., and Srinivasan R, 2011. Sediment Management Modelling in the Blue Nile Basin Using SWAT Model. Hydrology and Earth System Sciences 15 (3) (March 8): 807–818. doi:10.5194/hess-15-807-2011. http://www.hydrol-earth-syst-sci.net/15/807/2011/.

Bosch D D, Sheridan J M, Batten H L, and Arnold J G, 2004. Evaluation of the Swat Model on a Coastal Watershed. Transactions of the ASAE 47 (5): 1493–1506.

Gruenspecht, H, 2012. The U . S . Outlook for Shale Gas. In , 1–13. Washington, D.C.

Lillesand T.M., Kiefer R.W and Chipman J.W, 2004. Remote Sensing and Image Interpretation. 5th ed. New York: John Wiley & Sons, Inc.

Moriasi D N, Arnold J G, Van Liew M W, Bingner R L, Harmel R D, and Veith T L, 2007. Model Evaluation Guidelines for Systematic Quantification of Accuracy in Watershed Simulations 50 (3): 885–900.

Platt R V and Rapoza L, 2008. An Evaluation of an Object-Oriented Paradigm for Land Use / Land Cover Classification. The Professional Geographer 60 (1): 87–100.

Seyfried M S, and Wilcox B P, 1995. Scale and the Nature of Spatial Variability: Field Examples Having Implications for Hydrologic Modeling. Water Resources Research 31 (1): (1): 173–184.

Wegehenkel M, Heinrich U, Uhlemann S, Dunger V, and Matschullat J, 2006. The Impact of Different Spatial Land Cover Data Sets on the Outputs of a Hydrological Model: a

Modelling Exercise in the Ucker Catchment, North-East Germany. Phys. Chem. Earth 31: 1075–108.

Whiteside T and Waqar A, 2005. A Comparison of Object-oriented and Pixel-based Classification Methods for Mapping Land Cover in Northern Australia. In Proceedings of SSC2005 Spatial Intelligence, Innovation and Praxis: Melbourne, Australia.

Willhauck G, 2000. Comparison of object-oriented classification techniques and standard image analysis for the use of change detection between SPOT multispectral satellite images and aerial photos. International Archives of Photogrammetry and Remote Sensing XXXIII: 214–221.

CHAPTER 2: LITERATURE REVIEW

2.0 Image Acquisition Theory

Remote sensing is the science and art of acquiring and recording information about objects without physically being in contact with the object of interest; a process which is achieved through the use of a specialized remote sensing device (Yan, 2003). The specialized remote sensing device called the sensor, has the capability of recording electromagnetic energy emitted by or reflected from objects. Through the use of mathematically and statistically based algorithms, the remotely sensed electromagnetic energy data are subsequently analyzed to provide pertinent information about objects.

The amount of the recorded electromagnetic radiance that is measured in the instantaneous field of view (IFOV) of the sensor is a function of the wavelength, the size and location of the picture element (or pixel), temporal information, angular relationship between the sun, object of interest and the sensor, back-scattered energy and precision at which the recording is done by the sensor (radiometric resolution) (Jensen, 2005). Of particular importance to remote sensing is the spatial and spectral resolution of the sensed data. These characteristics bear a direct relationship to the specific sensor used in acquiring the data. Spectral resolution refers to the number and size of specific wavelength or bands that the sensor is sensitive to whiles spatial resolution is essentially a measure of the smallest angular or linear separation between two objects that the sensor has the capability of distinguishing.

The remote sensing device is typically operated aboard an airborne or spaceborne platform for the purposes of collecting information for inventory, mapping and specific information that will inform further decision making (Lillesand, 2001).

2.0.1 Airborne (Aerial) Image Acquisition

Aerial image acquisition is mainly achieved through high-quality photogrammetric cameras and is collected either ad hoc to support specific mapping or resource management projects or at regular intervals over extended periods of time to study environmental processes or economic development. For example, the United States Geological Survey (USGS) administers the National Aerial Photography Program (NAPP) that is designed to cover the lower 48 states every 5 to 7 years. NAPP was operational from 1987 to 2007 and consists of over a million images. Archived NAPP data and data from a number of remote sensing platforms both satellite and aerial photography (including NAPP images) are distributed to the public through the Earth Resources Observation and Science (EROS) center internet portal at eros.usgs.gov/find-data. Color digital NAPP photographs are acquired at an altitude of 6096 m (20,000 ft) with a 15.24 cm (6 in) focal length camera at a scale of 1:40,000. The data format is 22.86 X 22.86 cm (9 X 9 in) covering a ground swath of 8 km (USGS-NAPP, 2012). The photographs are solely acquired for the purpose of providing the USGS with accurate and cloud-free data for the creation and revision of topographic maps of the United States.

Other examples of a long-term acquisition project – and of particular importance to this study - is the United States Department of Agriculture Farm Service Agency (USDA-FSA) National Agricultural Imagery Program (NAIP) which is available for free download through the USDA geospatial data gateway internet portal at datagateway.nrcs.usda.gov. This data was hitherto acquired on a 5-year cycle but since 2009 has been acquired on a 3-year cycle. NAIP is acquired at a ground sample distance (GSD) of 1 meter and a horizontal accuracy that falls within 6 m of the photo-identifiable control points. The default spectral resolution is natural color Red Green Blue (RGB) but starting in 2007 a capability has been added to deliver RGB with Near Infra-Red

as well with a cloud cover of no more than 10%. Each individual image covers a 3.5 X 3.5 minute quarter quadrangle with a 300-m buffer on all four sides (USDA-FSA, 2011).

Other examples of hyperspectral aerial sensor systems are the Airborne Visible Infrared Imaging Spectrometer (AVIRIS) and the Airborne Terrestrial Applications Sensor (ATLAS). AVIRIS is operated by the National Aeronautics and Space Administration (NASA) Jet Propulsion Laboratory with the purpose of collecting data that can be used in characterizing the Earth's surface and atmosphere. The sensor acquires imagery at an altitude of 20 km with an IFOV of 20m with flights planned at regular times throughout the year and also on "on-demand" basis (Jensen, 2005; NASA-JPL, 2012; Howell and Green, 1987). The imagery can be obtained from the EROS data portal through the use of the earthexplorer utility. ATLAS is also designed and operated by NASA for purposes related to environmental, geographic information science, mineral exploration etc. The sensor provides various spatial resolutions in the range of 2 to 25 m depending on the flight altitude. ATLAS missions are flown on an "on-demand" basis (Sullivan et al., 2004; Quatrochi et al., 2000).

2.0.2 Satellite Image Acquisition

Satellite image acquisition is accomplished with unmanned aerial vehicles or satellites that have either analog or digital frame cameras orbiting the earth at significantly higher altitudes and ground coverage than airborne acquisition systems. Perhaps the two most popular satellite image acquisition sensors are the Landsat Multispectral Scanner (MSS) and Landsat Thematic Mapper (TM) sensor systems (Jensen, 2005).

The MSS was placed on Landsat 1 to 5 satellites. The sensor is an optical-mechanical system that scans the terrain perpendicular to the flight lines and focuses energy reflected or emitted energy from the terrain. MSS has five spectral bands (RGB and infrared) with an IFOV of 79 m X 79 m at nadir for bands 4 through 7 and 240 m X 240 m for band 8. Images are acquired at an altitude of 919 km with a swath width of 185 km. Each MSS scene contains 185 X 170 km ground coverage of the continuous swath of an orbit with a 10% overlap (Jensen, 2005).

The TM sensor also operates an optical-mechanical whiskbroom sensor that collects multispectral data that has higher spatial and spectral resolution than the MSS. The ground projected IFOV is 30 X 30 m for bands 1 through 5 and band 7; band 6 however has a 120 X 120 m ground projected IFOV with all images acquired at an altitude of 185 km. The spectral resolution of the sensor spans from 0.45 μm to 2.35 μm encompassing RGB and Infrared spectra (Jensen, 2005).

The main difference between the two sensors aside from the above stated respective characteristics is the fact that the original bandwidth of the MSS was selected based on their utility for vegetation inventories and geologic studies. On the other hand, the TM bands were selected based on their value for water penetration, discrimination of vegetation types etc. There other satellite image acquisition sensors other the two described above which are mostly made

for specialized purposes. One such sensor is the Advanced Very High Resolution Radiometer (AVHRR). One very popular application of this sensor is the study or the mapping of vegetation condition over wide areas of the earth surface through the computation of the Normalized Difference Vegetation Index (NDVI) and the mapping of sea-surface temperature.

Satellite and airborne image acquisition platforms have various respective advantages and disadvantages most of which depend to a large extent on the spectral and spatial resolutions of the respective sensor in a platform. Depending on the study objective, a critical analysis of the respective capabilities should be made in view of cost-benefits of each platform to determine the suitability and applicability.

2.1 Land-Use Land-Cover Change

Land-use is a term used to refer to the specific human or economic activity associated with a geographically defined piece of land (Lillesand, 2001). Therefore the land-use of a particular area could be said to be agricultural, transportation, commercial etc. The above shows that the land-use of a particular area is typically influenced by human activity but above all by the geographic location of the specific piece of land as well.

Land-cover is used to describe the type of feature that is present on the surface of a specific geographically defined area such as region, watershed, state etc. The land-cover description of any area can therefore be done with terms such as corn, bare land, grass, concrete etc. Land-use land-cover forms one of the major components of studies in the earth sciences (Townsend et al, 1994).

Land-use land-cover (LULC) change however, is a continual and dynamic process that is a major driving force in environmental change (Lambin, et al., 2000). This change can be driven by

economic, cultural and political factors (Brown et al., 2000) and in most cases are known to have improved conditions relating to cultural and economic aspects of people. However, there are negative implications of this change which is mostly seen in the environment relating to weather patterns (Chase et al., 1999; Stohlgren et al., 1998), changes in hydrologic regimes (Barr, 2008; Mejia, 1998), water quality and quantity (Tong and Chen, 2002; Faney et al., 2001; Aylward, 2002).

LULC change detection is there of critical importance in understanding the myriad of environmentally dependent factors in a region. Several methods of LULC change detection have been developed in literature. The major underlying principle is classification of multi-temporal remotely sensed data into land-use land-cover maps and subsequently performing statistical analyses of the relative change of the respective classes at the different acquisition times. The development of object-oriented image analysis methods has led to corresponding change detection methods such as presented by Das (2009). Niemeyer and Canty (2003) also detail pixel-based and object-based methodology for change analysis intended to take advantage of high-resolution imagery. Their approach involves the use of canonical correlation analysis in order to enhance the change information in the difference images and the use of bayesian techniques for the determination of significant thresholds. Changes that are determined to be significant are then analyzed explicitly with object-oriented techniques.

Advances in LULC change detection analysis have implications on hydrologic model interpretation and an understanding of the modeled system as well. For example, Wegehenkehl et al. (2006) found that a change of ~ 69% (2.9% to 4.9%) in the developed land class resulted in a 70% increase in surface runoff predictions. This makes it imperative to perform critical analyses in LULC regarding environmental studies so as to ensure an understanding of the

linkages between local environmental changes (hydrologic, weather, water quality etc) and LULC change detection. There are a number of studies in literature that deal with LULC change detection and others that explicitly tackle the relationship between LULC change and the attendant impact on hydrologic model simulation. In all, these studies either employ pixel-based or object-oriented classification techniques in their respective methodologies. Singh(1989) presents a comprehensive review of literature, methods and the theoretical basis of some outlined change detection techniques. Of particular importance in land cover change detection is the concept of thresholding. This basically involves decisions as to where to place threshold boundaries in order to separate areas deemed to have changed from those of no change. For example if in an image $I(x, y)$, a light object (represent a change) is found in a dark background (an area of no change) then these objects may be expressed by the simple mathematical thresholding equation

$$I(x,y) = \begin{cases} 1 \; I(x,y) > T \\ 0 \;\; I(x,y) \leq T \end{cases}$$

where T is the threshold value that is determined by empirical or statistical means. (Singh, 1989). Nelson (1983) also presents a tabular presentation of a variety of change detection approaches and details other studies that have used the respective approaches. A comparison of change detection techniques is also given in Maas (1999).

The ability to more closely depict responses in hydrologic processes due to changes in land cover has been a key research goal in remote sensing and hydrology (Miller et al., 2007) and a number of studies have touched on land cover change and the impact on hydrologic model outputs (Norbert and Jeremiah, 2012; Koch et al., 2012; Scott et al., 1993). A key similarity in such studies is that a variation or alteration in land cover data ultimately leads to noticeable change in

runoff and in some cases sediment yield. For example Alibuyog et al. (2009) showed with a SWAT model simulation of a catchment in the Philippines that land use change can impact the hydrology and sediment yield by between 3% to 14% and 200% to 273% respectively (Kock et al., 2012). Upward changes of 70% in runoff simulations have been reported in a study done in the Ucker Catchment, in North-East Germany.

2.2 Land-Use Land-Cover Mapping (Image Classification)

To better understand the basic concept of image classification there is the need to have an idea of the concept of feature space. This is a concept that illustrates with graphical plots the values of pixels in specific bands that make up a remotely sensed image.

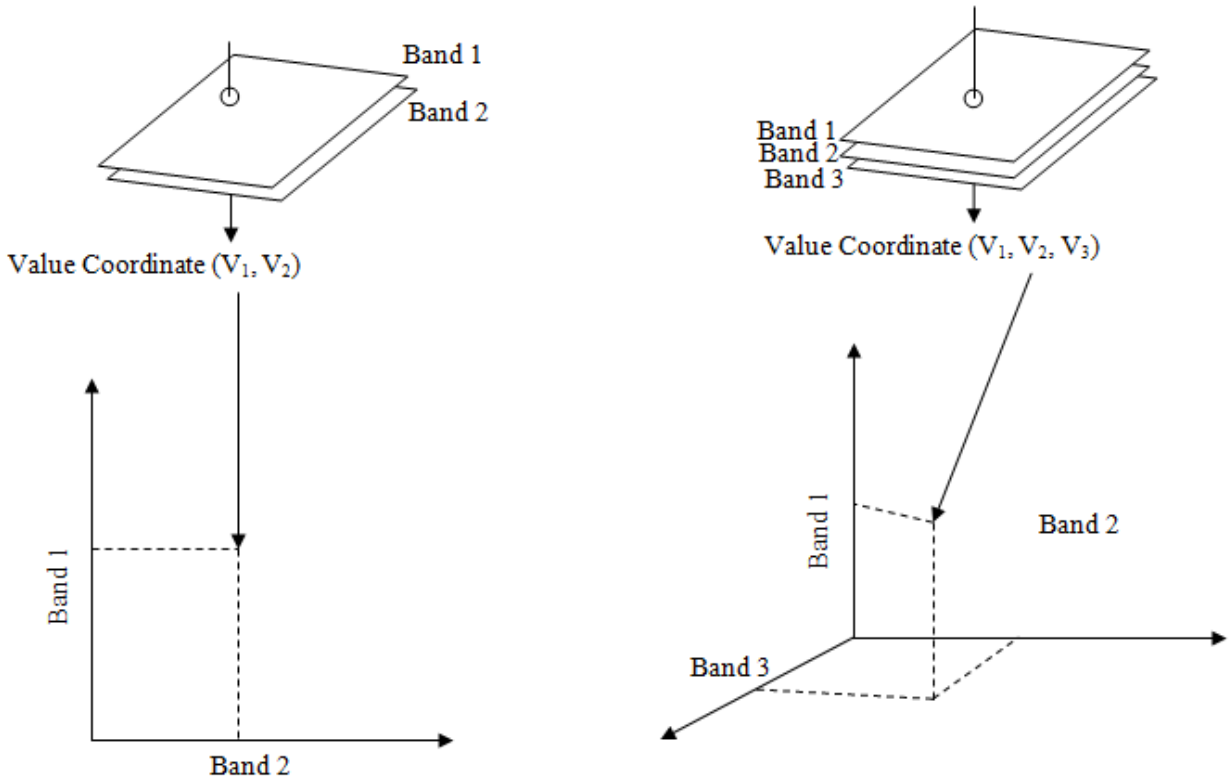

Figure 1: Feature space illustration (Jensen, 2001) as depicted in Gao (2003)

The number of bands in the image is effectively termed the dimensionality of the image. The illustrations below show feature space plots for 2-dimensional and 3-dimensional images (Gao, 2003). The underlying assumption in image classification is that a specific part of the feature space is representative of a specific class in the image data. Pixels are then compared to the identified classes in the feature space and a decision on pixel assignment is made based on a specific classification rule (Jensen, 2005).

2.2.0 Pixel-Based Image Classification

Pixel-based image classification refers to the classification of remote sensing data based on spectral properties of individual pixel that make up the image. It is sometimes referred to as "pixel by pixel" (Gao, 2003) manner of image classification in which a pixel can belong or be assigned to only one class. The two main criteria to be discussed under this method of image classification are the supervised and unsupervised classification methods.

2.2.0.0 Supervised Classification

In supervised classification the location and specific spectral characteristics of the land-cover classes of interest (urban, forest, agriculture, water etc) are known apriori (Jensen, 2005). This knowledge is acquired through and combination of field surveys and aerial image interpretation and personal experience (Hodgson et al., 2003). An analyst locates specific sites in the remotely sensed data that are representative of homogenous areas in the known land-cover types. These representative samples of class types are known as training sites (Jensen, 2001). The spectral characteristics of these known homogenous areas are used to train classifier for application in classifying the entire image. Also multivariate statistics such as means, standard deviations, covariance and correlation matrices are calculated for each training class or site. Pixels are evaluated with these training classes based on the respective statistics to determine the maximum

likelihood of that individual pixel belonging to that specific class. The importance of training classes in this regard requires that training samples of each class should be typical and encompass the spectral variability that class type (Mather, 1987). There is no known defined limit of pixels to be used in formulating a training class. However, in order to use statistically based classifiers, it is recommended that a theoretically lower limit of n + 1 (where n is the spectral bands) number of pixels must be used in a training class (Lillesand, 2001).

Pixel-based image analysis classifiers are classically hard classifiers that assign pixels membership to a class as either 1 or 0. With 1 expressing a pixel's membership to a class whiles 0 denotes that an individual pixel bear no membership to a particular class hence the term "hard classifiers" as they express in binary (yes or no) terms whether a pixel is a member or not a member of a class. The maximum-likelihood decision rule (classifier) is one of the most widely used of such a supervised classifier (Wu and Shao, 2002). It is a classification rule that is based on probability: it assigns each individual pixel to a specific class whose units are most probable or likely to have given rise to the feature vector (Atkinson and Lewis, 2000). The method assumes that the statistics of the training data for each class in each class is normally distributed. Therefore training data of n-modes in the histogram is not ideal and such a case implies the existence of unique classes (Jensen, 2005).

2.2.0.1 Unsupervised Classification

This method of image classification also referred to as clustering, partitions remote sensing data into multispectral feature space and subsequently extracting land-cover data (Loveland et al., 1999). Unlike supervised classification, this method only requires minimum input from the analyst; mainly because there is no requirement for training data. Therefore, the algorithm searches for natural groupings of the spectral characteristics of the pixels in a specific band as is

evident in the feature space. The process results in a classification map that consists of a number of spectral classes after which the analyst attempts an after the fact transformation of the spectral classes into class types (Jensen, 2001).

Among the numerous classification algorithms that are used to determine the natural groupings in an image is the "K-means" method. The approach in this algorithm requires the analyst to specify the number of clusters or data centers representing the potential individual classes. The algorithm then locates these number of cluster points in the multidimensional feature space. This is followed by assigning each pixel to the cluster based on the closest distance between the mean vector of the cluster and the pixel. The mean vectors of the clusters are then revised and are then used as the base to reclassify the data (Gao, 2003).

2.2.1 Object-Oriented Image Classification

Unlike the "per-pixel" classification which is mainly based on processing an entire image on pixel by pixel basis (Blaschke and Strobl, 2001), the object-oriented image analysis procedure allows for the decomposition of the image into many homogeneous objects known as segments. These segments are created at varying scales in the image leading to what is termed multi-resolution image segmentation (Baatz and Schape, 2000). Statistical characteristics of the defined objects are then used in traditional statistical or fuzzy logic classification algorithms. This method is often used on high-resolution imagery such as 1 m IKONOS or 0.6 m QuickBird Imagery.

2.2.1.1 Image Segmentation

Image segmentation is the process of aggregating pixels into homogenous image objects. Homogeneity in this sense is defined in terms of the spatial and spectral characteristics of the

discrete objects (Ryherd and Woodcock, 1996) and basically refers to the fact that within object variance is less than the variance between objects (Lalliberte et al., 2004). This process is the first step in a method that attempts to replicate the way humans perceive objects in the real world (Lang, 2008). There are several methods of image segmentation which can broadly be categorized into region-growing, spatial clustering, edge-based, area-based algorithms etc (Haralick and Shapiro, 1985; Blaschke and Strobl, 2001). More recent developments have yielded the Fractal Net Evolution Approach (FNEA) (Baatz and Schape, 2000) which is a multifractal approach to segmentation that is implemented in the eCognition software.

FNEA is a pair-wise clustering process that determines object areas of least spectral and spatial heterogeneity at a given scale, spectral and shape parameter set (Benz et al., 2004). Images are thus segmented at different scales which add a scale hierarchy to the analysis (Burnett and Blaschke, 2003). This multiscale approach determines the size of the image object which is also dependent on the inherent resolution of the image. With the scale parameter increase, so does the object size (Platt and Rapoza, 2008); therefore a specific scale level produces objects of specific sizes hence the term multiresolution segmentation. The process of segmentation stops when the smallest object exceeds the threshold that is set by the scale parameter (Lalliberte et al., 2004). Multiresolution segmentation as implemented in ecognition software is governed by the concept of minimizing the spectral heterogeneity between pixels making up an image object - thus minimizing within object spectral heterogeneity. Taking the size of objects into consideration the following simple equation that can be used to optimize the criterion of minimizing the spectral heterogeneity (Baatz and Schape, 2000)

$$h_{diff} = n_1(h_m - h_1) + n_2(h_m - h_2)$$

where h_{diff} is the difference in spectral heterogeneity, h_m is the spectral heterogeneity of the merged object, h_1 and h_2 are the spectral heterogeneities of the objects 1 and 2 to be merged with sizes n_1 and n_2 respectively.

The object-oriented image classification paradigm embedded in eCognition software employs nearest neighbor in addition to expert knowledge to assign objects to respective class types. The nearest neighbor classifier computes the Euclidean distance from the object to be classified to the nearest training data mean vector in feature space (as is applied in per-pixel method). Classification is subsequently done by assigning each object to the class that is closest to it in feature space (Schowengerdt, 1997).

Another classification method used in object-oriented image analysis is the fuzzy classification based on fuzzy logic theory. This is achieved through the use of membership functions. A membership function has output ranges from 0 to 1 for each object's feature values in relation to the object's assigned class (Lalliberte et al., 2004). The fuzzy rules allows for the definition of such criteria such as "all image objects with spectral values larger than x are natural gas well-pads".

2.3 Land-Use Land-Cover Map Accuracy Assessment

Land-use land-cover map accuracy assessment is necessary in order to provide a measure of certitude associated with the classified land-cover map. Perhaps the most important aspect of accuracy assessment is to clearly state the objective of the accuracy assessment in respect of the problem at hand, the classes of interest and method of data sampling (Jensen, 2005). In this research the object of accuracy assessment is to provide a degree of confidence that can be associated with the final classes in the produced land-cover map. There are many sources of error when it comes to the accuracy of the final thematic map. The most widely used method of

thematic map accuracy assessment; the error matrix is plagued with several sources of error. Congalton and Green (1993) detail these errors and explain how they affect the implications of the error or the accuracy assessment. In order to assess the accuracy of remotely sensed data or for that matter classified remotely sensed data, it is essential to evaluate both positional and thematic accuracy (Congalton, 2005).

2.3.0 Positional Accuracy

The most common measure of map accuracy is the measure of how closely the images represent the existing features on the ground. This is known as the positional accuracy (Congalton, 2005). The most important factor that affects positional accuracy is topography. The effect of topography on positional accuracy can be seen in figure 2.

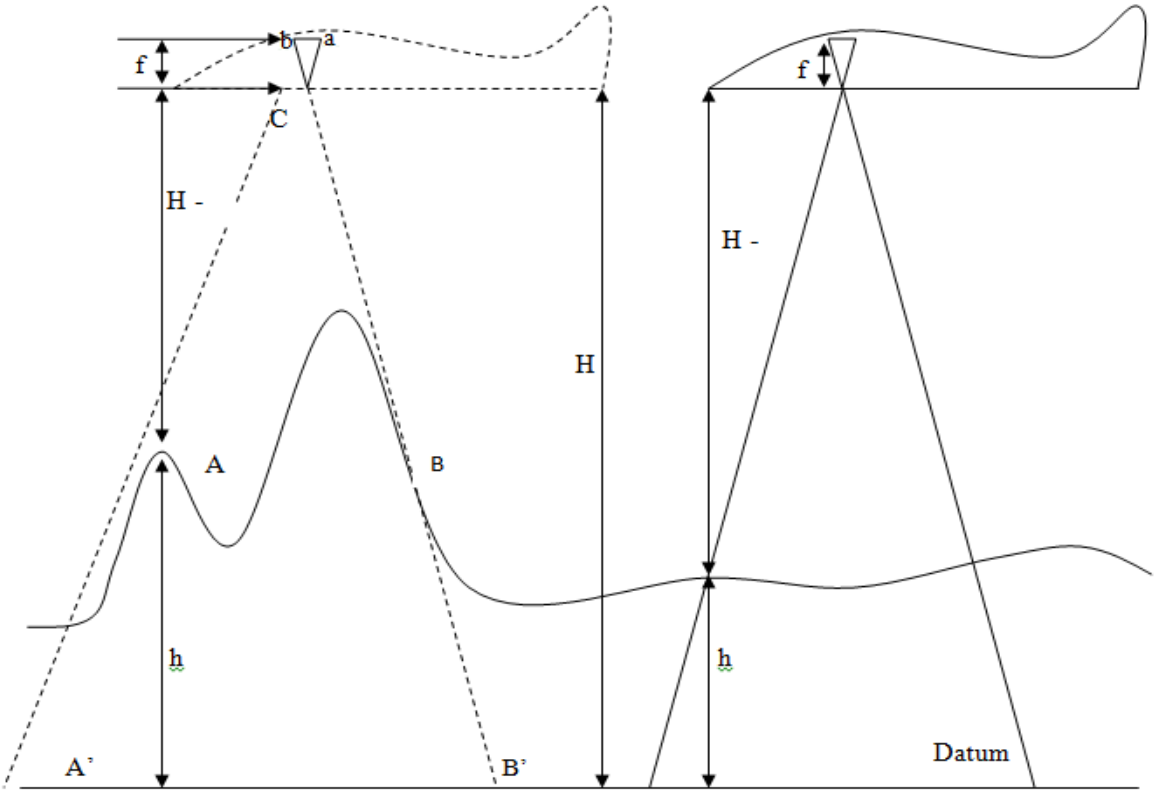

Figure 2: Illustration of terrain elevation differences on scale effects in aerial image acquisition

Sequence B Sequence A

To achieve positional accuracy it is imperative that the same exact location can be determined both on the image and on the ground and that scale effects are minimal. However as illustrated in figure 2, the relative scale in the images are at positions A and B are compromised due to terrain elevation effects. To better understand this one needs to understand the concept of scale as applied to aerial images. By using similar triangles

ΔabC ≈ ΔABC since $\overline{ab} : \overline{AB}$ Image distance is proportional to object (ground) distance

Again f: H (focal length of camera is proportional to height above datum)

Therefore,

$$\frac{f}{H-h} = \frac{\text{ab}}{AB} = \frac{1}{S}$$

Where S = scale of image

From the above it can be seen that the height or elevation, *h*, above the datum is the controlling factor in the scale for a given focal length at a specific pixel in an image. Therefore in figure 2, the pixel for image position A in sequence A will have a much different scale than the same pixel for image position A in sequence B. This phenomenon will invariably affect the positional accuracy of the acquired image as well.

Positional accuracy holds an important aspect of thematic map accuracy assessment. For example if a position is registered to the ground to within half a pixel size, using GPS in locating such a place on the ground to 15 m for instance, then using a single pixel as a sampling unit becomes impossible for assessing the thematic accuracy of such a map (Congalton, 2005). In this situation the GPS location must be located with a high degree of accuracy so as to prevent significant problems with regards to positional accuracy. Positional accuracy is measured in root mean square error (RMSE) computed as the sum of the squares of the differences between point

positions in one image layer in comparison to the point positions in another image layer (usually the ground) with the same data that has been used to register the images layers (Congalton, 2005).

2.3.1 The Error Matrix

Another measure of the accuracy of classified maps obtained from remotely sensed data is the thematic accuracy. This refers to the accuracy of a classified or mapped land-cover map obtained at a particular time in relation to the prevailing conditions on the ground at the time of classification (Congalton, 2005). This definition brings to the bear the fact that knowledge of the accuracy associated with a reference or ground-truth data is vital and that the reference data should in the least of cases have higher accuracy in order to ensure a fair accuracy assessment (Congalton, 1991).

The most common measures of accuracy assessment in classified remotely sensed imagery are the producer, user and overall accuracy (Story and Congalton, 1986); all based on the error or confusion matrix. The error matrix consists of a square array of numbers set out in rows and columns to express the number of pixels assigned to a particular classification category in relation to the actual category as determined using ground-truth (Congalton, 1991). The error matrix essentially provides a systematic way to compare pixels in the classified map and ground-truth data. The relationship between the two sets of data is expressed or summarized in the error matrix (Jensen, 2005). Table 1 is an error matrix used to illustrate the producer, user and overall accuracy measures. The columns represent the ground-truth data as the rows of the matrix correspond to the classified pixels. The diagonal of the matrix represents the number of pixels in each category that is deemed to be accurately classified as the off-diagonals represents the errors

in each classification class with respect to the ground-truth data (thus assuming the ground-truth data is error-free).

Table 1: Example of an error matrix (for demonstration purpose): modified from Congalton (1991)

Classified	**Reference Data**				
	Forest	Corn	Bare Soil	Well pad	Row Total
Forest	**96**	4	15	21	136
Corn	3	**89**	5	10	107
Bare Soil	2	5	**92**	43	142
Well pad	21	7	34	**97**	159
Column Total	122	105	146	171	**544**

Overall Accuracy = 374/544 = 68.75%

Producer's Accuracy (probability of a reference pixel being correctly classified)

Forrest: 96/122= 78.69% Corn: 89/105= 84.76% Bare Soil: 92/146= 63.01% Well pad: 97/171=56.73%

User's Accuracy (probability of a classified pixel representing the category on the ground)

Forrest: 96/136= 70.59% Corn: 89/107= 83.18% Bare Soil: 92/142= 64.48% Well pad: 97/159=61.01%

2.3.2 Land-Use Land-Cover Change Detection

Change detection is a remote sensing procedure that is intended to find alterations or changes in objects or phenomena of interest from images acquired at separate times (t_1, t_2, t_3,….t_n) (Niemeyer, 2003). Traditionally this has been achieved by comparing pixels from multitemporal images for time t_1 and t_2 and subsequently performing some sort of statistical analyses on difference data to determine a descriptive statistic with which to report change. Change detection algorithms mainly fall under;

- Write function memory insertion: This method involves the insertion of each individual band or any derivative of it acquired at different times, into each of the three write function memory (WFM) banks (red, green or blue) to identify changes in the scene (Jensen, 2005).
- Multi-date composite imagery: this mostly involves the subjection of the images to principal component analysis (PCA) to determine change (Fung and LeDrew, 1987; Maas, 1999).
- Band differencing: This in its simplest form can be explained as subtracting the brightness values of one image acquired at a specific time from the brightness values of another image acquired at a different time of the same scene. The normalized difference vegetation index method is perhaps one of the popular examples of this change detection method.
- Post-classification comparison: This involves performing a comparison on a pixel-by-pixel basis through the use of a change detection matrix obtained from a rectified and subsequently classified imagery data of the same scene at separate time periods (Yuan and Elvidge, 1998; Civco et al., 2002; Jensen et al., 1995).

There are a number of studies that have been done on change detection using the object-oriented approach as well (Tanathong et al., 2009; Lefebvre et al., 2008; Yuan and Elvidge, 1998; Chen et al., 2012). Tanathong et al., (2009) used the object-oriented approach to for post-disaster building assessment. Their approach mainly relies on knowledge based intelligent agents (Tenuci, 1998) for the recognition of buildings pre and post disaster. The process creates building objects (Jacobson, 1998) corresponding to the individual buildings in the image. The building objects not only contain properties of the building but also the computational process

that are used as decision rules for common properties of the buildings. The detection of change is achieved by interacting the individual building objects with each other to obtain matched-up pairs of pre and post disaster objects. Differences in the matched up pairs constitute the change in the scene. To more specifically address the issue of the choice of the above-named methods and algorithms for a particular task, it is essential to understand the rudimentary steps and scope of application. It is also important to note that each of the algorithms is optimized for a particular phenomenon of interest. Hence it becomes important to relate the choice of a specific algorithm to the dominant change theme or class in a change detection analysis of a scene or area. For example in this research land-use land-cover change of interest are particular related to urban, agricultural, forest and industrial (shale-gas related industrial change).

2.4 Data Bridging: Hydrologic Models and Remote Sensing Data Resolution

Integration of remote sensing data in hydrologic modeling has received some research attention. Notable among these are Gupta et al. (2011), Andersen (2008), Blankenship and Crosson (2012) and Schultz (1988). In this research what is of particular attention is the land-use land-cover (LULC) data of varying resolutions obtained from two fundamentally different methods of production. The role of LULC data is more prominent in distributed hydrologic models where the concept of hydrologic response unit (HRU) is a key driving factor in model set-up and parameterization. The HRU concept basically allows for the conceptualization of models in order to take account of the distribution of the physical characteristics of the watershed without having to resort to fully represent and perform model calculations at each individual discretization of the physical state of the watershed (Beven, 2005).

HRU discretization is highly aided by the introduction of geographic information science (GIS) in hydrological modeling. This is achieved through overlaying different hydrologic descriptive

indicators such as soil, land-use data and slope classes which have been properly spatially registered to the geographic region of interest. The definition of HRU in this way ultimately leads to irregular patterns as overlays are performed with vector and raster data layers. For calculation purposes, this concept has a significant advantage in that similar HRUs are grouped together into single units thereby simplifying calculations and reducing computing resource requirement. The crux of the concept is that sections of the catchment with similar characteristics will have similar responses and it is based on this that the predictions of the distribution of individual catchment responses are made (Beven, 2005).

The level of detail that a remotely sensed image is able to capture within an area is a measure of the resolution of the image. Therefore, in distributed or semi-distributed hydrologic models such as the Soil and Water Assessment Tool (SWAT), where model results have been shown to be dependent on the resolution of such data such as soils (Geza and McRay, 2008; Mukundan et al., 2010; Kumar and Merwade, 2009), DEM (Chaubey et al., 2005), land-cover data (Chen et al., 2005; Bosch et al., 2004), it becomes important to investigate the effect that methods of LULC data classification applied with the high resolution imagery in obtaining high resolution land-cover map. This is particularly important as computations in distributed surface hydrologic models such as SWAT depend to a large extent on the input land-cover data (Kepner et al., 2013; Arnold et al., 1998).

2.5 The Soil and Water Assessment Tool (SWAT)

The Soil and Water Assessment Tool (SWAT) is a continuous-time physical process-based model for the simulation of landscape processes at the watershed scale (Neitsch et al., 2005; Arnold et al., 1998). As described in the preceding section, the watershed is divided into discrete regions known as hydrologic response units (HRUs) based on the soil types, slope and land-use land-cover classes thus allowing for spatial detail in the simulation (Betrie et al., 2011). The major components of the model are hydrology, soil temperature, weather, soil erosion, crop growth, agricultural management etc.

Hydrologic prediction is done at the HRU level using the water balance equation (Arnold et al., 1998):

$$SWt = SWo + \sum_{i=1}^{n}(Rday - Qsurf - Ea - wseep - Qgw)$$

Where:

Rday (mm) = rainfall on day i

$Qsurf$ (mm) = amount of surface runoff on day i

Ea (mm) = amount of evapotranspiration on day i

wseep = amount of water that enters the vadose zone on day i

Qgw = the amount of return flow on day i

Surface runoff can be computed with a choice between the Green and Ampt infiltration method (Green and Ampt, 1911) or the Natural Resource Conservation Service Curve Number (CN) method (USDA-SCS, 1972; Betrie et al., 2011). Flow is calculated at the various HRUs and

routed to the nearest channel (Arnold et al., 1995) using either the variable storage coefficient method (Williams, 1969) or the Muskingum method (Chow, 1959).

2.6 The Concept of Equifinality

An important aspect of hydrologic modeling or any modeling exercise is the need to address the problem of model parameter calibration. Most calibrations involve the optimization of some parameter values through the comparison of simulated values with observed data until some "best-fit" parameter set satisfying an evaluation criterion or criteria are achieved (Beven, 2005; Chaubey and White, 2005; James and Burgess, 1982).

This method of calibration by optimizing parameter values assumes that observed data are error-free and the model at the end of a calibration exercise is a true representation of the system or data. However, in hydrologic modeling there can be significant errors in both observed data and model conceptualization (Beven, 2005). While one optimum parameter set may satisfy an objective function with a given threshold criterion, there may also be several other optimum parameter sets that may well present acceptable model simulations. This brings into focus the concept of equifinality that basically points out that the choice of one calibration optimum parameter set over another is at best described as arbitrary. Hence equifinality explains the concept that for a specific hydrologic model simulation there may be several optimum parameter sets that could produce acceptable fits to the observation data (Beven and Binley, 1992; Beven and Binley, 2001).

2.7 Accounting for Equifinality: The GLUE Method

Accounting for the limitations in distributed hydrologic models in terms of the calibration and the issue of equifinality has led to the development of methods that are based on the realistic estimation of the prediction uncertainty (Beven, 1989a). To this end, Binley and Beven (1991) outlined a general strategy for model calibration and uncertainty estimation in such complex distributed hydrologic models. The Generalized Likelihood Uncertainty Estimation (GLUE) method assumes that before any quantitative or qualitative information is added to any modeling exercise, any parameter set combination meant for the prediction of a specific model output should be deemed equally likely as a simulator of the system (Beven, 1989b). The glue method attempts to account for parameter non-uniqueness as there is no unique solution to a model outcome. The approach is to estimate degrees of belief that can be associated with models and parameter sets (Beven, 2005).

The method is simple and easy to implement. The base of the technique relies on the estimation of probabilities associated with different parameter sets. A posterior probability function is derived from a chosen likelihood function (mostly the Nash-Sutcliffe Index) which subsequently becomes the measure used to derive the predictive probability of the output variables (Abbaspour, 2011). The choice of a likelihood measure is somewhat subjective and can partly depend on the observational data available. Beven (2005) details the criteria for selecting an appropriate likelihood measure.

A GLUE analysis generally consists of the following steps:

- Define a “generalized likelihood measure”, L(α)

- Sample (Monte Carlo or Latin Hypercube or any appropriate sampling strategy) a large number of parameter sets from a prior distribution
- Define a threshold value for a "likelihood measure"
- Assess parameter sets as either acceptable (behavioral) or unacceptable (non-behavioral) based on a comparison with the give threshold value for the likelihood measure
- Assign weights to each behavioral parameter set using

$$Wi = \frac{L(\alpha \mathrm{i})}{\sum_{j=1}^{n} L(\alpha \mathrm{j})}$$

  Where n is the number of acceptable parameters
- The prediction uncertainty is then presented as a quantile from the cumulative distributions of all the weighted parameter sets. (Abbaspour, 2011; Beven, 2005)

Implementing the method ultimately requires key decisions to be made regarding the choice of a sampling strategy, appropriate likelihood measure, feasible parameter range and behavioral model threshold. Details regarding these are further discussed in Beven (2005).

2.8 Prior Applications of SWAT in Best Management Practice (BMP) Implementation

The SWAT model has been used in several studies to evaluate the Best Management Practices (BMPs). These studies encompass areas such as nutrient loading of water bodies, application of agricultural chemicals (YunSheng et al., 2005), fate and transport of chemicals and sediments (Zhang and Minghua, 2011), sediment control (Betrie et al., 2011), storm-water control etc. The model was used to evaluate the effectiveness of five BMPs scenarios in reducing nutrient loading in a watershed located in the Inland Bays in southern Delaware (Sood and Ritter, 2010). It has also been used in predicting non-point source pollution nitrates nitrogen and total phosphorous

loading through evaluation and assessment of large number of scenarios in a watershed in Greece (Panagopoulos et al., 2012).

The model has also been adopted by the United States Environmental Protection Agency's (USEPA) Better Science Integrating Point and Non-Point Sources (BASINS) software package for analyses pertaining to development of Total Daily Maximum Load (TMDL) guidelines for various water bodies in the United States. A review presented by Kalin and Hantush (2003) regarding key features of hydrologic models widely cited for the ability of the models to represent BMPs indicated that the SWAT model offers the largest number of management alternatives.

Perhaps a short fall to the use in management representation is that it offers no numerical guidelines for the representation of management scenarios. The lack of numeral representation of practice performance has been addressed as a vital research need in Nietch et al., (2005) and Arabi et al., (2007).

References

Andersen F H, 2008. Hydrological Modeling in a Semi-arid Area Using Remote Sensing Data. PhD Thesis, University of Copenhagen, Copenhagen, Denmark.

Arnold J G, Srinivasan R, Muttiah R S and Williams J R, 1998. Large Area Hydrologic Modeling and Assessment: Part I. Model Development. Journal of American Water Resource Association 34 (1): 73–89.

Atkinson P M, and Lewis P, 2000. Geostatistical Classification for Remote Sensing: An Introduction. Computers and Geosciences 26 (4): 361–371.

Aylward B, 2002. Report to the World Bank as Part of the Program for the Sustainable Management of the Rural Areas in the Panama Canal Watershed. Falls Church, VA.

Baatz M and Schäpe A, 2000. Multiresolution Segmentation: An Optimization Approach for High Quality Multi-scale Image Segmentation. Angewandte Geographische Informationsverarbeitung. Heidelberg: Wichmann-Verlag.

Barr S, 2008. Environment and Society: Sustainability, Policy and the Citizen. Ashgate publishing

Benz U C, Hofmann P, Willhauck G, Lingenfelder I and Heynen M, 2004. Multi-resolution, Object-oriented Fuzzy Analysis of Remote Sensing Data for GIS-ready Information. ISPRS Journal of Photogrammetry and Remote Sensing 58 (3-4) (January): 239–258. doi:10.1016/j.isprsjprs.2003.10.002. http://linkinghub.elsevier.com/retrieve/pii/S0924271603000601.

Betrie G D, Mohamed Y A, van Griensven A and Srinivasan R, 2011. Sediment Management Modelling in the Blue Nile Basin Using SWAT Model. Hydrology and Earth System Sciences 15 (3) (March 8): 807–818. doi:10.5194/hess-15-807-2011. http://www.hydrol-earth-syst-sci.net/15/807/2011/.

Beven K J and Binley A M, 1992. The Future of Distributed Models: Model Calibration and Uncertainty Prediction. Hydrological Processes 6: 279–298.

Beven K J, 2005. Rainfall Runoff Modeling. John Wiley & Sons, Inc.

Blankenship C B and Crosson W L, 2012. Ensemble Kalman Filter Data Assimilation of AMSR-E Soil Moisture Estimates into the SHEELS Land Surface Model. In 92nd American Meteorological Society Annual Meeting. New Orleans.

Blaschke T and Strobl J, 2001. What's Wrong with Pixels? Some Recent Developments Interfacing Remote Sensing and GIS. GeoInformation Systems 14 (6): 12–17. http://courses.washington.edu/cfr530/GIS200106012.pdf.

Bosch D D, Sheridan J M, Batten H L, and Arnold J G. 2004. Evaluation of the SWAT model on a coastal watershed. Transactions of the ASAE 47 (5): 1493–1506.

Brown D G, Duh J and Scott A D, 2000. Estimating Error in an Analysis of Forest Fragmentation Change Using North American Landscape Characterization (NALC) Data. 117 (June 1999): 106–117.

Burnett C, and Blaschke T, 2003. A Multi-scale Segmentation/object Relationship Modelling Methodology for Landscape Analysis. Ecological Modelling 168 (3) (October): 233–249. doi:10.1016/S0304-3800(03)00139-X. http://linkinghub.elsevier.com/retrieve/pii/S030438000300139X.

Chase T N, Pielke R A Sr., Kittel T G F, Nemani R R, and Running S W. 2000. Simulated Impacts of Historical Land Cover Changes on Global Climate in Northern Winter. Climate Dynamics 16 (2-3) (February 4): 93–105. doi:10.1007/s003820050007. http://www.springerlink.com/openurl.asp?genre=article&id=doi:10.1007/s003820050007.

Chaubey I, Cotter A S, CostelloT A, and Soerens T S, 2005. Effect of DEM Data Resolution on SWAT Output Uncertainty. Hydrological Processes 19 (3) (February 28): 621–628. doi:10.1002/hyp.5607. http://doi.wiley.com/10.1002/hyp.5607.

Chen G., Hay G.J., Carvalho L.M.T. and Wulder M.A., 2012. Object-based change detection. International Journal of Remote Sensing, 33:14, 4434-4457

Chen L and Michael H Y, 2006. Green-Ampt Infiltration Model for Sloping Surfaces. Water Resources Research 42 (7): 1–9. doi:10.1029/2005WR004468. http://www.agu.org/pubs/crossref/2006/2005WR004468.shtml.

Chen P, Di Luzio M, and Arnold J G, 2005. Impact of two land-cover data sets on stream flow and total nitrogen simulations using a spatially distributed. In Pecora 16, “Global Priorities in Land Remote Sensing”. Sioux Falls, SD.

Chow V T, 1959. Open-channel Hydraulics, McGraw-Hill, New York.

Civco D L, Hurd J D, Wilson E H, Song M, and Zhang Z, 2002. Acomparison of land use and land cover change detection methods. In Proceedings, ASPRS-ACSM Annual Conference and FIG XXII Congress, American Society for Photogrammetriy & Remote Sensing, 10. Bethesda, MD.

Congalton R G, and Green K, 1993. A practical look at the sources of confusion in error matrix generation. Photogrammetric Engineering and Remote Sensing 59 (5): 641–644. http://cat.inist.fr/?aModele=afficheN&cpsidt=4739878.

Congalton, Russell G. 1991. A Review of Assessing the Accuracy of Classifications of Remotely Sensed Data. Remote Sensing of Environment 46 (October 1990): 35–46.

Congalton R G, 2005. Thematic and positional accuracy assessment of digital remotely sensed data. In proceedings of the seventh annual forest inventory and analysis symposium, 149–154.

Das T, 2009. Land Use / Land Cover Change Detection : an Object Oriented. http://www.igeo.pt/gdr/pdf/Tese_Tanmoy_Das.pdf.

Fung T and LeDrew E, 1987. Application of Principal Components Analysis to Change Detection. Photogrammetric Engineering and Remote Sensing Remote Sensing 53: 1649–1658.

Geza M and McCray J E, 2008. Effects of Soil Data Resolution on SWAT Model Stream Flow and Water Quality Predictions. Journal of Environmental Management 88 (3): 393–406.

Green W H and Ampt G A, 1911. Studies on Soil Physics, J. Agric. Sci., 4(1), 1 – 24. Journal of Agricultural Science 4 (1): 1–24.

Haralick R M and Shapiro L G, 1985. Image Segmentation Techniques. Computer Vision, Graphics, and Image Processing 29 (1): 100–132.

Hodgson, Michael E, John R Jensen, Jason A Tullis, Kevin D Riordan, and Clark M Archer. 2003. "Synergistic Use of Lidar and Color Aerial Photography for Mapping Urban Parcel Imperviousness." Photogrammetric Engineering and Remote Sensing 69 (9): 973–980.

Howell K J and Green R O, 1987. AVIRIS User's Guide. URL: ftp://popo.jpl.nasa.gov/pub/docs/workshops/95_docs/29.PDF . Date accessed: August, 2011

Jacobson, I., 1992. Object Oriented Software Engineering: A Use Case Driven Approach, Addison-Wesley, 43-69.

James, L. D., and Burgess S. J. 1982. "Selection, Calibration and Testing of Hydrologic Models." In Hydrologic Modelling of Small Watershed.

Jensen, John, R. 2005. Introductory Digital Image Processing. 3rd ed. Upper Saddle River, NJ: Prentice Hall.

Kepner W G, Semmens D.J., Hernandez M. and Goodrich D C, 2013. Evaluating hydrological responses to forecasted land use change. North American Land-Cover Summit. URL: http://www.aag.org/galleries/nalcs/CH15.pdf. Date accessed: January 2013

Koch F J, van Griensven A, Uhlenbrook S, Tekleab S., Teferi E., 2012. The effect of land use change on hydrological responses in the Choke mountain range (Ethiopia) - A new approach addressing land use dynamics in the model SWAT. 2012 International Congress on Environmental Modeling and Software. URL: http://www.iemss.org/sites/iemss2012//proceedings/I4_0780_Koch_et_al.pdf. Date accessed: May 2013

Kumar S, and Merwade V, 2009. Impact of watershed subdivision and soil data resolution on swat model calibration and parameter uncertainty. Journal of American Water Resources Association 45 (5): 1179–1196.

Laliberte A S, Rango A, Havstad K M, Paris J F, Beck R F, McNeely R, and Gonzalez A L, 2004. Object-oriented image analysis for mapping shrub encroachment from 1937 to 2003 in southern New Mexico. Remote Sensing of Environment 93 (1-2) (October): 198–210. doi:10.1016/j.rse.2004.07.011. http://linkinghub.elsevier.com/retrieve/pii/S0034425704002147.

Lambin E F, Rounsevell M, and Geist H, 2000. Are Current Agricultural Land Use Models Able to Predict Changes in Land Use Intensity? Agriculture, Ecosystems & Environment (1653): 1–11.

Lang S. 2008. Object-based Image Analysis for Remote Sensing Applications: Modeling Reality – Dealing with Complexity. Earth and Environmental Science: 3–27. doi:10.1007/978-3-540-77058-9_1.

Lefebvre A, Corpetti T and Hubert-Moy L, 2008. Object-oriented approach and texture analysis for change detection in very high resolution images. Geoscience and Remote Sensing symposium, Boston, Massachusetts , 4: 663 - 666

Lillesand, T M, Riera J, Chipman J, Gage J, Janson M, Panuska J, and Webster K, 2001. Integrating Multiresolution Satellite Imagery into a Satellite Lake Observatory. In Proceedings, Annual Meeting of the American Society for Photogrammetry and Remote Sensing. St. Louis, MO.

Maas J F, 1999. Monitoring Land-cover Changes: a Comparison of Change Detection Techniques. International Journal of Remote Sensing 20 (1): 139–152.

Mather P M, 1987. An Introduction. In Computer Processing of Remotely-Sensed Images, 206–209. Chichester, New York, Weinheim, Brisbane, Singapore, Toronto: John Wiley & Sons, Inc. ftp://ftp.ecn.purdue.edu/jshan/ce697v/project 1/Hather_pages.pdf.

Miller S N, Guertin D P and Goodrich D C, 2007. Hydrologic Modeling Uncertainty resulting from land cover misclassification. Journal of the American Water Resources Association (JAWRA) 43(4):1065-1075. DOI: 10.1111⁄j.1752-1688.2007.00088.x

Mukundan R, Radcliffe D E and Risse L M, 2010. Spatial Resolution of Soil Data and Channel Erosion Effects on SWAT Model Predictions of Flow and Sediment. Journal of Soil and Water Conservation 65 (2) (March 24): 92–104. doi:10.2489/jswc.65.2.92. http://www.jswconline.org/cgi/doi/10.2489/jswc.65.2.92.

NASA-JPL, 2012. Airborne Visible Infrared Imaging Spectrometer (AVIRIS). URL: http://aviris.jpl.nasa.gov/index.html. Date accessed: June, 2012.

Neitsch, S L, Arnold J G, Kiniry J R, Srinivasan R and Williams J R, 2005. Soil and Water Assessment Tool Theoretical Documentation, Version 2005. Temple, TX: Grassland, Soil and Water Research Laboratory, Agricultural Research Service. Available a.

NELSON R F, 1983. Detecting forest canopy change due to insect activity using Landsat MSS. Photogrammetric Engineering and Remote Sensing, 49, 1303-1 3 14.

Niemeyer I and Canty M J, 2003. Pixel-based and Object-oriented Change Detection Analysis Using High-resolution Imagery. http://esarda2.jrc.it/db_proceeding/mfile/P_2003_Stockholm_062-a-niemeyer.pdf.

Platt R V and Rapoza L, 2008. An evaluation of an object-oriented paradigm for land use / land cover classification. The Professional Geographer 60 (1): 87–100.

Quattrochi D, Luvall J, Rickman D, Estes M, Laymon C, Howell B, 2000. A decision support system for urban landscape management using thermal infrared data, Photogrammetric Engineering and Remote Sensing, 66(10), 1195-1207

Ryherd S and Woodcock C E, 1996. Combining Spectral and Texture Data in the Segmentation of Remotely Sensed Images. Photogram- Metric Engineering b Remote Sensing 62: 181–194.

Schowengerdt R A, 1997. Remote Sensing: Models and Methods for Image Processing. Academic Press.

Schultz G A, 1988. Remote Sensing in Hydrology. Journal of Hydrology 100.

Scott J M, Davis F, Csuti B, Noss R, Butterfield B, Groves C, Anderson H, Caicco S, D'Erchia F, Edwards T C Jr., Ulliman J and Wright R G, 1993. Gap analysis: a geographical approach to protection of biological diversity. Wildlife Monographs 123.

Singh A, 1989. Digital Change Detection Techniques Using Remotely Sensed Data. International Journal of Remote Sensing 10(6), 989-1003

Stohlgren T J, Chase T N, Pielke R A Sr., Kittel T G F and Baron J S, 1998. Evidence That Local Land Use Practices Influence Regional Climate , Vegetation , and Stream Flow Patterns in Adjacent. Global Change Biology 4: 495–504.

Story M and Congalton R G. 1986. Accuracy Assessment: a User's Perspective. Photogrammetric Engineering and Remote Sensing 52: 397–399.

Sullivan D G, Shaw J N, Mask P L, Rickman P, Guertal E A, Luvall J and Wersinger J M, 2004. Evaluation of multispectral data for rapid assessment of wheat straw residue cover. Soil Science Society of America Journal, 68: 2007–2013.

Tanathong S, Rudahl K T and Goldin S E, 2009. Object-oriented change detection of buildings after a disaster. ASPRS 2009 Annual conference. Baltimore, Maryland, USA

Tecuci G, 1998. Building Intelligent Agents: An Apprenticeship, Multistrategy Learning Theory, Methodology, Tool and Case Studies, Academic Press, 1-178.

Tong S T Y and Chen W, 2002. Modeling the Relationship Between Land Use and Surface Water Quality. Journal of Environmental Management 66 (4) (December): 377–393. doi:10.1006/jema.2002.0593. http://linkinghub.elsevier.com/retrieve/pii/S0301479702905931.

U.S. Department of Agriculture - Soil Conversation Service (USDA-SCS). 1972. Estimation of Direct Runoff From Storm Rainfall. U.S. Department of Agriculture, Soil Conservation Service, Washington, D.C., Pp. 10.1-10.24. SCS National Engineering Handbook, Section 4, Hydrology. Chapter 10.

USDA-FSA, 2011. National Agriculture Imagery Program (NAIP). http://www.fsa.usda.gov/FSA/apfoapp?area=home&subject=prog&topic=nai. Date Accessed: May 2011

USDA-NAPP, 2012. National Aerial Photography Program (NAPP). URL: https://lta.cr.usgs.gov/NAPP. Date Accessed: January 2012

Wegehenkel M, Heinrich U, Uhlemann S, Dunger V and Matschullat J, 2006. The Impact of Different Spatial Land Cover Data Sets on the Outputs of a Hydrological Model: a Modelling Exercise in the Ucker Catchment, North-East Germany. Phys. Chem. Earth 31: 1075–108.

Weiss N and Barr S, 2009. Environment and Society : Sustainability , Policy and the Citizen. 4 (1): 105–106.

White K L and Chaubey I, 2005. Sensitivity analysis , calibration , and validations for a multisite and multivariable SWAT model. Journal of American Water Resource Association 72701: 1077–1089.

Williams J R, 1969. Flood Routing with Variable Travel Time or Variable Storage Coefficients. Transactions of the ASAE 12 (1): 100–103.

Wenchun W and Shao G, 2002. Optimal Combinations of Data, Classifiers, and Sampling Methods for Accurate Characterizations of Deforestation. Canadian Journal of Remote Sensing 28 (4): 601–609.

Yan G, 2003. Pixel Based and Object Oriented Image Analysis for Coal Fire Research."

Yuan D and Elvidge C, 1998. NALC Land Cover Change Detection Pilot Study: Washington D.C. Area Experiments. Remote Sensing of Environment 66: 166–178.

CHAPTER 3: OBJECTIVE ONE

ABSTRACT

The aim of this study is to evaluate the respective impacts of high-resolution land-use land-cover (LULC) data classified with the Object-Oriented Image Analysis (OOIA) method and a relatively lower-resolution LULC data classified with the maximum-likelihood method on stream-flow predictive reliability of the Soil and Water Assessment Tool (SWAT) model. In essence, the objective was to investigate how the model performs with methods of LULC data classification and LULC data type resolution. The predictive reliability of the model as used in this study is primarily evaluated with two descriptive statistic measures; the p-factor and the r-factor. The p-factor is used to quantify the percentage of the observed data that a calibrated model is able to capture whiles the r-factor quantifies the level of uncertainty associated with the calibrated model. Statistically, the r-factor measures the thickness of the uncertainty band around the best possible model simulation divided by the standard deviation of the observation values. The hypothesis was that a combination of GIS-based hydrologic modeling and the promise of LULC data obtained from object-oriented image classification method significantly improve SWAT flow predictive reliability. Two SWAT models were set-up and calibrated at a gaging station located within the study area. The study area is the Little Red River Watershed (LRRW) with an approximate area of close to 4700km^2 located in the north-central portion of Arkansas within the Fayetteville Shale Play. After manual and auto-calibration, results showed that the high-resolution data classified with object-oriented image analysis method does not present any significant advantage in terms of predictive reliability.

Keywords: *SWAT modeling, land-use land-cover, remote sensing, high and low-resolution.*

3.0 Introduction

The object-oriented image analysis method (Baatz et al., 2001) is a method of land-use land-cover (LULC) classification that was developed to optimize classification accuracy by utilizing the inherent spectral characteristics and image resolution of remotely sensed images. This method has been shown to yield better results in studies regarding LULC change analyses (Gao, 2003; Rutherford and Platt 2008). The resultant classified image can be ultimately used in investigations concerned with the corresponding environmental impacts such as changes on the hydrologic balance of watersheds.

The change to the hydrologic balance can be assessed using hydrologic modeling methods (Conly and van der Kamp, 2001; Peterson et al., 2000; Zhang et al., 1999). Also, results of hydrologic models such as the Soil and Water Assessment Tool (SWAT) (Arnold et al., 1998) have been shown to be affected by the input LULC data (Bosch et al., 2004; Huang et al., 2013). However, there is a lack of assessment of the resolution and methods of LULC data classification on SWAT model simulations particularly in a shale-gas impacted watershed. The objective of this study is to evaluate the impact of LULC data method of classification performed on imagery of different spatial resolutions on the predictive reliability of SWAT flow models. Specifically, this study aims to show the difference (if any) in the predictive reliability of SWAT flow models simulated with high resolution LULC data that is classified with the object-oriented image analysis method and low-resolution LULC data classified with the maximum-likelihood method in a shale-gas impacted watershed.

3.1 Background and Significance

Generally, research on the effect of high-resolution LULC input data on various SWAT outputs seem to show that, high-resolution data do not necessarily result in better SWAT stream-flow simulations (Chen et al., 2005). This result may arise in part from the fact that traditional pixel-based image classification methods designed for low-resolution images are not well-suited to deal with the spectral variance inherent in higher resolution images. More modern computer-vision based classification methods have shown great potential and one, object-oriented image analysis (OOIA) method, has been used extensively in small and large scale studies (Laliberte et al., 2004; Rutherford and Platt, 2008).

This method is based on a hierarchical, multi-scale segmentation and subsequent classification using shape, texture and spectral properties of the segmented image. OOIA is particularly optimized for high-resolution data with particular emphasis on spatial and spectral homogeneity of the underlying data. Although the differential effect of high or low-resolution LULC data on SWAT outputs has been studied (Bosch et al., 2004), we are currently not aware of any study that deals with the impact of the respective classification methods and how the accuracy with which the respective methods of classification can be used to correctly extract land use related to local LULC changes such as shale-gas-related infrastructure (Myint et al., 2011) affect the reliability of model outputs.

Several studies have reported that combined with high-resolution data, OOIA produces LULC data of significantly better classification accuracy than traditional pixel-based maximum-likelihood (PBML) methods (Devi and Krishna, 2012; Pham et al., 2009; Yan, 2003). Furthermore, it is also known that the relative increase or decrease in a particular land-use class can have significant impacts on distributed hydrologic model results. For instance Wegehenkel et

al. (2006) found that a two percentage increase (2.9% to 4.9%) in the developed land class of a watershed resulted in 70% increase in the surface runoff predictions in their study. This implies, in particular reference to this study that, it is important to consider the spatial resolution, accuracy and the method of classification of LULC data in evaluating the model's predictive reliability based on LULC datasets obtained from high and low-resolution imagery and classified with different methods (in this case the object-oriented and pixel-based methods respectively).

In considering major economic activities that drive LULC changes in this study, general agriculture and urbanization activities have in addition to the increase in shale-gas related activities resulted in significant LULC change in the general area of the Fayetteville Shale Play (FSP) located in north-central Arkansas. Such LULC change has also been shown to have negative impacts on stream water quality (Tang et al., 2005; Zampella et al., 2007) and water quantity (Bronstert et al., 2002; White and Greer, 2006).

Albeit there have been rapid changes in LULC mostly related to urban, residential, commercial and agricultural activities, higher projected economic growth rate for the counties with oil and gas operations (Deck and Riiman, 2012) can lead to land-cover changes that will be exacerbated as well. Land-cover change in forested watersheds mostly leads to the exposure of the land; this is known to have negative impacts such as decreased water quality, increase runoff velocity and volume, reduced groundwater recharge, greater peak flows, increased flood frequency etc. (Scanlon et al., 2005; Carlson and Arthur, 2000; Pitman and Narisma, 2004). The increase in shale-gas related activities requires that studies be done on the respective shale-plays to determine an adequate balance between the need for the energy resource whilst sustaining minimal change to the watershed's hydrology. This requires the development of accurate hydrologic models to study the impacts of several LULC change scenarios on stream flow. To

achieve this there is the need to investigate the applicability of methods, input data and the hydrologic models to be used in such settings.

3.2 Study Area Description

Located in north-central Arkansas, the Little Red River watershed (LRRW) is one of the biggest watersheds which see significant activities from shale-gas operators in the Fayetteville Shale Play. The watershed is completely located within the Fayetteville Shale play and is approximately 4668km^2 in area with roughly 70% of this area being classified as mixed forest land (CAST, 2006). The area has an average annual precipitation range of 1270 – 1320 mm with winter and summer average temperatures of 2^{o}C and 30^{o}C respectively. Mean annual high and low temperatures are 5^{o}C and 17^{o}C respectively (NOAA, 2012). Precipitation normally occurs less frequently during the months of June, July and August; summers are hot and humid while winters are relatively mild and short. A 2006 LULC analysis revealed that the watershed is approximately 70% forest land, 16% pasture, 2% cropland, 3.69% Urbanized, 3.33% water and 5% herbaceous (CAST, 2006). There are three main population centers within the watershed; namely Searcy, Heber Springs and Clinton with population density of 44 persons per square mile (CAST, 2006); averaged for the combined area of the three counties encompassing the centers. The watershed lies within the physiographic regions of Mississippi Alluvial Valley, Arkansas River Valley and Ozark Plateaus, with an elevation range of roughly 52 to 630 m respectively. The Ozark Plateau Region is made up of steep valleys; it is further divided into three broad plateau surfaces (Springfield Plateau, Salem Plateau and Boston Mountains) mainly based on elevation and age of surface rock. The Arkansas Valley is a low-lying region surrounding the valley of the Arkansas River and the Mississippi Alluvial Valley which is relatively level plain

land (Arkansas Geological Survey, 2012). The main river in the watershed is the Little Red River which flows in a mainly south-east direction.

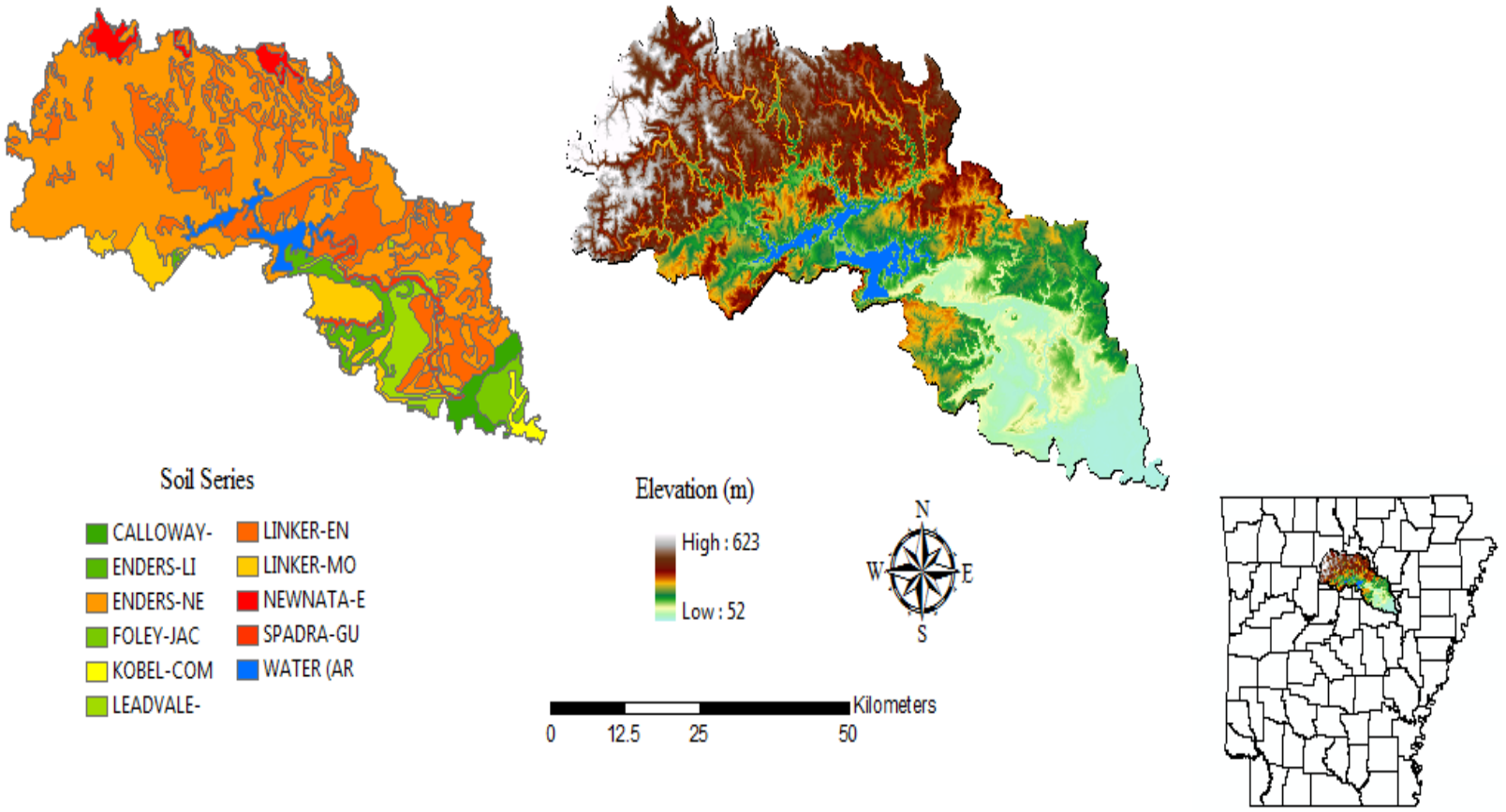

Figure 1: Soils and elevation characteristics of the study area: Little Red River Watershed (LRRW)

3.3 Methodology

To determine the impact of high and low-resolution LULC data and their respective methods of classification on SWAT flow model predictive reliability in a shale-gas watershed, we used a combination of Geographic Information Science (GIS), digital image analysis and hydrologic modeling.

3.3.1 Image Classification

Two main datasets were used as the input LULC data for the LRRW flow models. A low-resolution (28.5m) data produced by the University of Arkansas Center for Advanced Spatial Technologies (CAST) through maximum-likelihood classification from a 2006 Landsat 5 thematic mapper UTM orthorectified imagery and a high-resolution (4 m) LULC data classified with object-oriented image analysis acquired from a 2006 National Agricultural Imagery Program (NAIP) orthorectified aerial imagery. This pixel-based maximum-likelihood method essentially identifies the class of each pixel by comparing the value of individual pixels with sampled training classes and assigns the pixel to a specific class based on a set algorithm (Lillesand et al., 2004). The map which was created from the Landsat 5 TM data depicts the land cover of the study area and was considered to represent current conditions. The classification was obtained from Landsat 5 TM scenes of the watershed with the following classes; agriculture, urban, forest, crops, water and grasses.

The high-resolution (4 m) LULC data was derived from the National Agricultural Imagery Program (NAIP) aerial imagery of 1 m pixel size that was resampled to 4 m and classified with object-oriented image analysis method using Trimble eCognition Developer 8 (Trimble, 2012). Object-oriented image analysis incorporates a multi-scale segmentation approach that groups

pixels into homogenous image objects based on defined shape, texture, spatial and spectral characteristics of the pixels (Baatz et al., 2001). This approach results in discrete regions that are spectrally and spatially homogenous and allows for the identification of object features at specific scales of segmentation. Homogeneity in this regard refers to the fact that the spectral variance within an object is less than the spectral variance between objects (Laliberte et al., 2004). A segmentation procedure known as multi-resolution segmentation based on defined scale parameters was used. The scale of a particular segmentation process determines the size of objects created at that scale. Through a trial and error method, we determined appropriate parameter values for scale, compactness and smoothness for four main levels of segmentation; 350, 150, 35 and 5 (depending primarily on scale).

The objective of the classification at level 350 of the object hierarchy was to determine the largest size of objects in the imagery that represent the aggregated homogenous pixels. The subsequent levels of segmentation were determined to break down the super objects at the previous scale in order to attain objects of interest belonging to specific classes of interest for accurate classification. In general, classifications of segmented objects into their respective classes were done by an assignment classification based on the mean spectral properties of the various image channels, specific homogeneity criteria and thematic data attribute values. Other classification rules were determined by using either the nearest-neighbor or membership function classifier based on fuzzy-logic and supplemented with user supplied knowledge. For example, the classification of urban area and road networks were aided with a thematic layer containing urban areas and road networks within the area of classification. The land-use classes were broadly categorized to include all the classes as used in the low-resolution data; which are agriculture, barren, forest, roads, transitional, urban and water.

The most common measures of accuracy assessment in classified remotely sensed imagery are the producer, user and overall accuracy (Story and Congalton, 1986); all based on the error or confusion matrix. The error matrix is simply a square array of numbers set out in rows and columns to express the number of pixels assigned to a particular classification category in relation to the actual category as seen on the ground (Congalton, 1991). A maximum of 30 sample objects were selected for each classification category for the creation of test and training area (TTA) mask. The TTA mask (which essentially represents ground reference data) was used to generate an error matrix for accuracy assessment in eCognition software.

3.3.2 SWAT Model Description

SWAT is a physically based and continuous time semi-distributed parameter model that is developed to simulate the effects of land management practices on water, sediment, and agricultural chemicals in large and complex watersheds over long periods of time (Arnold et al., 1998). The version of the model that was used for this study is SWAT2009; an ArcGIS extension (ArcSWAT) that provides a graphical user interface for SWAT was used as a means of coupling the modeling framework within a GIS. Albeit newer versions of SWAT were available, we used this version due to GIS software compatibility issues and also the fact that the newer versions did not include significant changes in flow simulation. The model requires input data in DEM, land use data, soils and slope classes for the delineation of Hydrologic Response Units (HRUs). HRUs are created through an overlay of respective slope classes, soils and land-use data. Aggregations of overlays of the same slope class, land-use and soil type are grouped into the same HRU. Figure 2 illustrates the creation of HRUs in the ArcSWAT environment.

The HRU is the basic computational unit of the model and helps to ensure efficient computation. SWAT simulates the hydrology at each HRU using the water balance equation, comprising

precipitation, runoff, evapotranspiration, percolation and base flow components. Runoff is computed with either the Soil Conservation Service Curve Number method (USDA-SCS, 1972) or the Green and Ampt infiltration method (Green and Ampt, 1911) and routed to the closest channel using the Muskingum method (Chow, 1959).

3.3.3 SWAT model setup

The models were was set-up in a GIS framework with the ArcSWAT extension of SWAT version 2009 is as shown in figure 4. The watershed was delineated based on an input 10 m digital elevation model (DEM). Soils data for all the counties in the study area were obtained from the Soils Survey Geographic database (SSURGO) of the Natural Resources Conservation Service (NRCS). The respective high and low-resolution LULC input data models were subsequently divided into hydrologic response units (HRUs) with specific threshold values based on soils, slope and land-use. These thresholds were obtained through a trial and error procedure to pick the optimum values for the data categories so as to ensure that significant areas of land-use and soils are not excluded and insignificant areas are not included; thus reducing computational overhead and presenting the most likely accurate representation of the watershed in the model. To ensure that the land-cover classes were uniform in both datasets, the land-use refinement option in the HRU definition component was used to refine the land-use categories in both models. The overlay of soil, slope and land-use and subsequent HRU definition operation resulted in the creation of a total of 735 and 367 HRUs for high and low-resolution LULC data models respectively. SWAT formatted observed daily rainfall and temperature data from 1950 to 2010 were obtained from the United States Department of Agriculture's Agricultural Research Service (USDA-ARS) climate database (USDA-ARS, 2012) for the weather stations shown (figure 3). Greers Ferry Lake, located in the mid-section of the watershed was simulated as a

reservoir with estimated monthly outflow derived from the reservoir daily outflow data. This data was obtained from the National Inventory of Dams database of the United States Army Corps of Engineers (NID-USACE, 2011).

A third model was added purposely to further evaluate and place the analysis in a broader perspective in terms of the results of the above-described data and in respective of the methods of classification. This model was set-up with LULC obtained from the 2006 National Land Cover Data (NLCD). The NLCD LULC is a 30 m Landsat 6 enhanced thematic mapper+ (ETM+) with classification based on unsupervised classification method (NLCD2006, 2011). The models were calibrated from 1997 to 2006 and validated from 2007 to 2009 with the data from January-1997 to December-1999 serving as the period for computation of model initial (warm-up period) parameters.

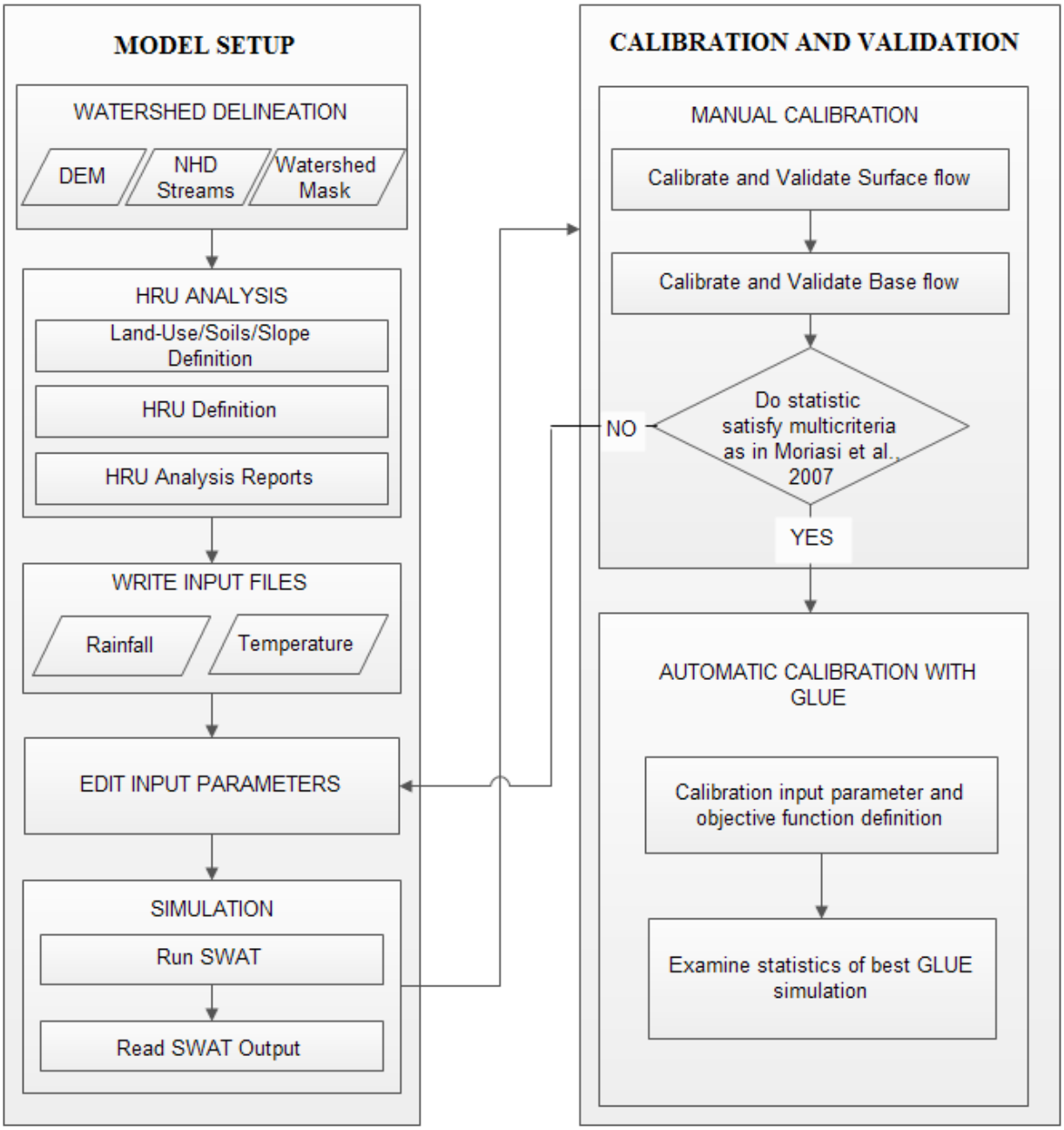

Figure 4: Workflow of modeling framework

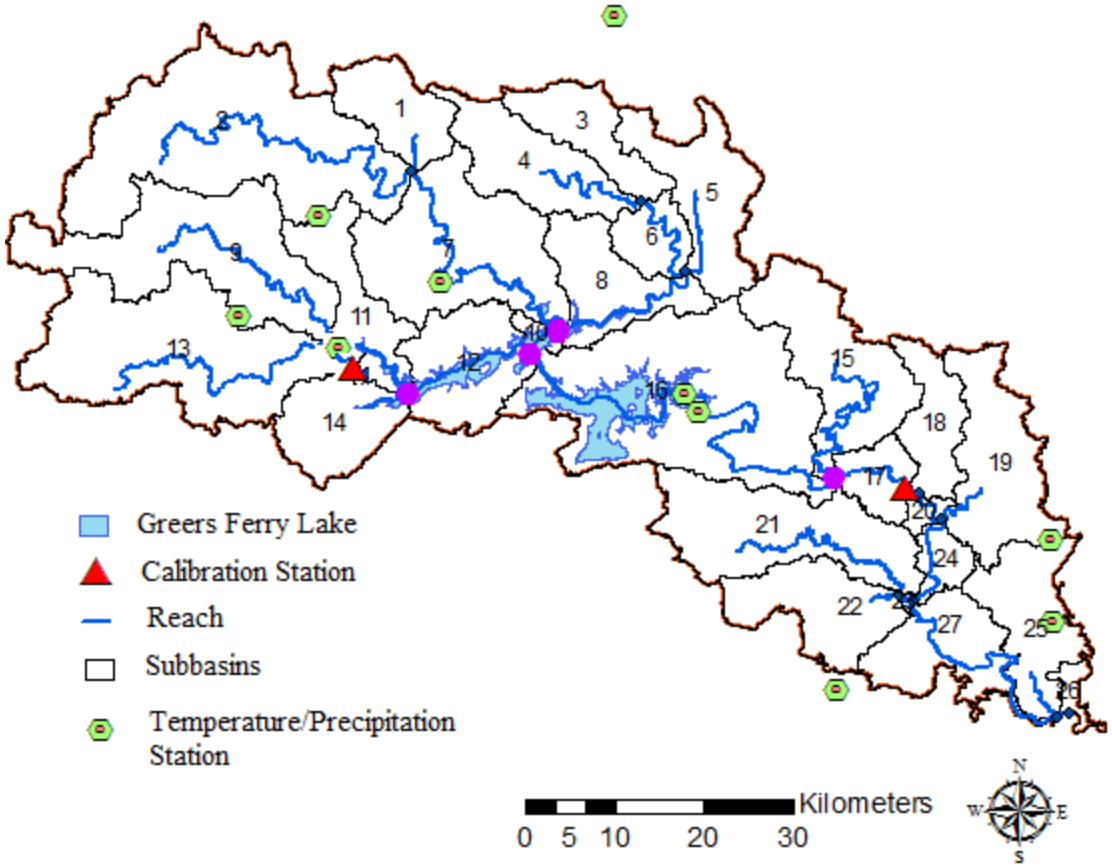

Figure 5: General model Set-up parameter and features

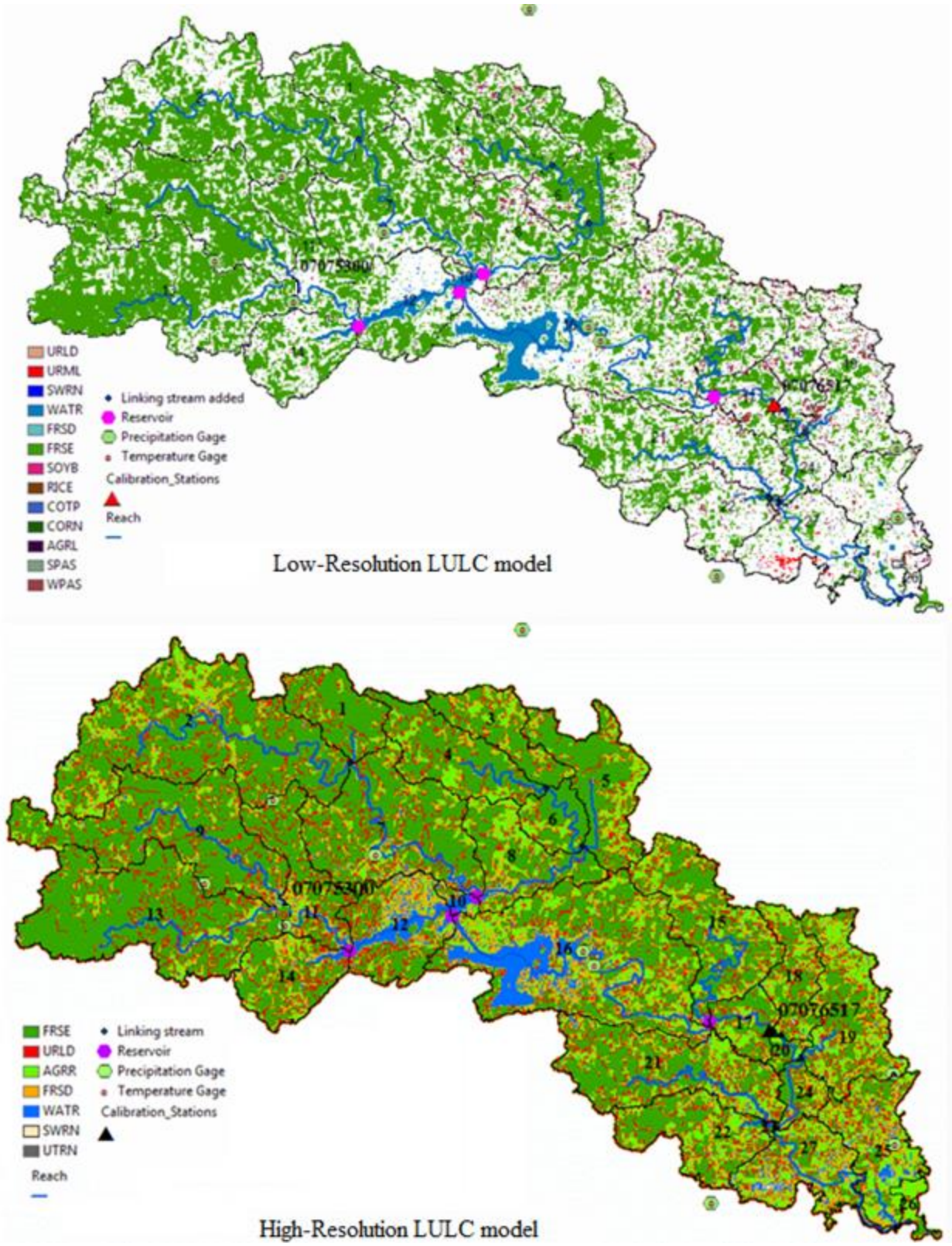

Figure 6: Low and High-Resolution LULC data models after model set-up

3.3.4 Model Calibration

The model was calibrated against observed data obtained from January 1997 to December 2009 for the calibration station located near Dewey, AR with USGS station number 07076517 (indicated on study area map with red triangle). For manual calibration, parameters identified from literature to be sensitive to flow were iteratively changed till the simulated output satisfied the best fit scenario as defined by the multi-criteria in Moriasi et al., (2007). According to Moriasi et al., (2007), model simulations for stream-flow are determined to be satisfactory if NSE > 0.5 and PBIAS = ± 25%. The stages and steps for the model calibration are as shown in figure 2. Total-flow is expressed in SWAT as a combination of surface-flow and subsurface-flow components. A base-flow filter program obtained from the SWAT model website was used to separate observed total stream-flow into surface and subsurface components for calibration purposes. This program uses an automated base-flow separation method using a digital filter which has been tested to be comparable to manual hydrograph separation methods with an efficiency of 74% (Arnold et al., 1995).

Calibration was sequentially performed on surface-flow and base flow components. Parameters identified to be sensitive to surface-flow from literature search were canopy maximum storage (CANMX), soil evaporation compensation factor (ESCO), curve number, threshold depth in the shallow aquifer required for return flow to occur (GWQMIN), soil available water content (AWC) etc, (White and Chaubey, 2005; Betrie et al., 2011). We further performed sensitivity analysis to verify the above literature identified flow sensitivity parameter as we could not locate any such study done in a shale-gas impacted watershed. Surface-flow calibration was subsequently followed by subsurface-flow calibration.

Auto-calibration was added to the modeling protocol after manual calibration. In models such as SWAT, no one set of parameter values can be considered as the optimum parameter set as there are several sets of parameter values that can provide an "acceptable" fit for the objective function. This problem is known as equifinality (Beven and Binley, 1992). To account for this problem, a method known as generalized likelihood uncertainty estimation (GLUE) (Beven and Binley, 1992) is applied.

GLUE is coupled with SWAT in a software of uncertainty estimation programs known as SWAT-CUP (SWAT Calibration and Uncertainty Programs), (Abbaspour, 2011). The basic approach of the GLUE program is to estimate uncertainties associated with model predictions through the prior determination of respective probabilities associated with each individual parameter set which are all part of a large collection of parameter sets. The exact algorithm as implemented in the coupling of GLUE with SWAT can be found in Abbaspour (2011). The Nash-Sutcliffe efficiency (NSE) criterion of model performance evaluation was selected as the objective function with a threshold value of 0.5 and a maximum number of 7000 GLUE simulations for both models respectively.

3.4 Results

3.4.1 Image Classification

During the image classification stage, only object-oriented image analysis was performed as the low-resolution LULC data obtained from the University of Arkansas Center for Advanced Spatial Technologies (CAST) was classified with the pixel-based maximum-likelihood classification method. The pixel-based method operates at the pixel level and does not involve the incorporation of any user supplied knowledge of the inherent spectral and spatial difference in the scene. The primary classifier uses the optimized feature space spectral variances. The

relative proportion of the total watershed area occupied by each class category as determined from each classification method is presented in table 2.

Table 2: Percentage of the total watershed area occupied per class from both methods

CLASS NAME	PIXEL-BASED	OBJECT-ORIENTED
Agric	17.80	20.26
Barren	0.07	0.002823
Forest	75.17	70.45
Water	3.31	4.32
Urban	3.65	4.97

3.4.2 Accuracy Assessment

The low-resolution classified data had a reported overall classification accuracy of roughly 88%; however to derive the respective user's and producer's accuracy measures, the classified data was reassessed for accuracy with a minimum of 30 selected reference points per class in the original image and was subsequently used as ground-truth data to derive the error matrix (Gorham, 2013). Further information concerning accuracy assessment of the low-resolution data can be obtained from CAST (2007).

For the object-oriented image analysis, we used the test and training area utility embedded in eCognition software with random sampling of a minimum of 30 training areas per class for accuracy assessment. Training areas were selected for each classification category and used as the ground reference data. Accuracy assessment was evaluated in terms of the user's, producer's and overall accuracies. The user's and producer's accuracies were above 70% for all classes except the agriculture class which had the lowest accuracy in both measures. The average user's and producer's accuracies were approximately 78% and 86% respectively. The overall classification accuracy was also approximately 86% as compared to 88% of the low-resolution data classification. The respective error matrices are presented in Tables 3 and 4.

Table 3: Error matrix for accuracy assessment of object-oriented classification

User \ Reference	Forest	Urban	Agriculture	Transitional	Water	Barren	Roads	Sum
Forest	6113	1	802	274	0	9	64	7263
Urban	0	5236	0	350	0	3	277	5866
Agriculture	299	774	3978	236	160	66	136	5649
Transitional	255	0	9	2479	0	0	74	2817
Water	0	0	2	0	9491	127	0	9620
Barren	0	0	0	0	0	219	0	219
Roads	52	154	806	78	0	57	3206	4353
Sum	6719	6165	5597	3417	9651	481	3757	
Accuracy								
Producer	0.910	0.849	0.711	0.725	0.983	0.455	0.853	
User	0.842	0.893	0.704	0.880	0.987	1.000	0.737	
Overall	0.858							
KIA($\bar{K}$)	0.826							

Table 4: Error matrix for accuracy assessment of maximum-likelihood classification

User \ Reference	Agriculture	Forest	Urban	Roads	Transitional	Barren	Water	Sum
Agriculture	33903	0	8324	1766	3631	73	332	48029
Forest	0	32957	719	0	1132	0	0	34808
Urban	0	0	18797	0	0	0	356	19153
Roads	0	0	797	155	0	0	0	952
Transitional	0	4199	0	0	19285	0	736	24220
Barren	0	0	0	0	0	128	0	128
Water	0	0	0	0	1374	0	28541	29915
Sum	33903	37156	28637	1921	25422	201	29965	151205
Accuracy								
Producer	1.000	0.887	0.656	0.081	0.759	0.637	0.952	
User	0.706	0.947	0.981	0.163	0.796	1.000	0.952	
Overall Accuracy	0.885							
KIA($\bar{K}$)	0.853							

To determine if the values for the respective overall accuracies were significantly different (statistically significant), the Kappa index of agreement (KIA) and a pairwise Z-score test (Congalton and Green, 1999; Weih and Riggan, 2013) were calculated for both methods of classifications based on the following equations.

$$\overline{K} = \frac{\mathrm{Po} - \mathrm{Pc}}{1 - \mathrm{Pc}}$$

$$Z = \frac{\left|\overline{\mathrm{Ka}} - \overline{\mathrm{Kb}}\right|}{\sqrt{var(\overline{\mathrm{Ka}}) + var(\overline{\mathrm{Kb}})}}$$

Where Po and Pc are the respective overall and chance classification measures, $\overline{K}$ is the kappa index (with a and b subscripts designating the respective error matrix measures) and $var(\overline{\mathrm{Ka}})$, $var(\overline{\mathrm{Kb}})$ are the respective variances related to the two kappa indices. The KIA index measures the agreement between two observed and predicted values and is also used to determine whether the agreement is by chance; the index ranges from 0 to 1 with values closer to 0 indicating chance agreement (Congalton and Green, 1999). KIA values that are higher than 0.8 represent a strong agreement between the classified and the reference data while those between 0.4 and 0.8 indicate moderate agreement (Congalton and Green, 1999; Congalton, 2005).

For the low-resolution data classification, the derived KIA was 0.85 while that for the high-resolution object oriented classification was 0.82. This indicates a slightly stronger agreement between the maximum-likelihood method classification and reference samples than the object-oriented method and its corresponding reference data. Additional calculations were performed on variances relative to the kappa statistic using a method outlined in (Congalton and Green, 1999) and obtained values of 0.23 and 0.16 for the object-oriented and maximum-likelihood methods

respectively. This further showed that the maximum-likelihood classification yielded a slightly better agreement with the reference data.

In comparing the two methods by their respective error matrices, the pairwise Z-value computed from the stated equation was 0.032 which is less than 1.96, taking a confidence level of 95% on the standardized normal distribution. This shows that there is no statistically significant difference (at the 95% confidence level) between the classification methods as applied in this study.

3.4.3 Image Classification Discussion

The feature space optimization algorithm of the maximum-likelihood method results in pixels that are spectrally more homogenous within a specific class than they are to other classes. Therefore the classification is based on pixels within a land-cover class that are spectrally similar in the feature space. However, this is not always true in complex environments (Burnett and Blaschke, 2003) like in our study area. This is seen in the pixel-based method classified data in figure 7. It can be seen that spatial continuity of the classified classes is not as strong as that of the object-oriented classified image on the left. This is also attributable to the fact that no spatial relationship is used in the maximum-likelihood classification method. Another feature which is apparent from the pixel-based classified image is that the data appears to depict more isolated pixels are classes within the land surface. This effect known as the "salt and pepper effect" (Lang et al., 2006) arises from the fact that pixels are potentially classified differently but that they may actually belong to the same class. Thus as this method accounts for spectral autocorrelation, the lack of spatial knowledge in the classification algorithm potentially leads to wrongful classification. This is eliminated in the object-oriented classified image through segmentation.

Segmentation in the object-oriented classification uses spatial, textural, shape and spectral information to group pixels into object for subsequent classification. This increases the probability of a reference pixel being accurately classified (producer accuracy). The forest cover therefore had the highest producer's accuracy (table 3) due in part to the fact that the watershed is predominantly forested and was well aggregated than the other classes based on the previously stated factors used in the segmentation. This also in part, explains the low producer's accuracy obtained for the barren land class (table 3). Another reason for this low value for the barren class is that the barren land bears similar spectral, spatial and textural qualities to the urban class.

However in this study the similar overall accuracy values obtained from both methods of classification represent a marked difference from studies such as Gao (2003) and Rutherford and Platt (2008) that reported significantly higher accuracies for the object-oriented method than the pixel-based method. Generally, the object-oriented image classification method is known to offer higher overall classification accuracy. This departure from the general trend could be as a result of the lack of heterogeneity in the greater percentage of the study area. As mentioned the study area is predominated forested, therefore an approach such as the object-oriented method as used in this study with a ruleset which optimizes characteristic of the scene with a much higher precedence than the spectral signature may not prove significantly advantageous.

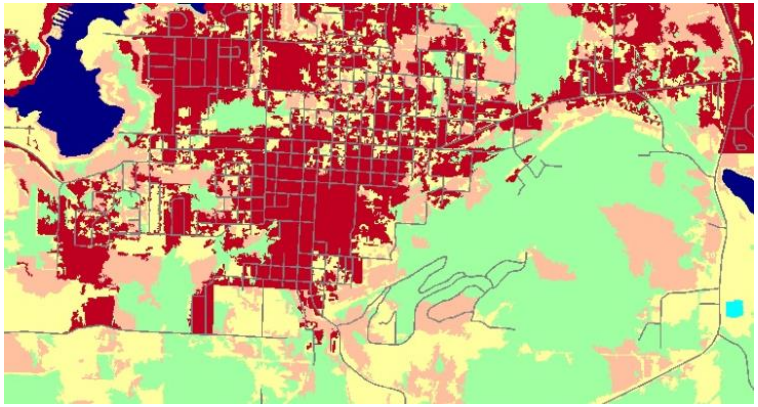

Object-Oriented/high-resolution classified image of study area

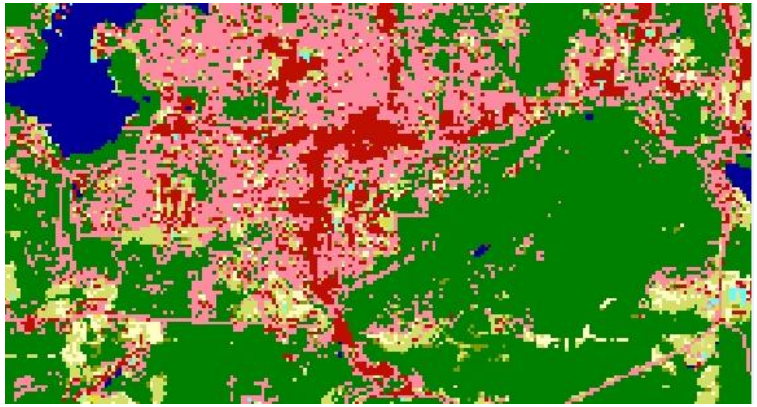

Maximum-likelihood/low-resolution classified image of study area

Raw image of part of study area

Figure 7: Illustration of high and low-resolution LULC data as derived with both methods

3.4.4 Pre-Calibration Model Results

As the separate models are set-up with LULC data of different spatial resolutions, the discretization of HRUs are consequently different and results in separate numbers for each model – ideally higher for high resolution data of all categories (soils, land-cover etc.). This has the potential to affect the objectivity of the comparisons to be made among the models (DiLuzio, 2013). This effect was accounted for on the comparison by the use of the GLUE methodology (Beven and Binley, 1992) in the auto-calibration stage in order to minimize the effect of equifinality. Table 4 gives the results of pre-calibrated output from each model.

Table 5: Pre-Calibration Results for Models with different LULC data

Criteria	30 m Landsat 6 ETM+	28.5 m Landsat 5	1 m NAIP
Calibration Period			
NSE	-2.06	-2.44	-2.40
R^2	0.27	0.26	0.24
PBIAS	-90.95	-100.42	-94.27
RSR	8.27	8.04	8.72
RMSE	5.74	6.09	6.05
Total Water Yield /mm	665.94	703.10	672.15
Validation Period			
NSE	-0.85	-1.00	-0.97
R^2	0.35	0.33	0.32
PBIAS	-59.63	-63.29	-59.57
RSR	1.02	1.06	1.03
RMSE	73.95	76.80	76.26
Total Water Yield /mm	119.66	117.67	115.20
P-Factor*/%	36	37	32
R-Factor*	0.14	0.14	0.17
Number of HRUs	522.00	367.00	735.00

*Determined through auto-calibration with GLUE

The addition of the 30 m Landsat 6 ETM+ model provides more information that ultimately gives further insight into model behavior regarding different HRU discretization and hence different number of calculation points.

3.4.5 Manual Calibration and Validation Results for Low-Resolution LULC data Model

The low-resolution LULC model was manually calibrated against monthly flow data from 2000 to 2006 and subsequently validated from 2007 to 2009. Observed stream-flow data constituted the observed total water yield from the contributing sub-basins to the gaging (calibration) station location (figure 5). The proportion of total water yield contributed by subsurface-flow was estimated to be an average of 42% from the base-flow filter program. The remainder of the total water yield was the proportion contributed by stream-flow.

The average monthly simulated and observed total stream-flow was 37.11 m^3s^{-1} and 40.21 m^3s^{-1} respectively. The NSE computed for both the calibrated and validated models were 92% and 97% with simulation biases (PBIAS) of +7.7% and +1.9% respectively; implying that the model is capable of accounting for 92% of the variance in the calibration period and 97% of the variance in the model for the validation period. The inclusion of ponds and other smaller reservoirs from data prepared by CAST had insignificant impact on the total stream-flow volume.

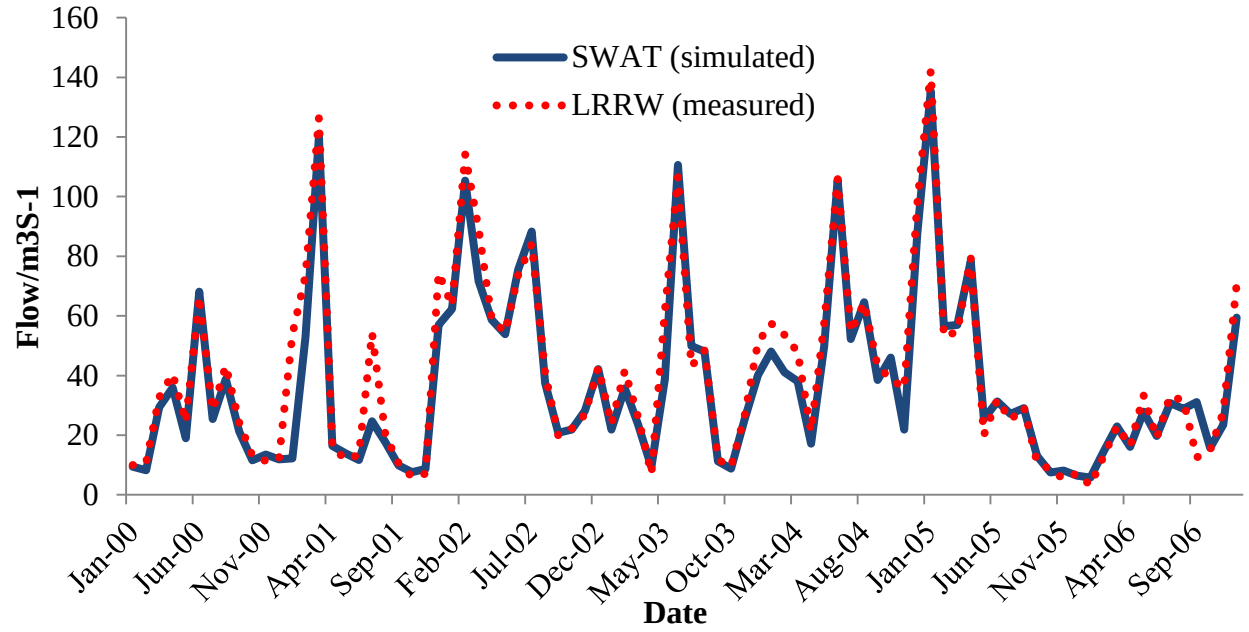

Figure 8: Calibrated monthly SWAT total flow model with low-resolution LULC data

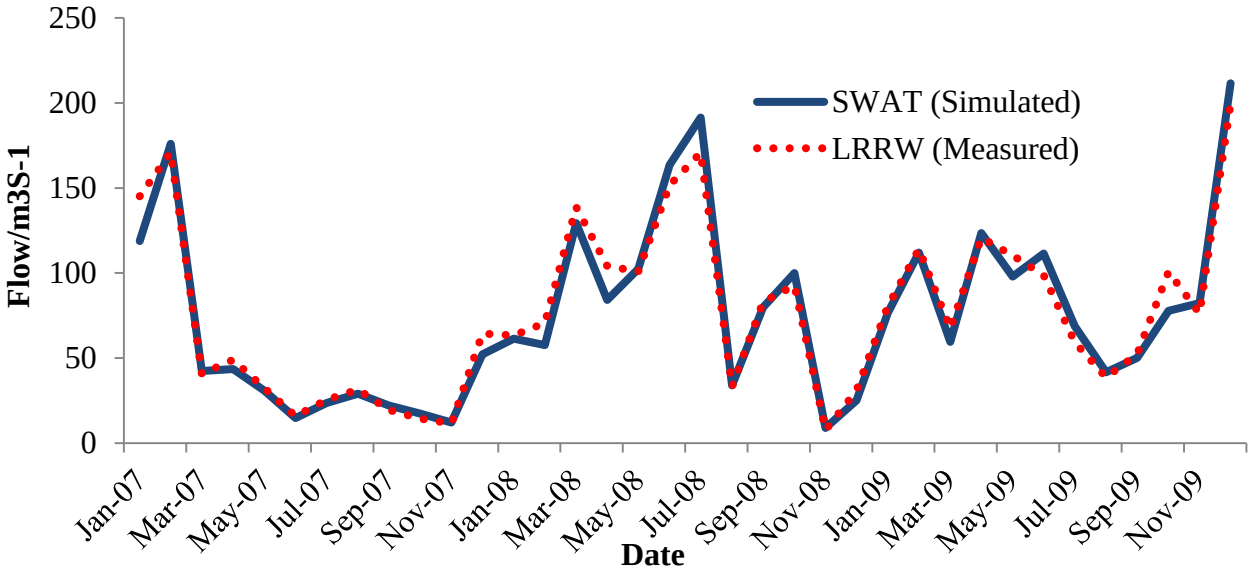

Figure 9: Validated monthly SWAT total flow model with low-resolution LULC data

3.4.6 Manual Calibration and Validation Results for High-Resolution LULC data Model

Results for calibration and validation for the high-resolution LULC data model were similar to the low-resolution LULC data model. As in the low-resolution model, parameters identified to be sensitive to flow from literature search (Betrie et al., 2011; White and Chaubey, 2005) were iteratively changed between successive runs. Among these the most sensitive parameters to flow simulations identified through sensitivity analysis in our study are listed in table 6. The average monthly simulated and observed total stream-flow was 36.81 m^3s^{-1} and 40.01 m^3s^{-1} respectively. The computed NSE for both the calibrated and validated models were 91% and 97% with simulation biases (PBIAS) of +10.78% and +3.23% respectively; implying that the model is capable of accounting for 91% of the variance in the calibration period and similarly for the validation period.

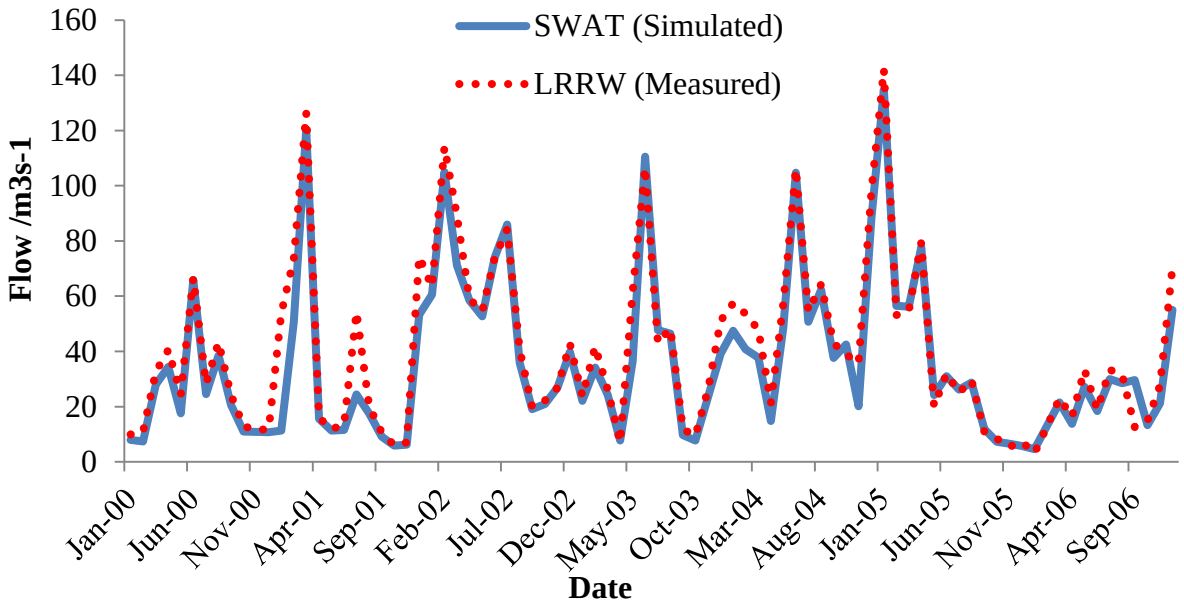

Figure 10: Calibrated monthly SWAT total flow model with High-resolution LULC data

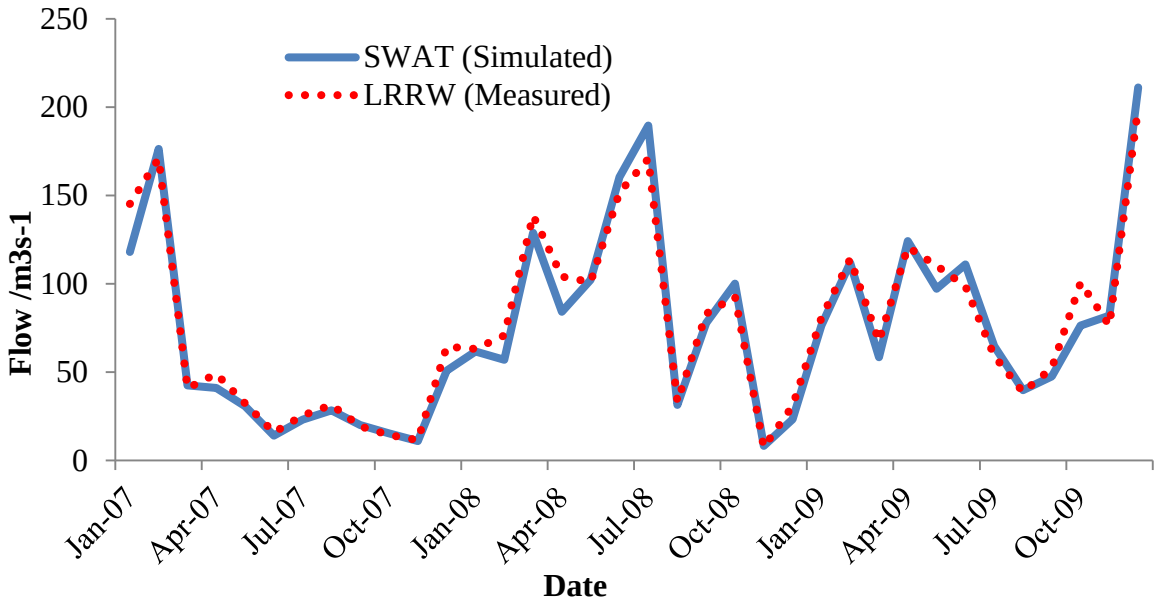

Figure 11: Validated monthly SWAT total flow model with high-resolution LULC data

Table 6: Sensitive parameters and parameter ranges in decreasing order of sensitivity

*Parameter	Values				Parameter Description
	Min	Max	**Average Chosen value		
	***	***	HR	LR	
r_CN2.mgt	-0.2	0.2	78	83	Curve Number
v_GW_DELAY.gw	1.0	30	20	10	Groundwater Delay Time/days
r_SOL_BD.sol	-0.5	0.6	1.45	1.45	Soil Moist Bulk Density/gcm^{-3}
v_ALPHA_BNK.rte	0.0	1.0	0	0	Base Flow Alpha Factor for Bank Storage/days
v_GW_REVAP.gw	0.0	0.2	0.09	0.05	Groundwater revap Coefficient
v_ESCO.hru	0.8	1.0	0.2	0.9	Soil evaporation compensation factor
v_GWQMN.gw	0.0	2.0	1	0	Shallow aquifer threshold depth /mm
r_SOL_K.sol	-0.8	0.8	9.993	9.993	Saturated Hydraulic Conductivity/$kmhr^{-1}$
r_SOL_AWC.sol	-0.2	0.4	0.11	0.11	Soil Available Water Capacity/mm/mm
v_CH_K2.rte	5	15	5	5	Channel Hydraulic Conductivity/$mmhr^{-1}$
v_CH_N2.rte	0.0	0.3	0.014	0.014	Manning's n Value for main channel
v_ALPHA_BF.gw	0.0	1.0	0.048	0.0112	Base Flow Alpha Factor/days
v_SFTMP.bsn	-5.0	5.0	1	1	Snowfall Temperature/^0C

***** r_means the existing parameter value is to be multiplied by (1+ given parameter value)

v_means the existing parameter value is to be replaced by the given value

******HR: Areally averaged high-resolution LULC data model, LR: low-resolution LULC data model

***Minimum and maximum value ranges used during auto-calibration

3.4.7 Auto-calibration Results for Low-Resolution LULC data model

The GLUE method was used in a coupled SWAT software system (SWAT-CUP) (Abbaspour, 2011) to automatically calibrate the models with model parameters constrained to limits that depict the prevailing watershed. The GLUE method allows for the evaluation of the models based on the uncertainties associated with the sampled parameter sets.

From 7000 simulations, 6997 of the simulations had NSE values of 50% or above (termed behavioral model runs). The NSE for the best simulation was 92% with RMSE of 8.3; determined from the validation period. The predictive reliability of the model was evaluated based on uncertainty quantifications as determined from two main parameters output from the GLUE analysis; the *P-factor* and *R-factor*. A larger *P-factor* indicates a good fit and ranges between 0 and 100% whiles *R-factor* ranges from 0 to ∞ with lower values depicting a good fit (Abbaspour, 2011).

With the low-resolution model, auto-calibration resulted in *P* and *R-factors* of 37% and 14% respectively. This essentially implies that 37% of the observed flow data can be accounted for by the model at the 95% prediction uncertainty level. We assumed that all the uncertainty in the model is attributable to the uncertainty in the observed data as other system uncertainties were deemed improbable to quantify with our knowledge of the watershed.

P and *R-factors* results for the simulations run to validate the calibration model were 32% and 18% respectively. Figure 12 shows a graph of the calibration output with the best simulation and uncertainty band.

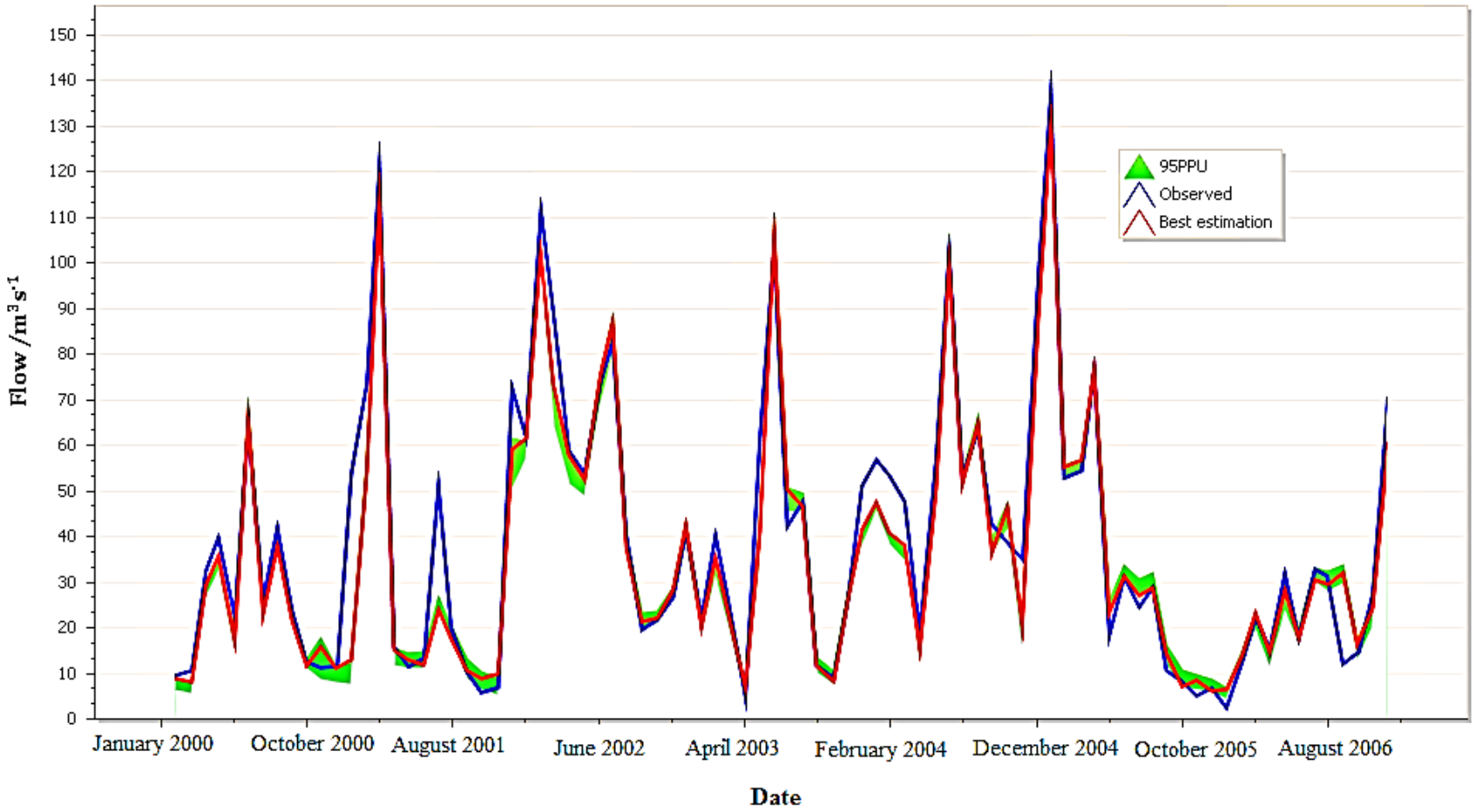

Figure 12: Auto-calibration output of low-resolution LULC model with best simulation and 95 percent prediction uncertainty band

3.4.8 Auto-calibration Results for High-Resolution LULC data model

Similar to the low-resolution model simulations, 7000 auto-calibration runs were performed for the high-resolution data model; out of which 6997 (same as in the low-resolution) were behavioral. The calibration NSE for the best simulation was 92% with RMSE of 8.3 at *P* and *R-factors* of 39% and 14% respectively. Therefore, the model is able to account for 39% (slight increase from 37% of the low-resolution LULC model) with the same uncertainty band of 14%. This implies that in spite of the higher number of HRUs which also implies a more detailed discretization of the model, the high-resolution LULC model could account for 39% of the measured discharge data; this represent a slight increase of 2% over the low-resolution data model. The model was further validated for same period as in the low-resolution LULC model; results of the validation showed obtained *P* and *R-factors* values of 0.32 and 0.17 respectively. Furthermore, among the 13 parameters that were optimized (listed in table 2), groundwater delay (GW_DELAY), evapotranspiration compensation factor (ESCO), soil bulk density (SOL_BD), curve number for antecedent moisture condition II (CN2), soil available moisture content (SOL_AWC) and soil hydraulic conductivity (SOL_K) (in decreasing order of sensitivity) were determined to be most sensitive through sensitivity analysis performed in SWAT-CUP (Abbaspour, 2011).

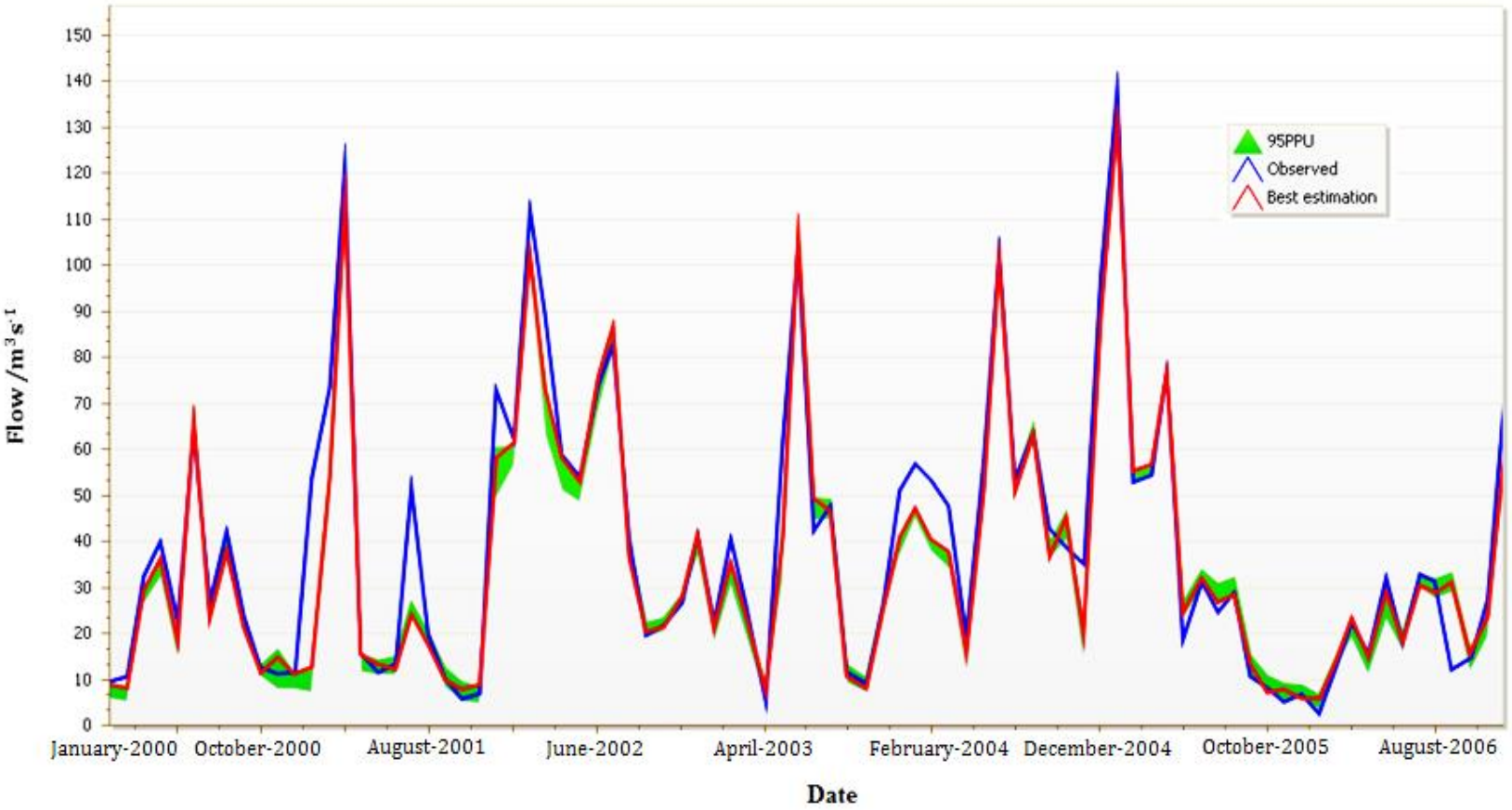

Figure 13: Auto-calibration output of high-resolution LULC model with best simulation and 95 percent prediction uncertainty band

3.4.9 NLCD Land-Cover data Model Results

This model was calibrated with LULC data of 30 m resolution, classified with unsupervised classified method (USGS, 2007) with DEM, soils data and slope specified in the same way as the previous models. Over all, 522 HRUs were discretized for this model compared to the 367 and 735 for low and high LULC models. The results of the flow calibrations and validation were also determined similarly to the previous LULC data models; calibrated and validated against observed monthly stream-flow from 2000 to 2006 and 2007 to 2009 respectively.

The simulated monthly stream-flow showed acceptable results for the calibration period with NSE, PBIAS, RSR, R^2 and RMSE values 0.91, 10.84%, 0.24, 0.93 and 0.99 respectively according to multi-criteria outlined in Moriasi et al., (2007). For the validation period, the measured aggreement between observed and simulated flow values was indicated by NSE, PBIAS, RSR, R^2 and RMSE values of 0.96, 3.24%, 0.19, 0.97and 10.2 respectively. By this, it is can be inferred that the model slightly under-predicts the system stream-flow response by 3.24% while showing a correlation of 97% of the simulated stream-flow to the observed stream-flow. Through auto-calibration using GLUE, the NLCD model was determined to capture 36% of the observation with r-factor of 0.14 at the 95% prediction uncertainty level, correlation coefficient of 92% and NSE of 0.92. Out of the 7000 simulations, 6997 were determined to provide acceptable results; the same number as the previous models.

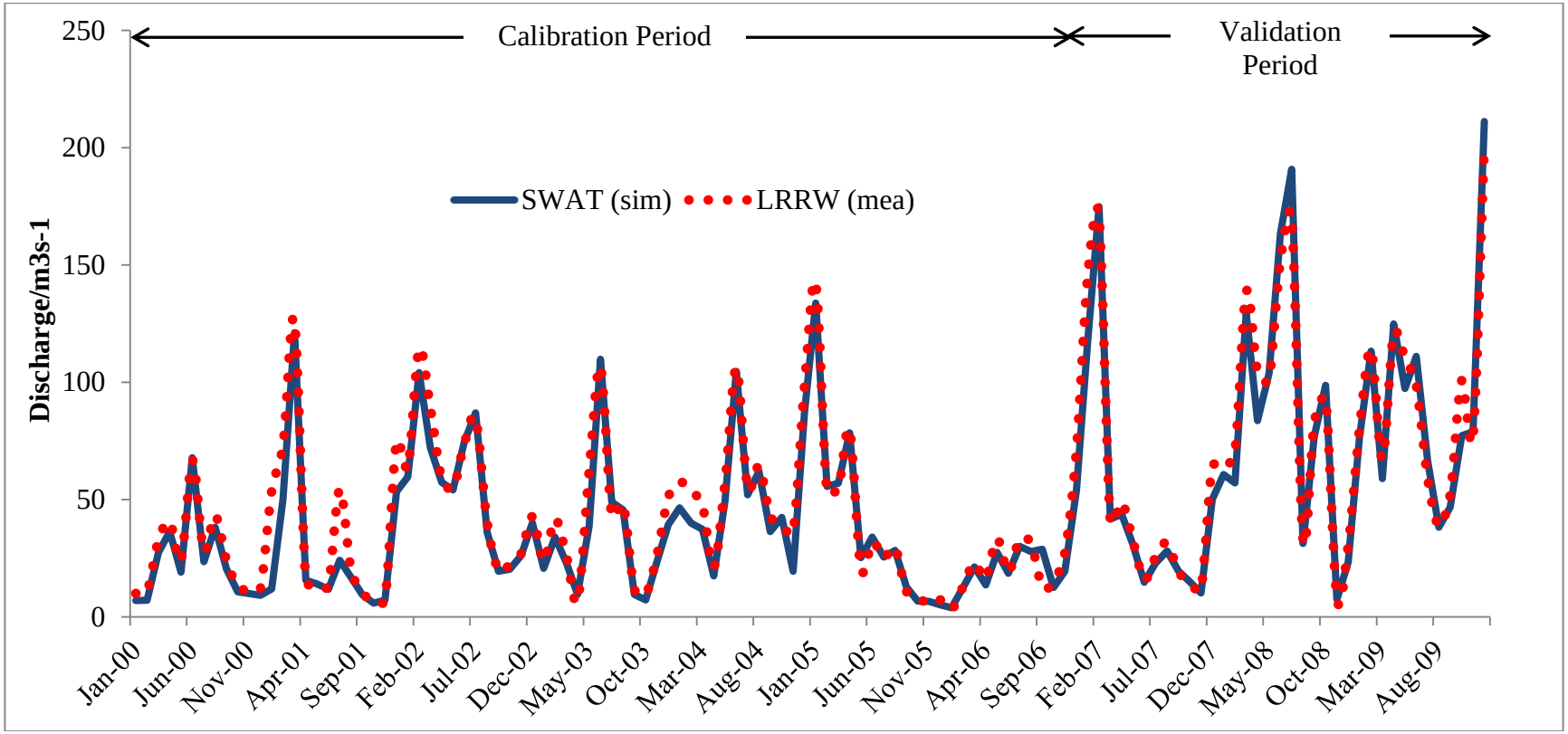

Figure 14: SWAT monthly total flow model with NLCD LULC data (Manual Calibration)

3.4.10 Model Prediction Bias for high and low-flow Regimes

In the watershed, water-yield is generally low in August (shown in figure 15). For the entire period of the simulation (2000 to 2009) in the NLCD LULC data model, the simulated flow represented a general over-prediction. August stream-flow was under-predicted for all the ten years of simulation. Similarly for high water-yield which normally occurs around the months of March, April and May, the model under and over-predicted the system stream-flow; in May-2001, 2005 and2008, the model over-predicted the stream-flow by 17%, 25% and 2% respectively. The lowest under-prediction occurred in May-2003 (under-predicted by 37%). Generally the model under and over-predicted stream-flow in the high-flow season by an average value of 15% respectively.

For the low and high-resolution LULC models, there was only a slight over-prediction of August low stream-flow of 2% and 7% respectively for two (2008 and 2009) out of the ten years of simulation in the case of the low-resolution LULC model. For the high-resolution LULC data model, low stream-flow for August was slightly over-predicted one out of the ten simulation years; by 3% for 2009. The average under-prediction was 7% for both low and high-resolution models respectively. Again to offer some more perspective on these two model results, the NLCD model generally over-predicted August stream-flow by an average value of 8%. Table 3 shows the comparison of model results for the average simulation prediction bias for high and low stream-flow periods in the watershed.

Table 7: Model average percentage prediction bias for low and high-flow regimes

Model	High-Flow Regime		Low-Flow Regime	
	Under-Predicted	Over-Predicted	Under-Predicted	Over-Predicted
NLCD LULC Model	15.47	-15.37	8.14	None
Low-Resolution LULC Model	10.62	-8.83	6.93	-3.36
High-Resolution LULC Model	11.64	-6.74	7.12	-3.22

*-ve values represent over-prediction and vice versa

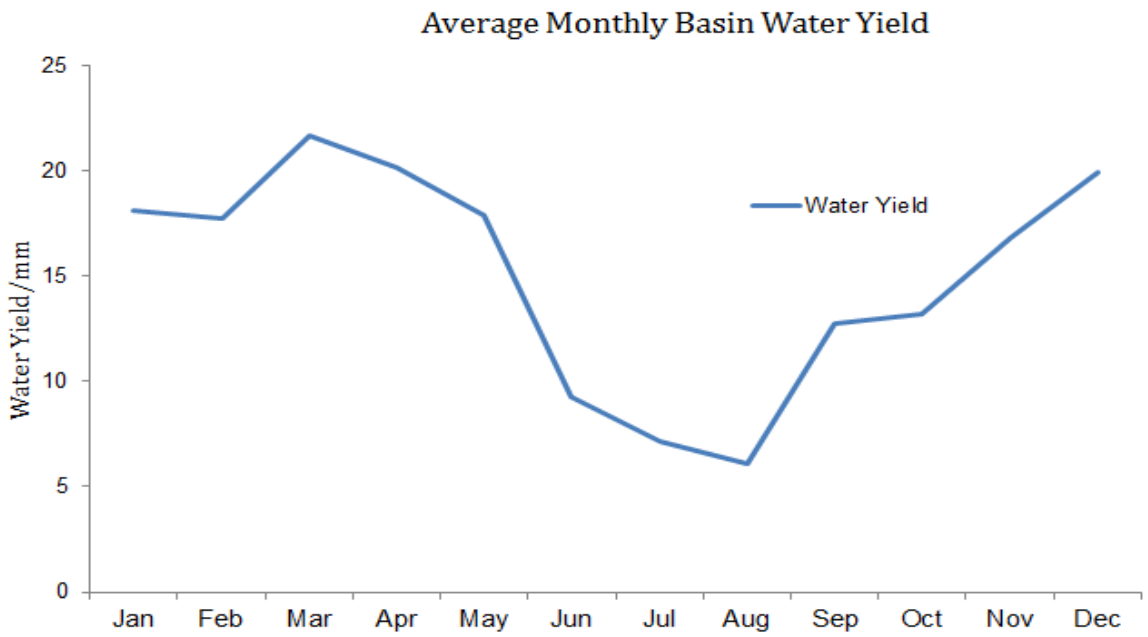

Figure 15: Average monthly basin water yield for the entire simulation period (2000-2009)

In highly managed watersheds, primary controlling hydrological processes take a secondary role in dictating the hydrological responses of the entire watershed (Abbaspour, 2011). This is certainly the case in our study with regards to the calibration site. It does not take a keen observation to realize that the calibration and validation values of the two LULC dataset models

are near “perfect”. This is inferred to be contributed by the fact of the presence of the Greers Ferry Lake from which water is released at specific times of the day. The measured release rate we incorporated into the models in order to ensure an accurate calibration. This however, introduces the problem of a highly managed watershed as discussed in Abbaspour (2011) hence the in the above model calibrations, the primary controlling hydrological processes in the system take a secondary role in the model. In order words, our models as calibrated do not adequately reflect the other prevailing environmental processes that might affect the hydrology of the system if the Greers Ferry Lake had not been present in the system. To account for this short-coming in the study, the models were calibrated against data from a gaging station located upstream of the Greers Ferry Lake. The results from the manual and automatic calibrations are presented in table 8.

Table 8: Model calibration for high-resolution LULC model (Upstream gaging station)

Calibration	
Criterion	**Criterion Value**
NSE	0.58
R^2	0.6
BIAS	-1.32
RSR	0.87
Total Water Yield /mm	472.04
Validation	
NSE	0.87
R^2	0.9
PBIAS	13.96
RSR	0.48
Total Water Yield /mm	363.6
r-factor	0.33
p-factor	0.27

Table 9: Model calibration for low-resolution LULC model (Upstream gaging station)

Calibration	
Criterion	**Criterion Value**
NSE	0.6
R^2	0.6
BIAS	-2.31
RSR	0.83
Total Water Yield /mm	469.25
Validation	
NSE	0.88
R^2	0.9
PBIAS	11.39
RSR	0.44
Total Water Yield /mm	322.6
r-factor	0.73
p-factor	0.55

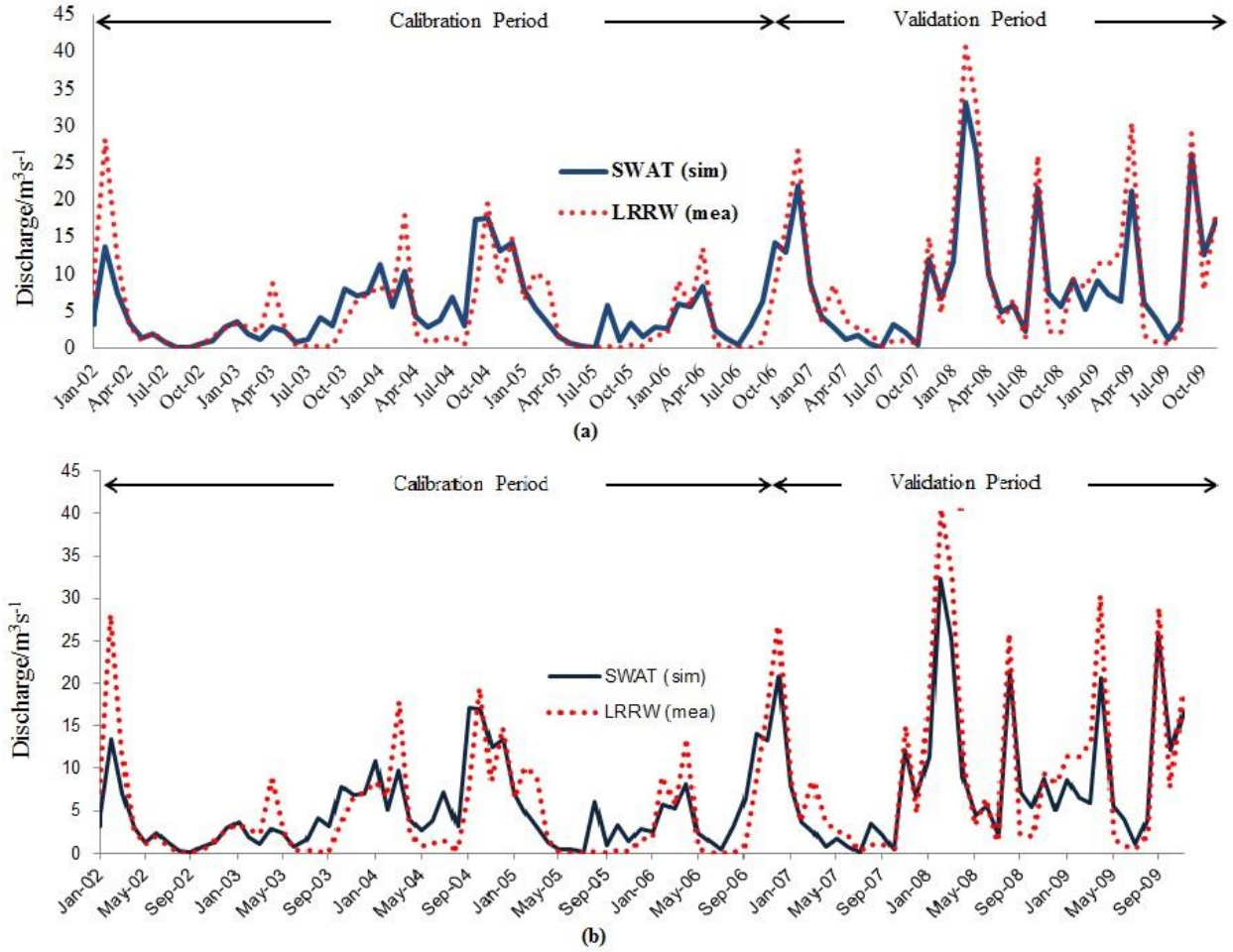

Figure 16: Hydrograph of low-resolution LULC model (a) and high-resolution LULC model (b) calibrated at the upstream gaging station

One key question of interest with regards to this study is as to how low-resolution imagery classified with object-oriented image classification method performs with the SWAT flow model calibration and subsequent predictive reliability. This question becomes particularly pertinent to the study in view of the fact that the object-oriented image classification technique is optimized for high resolution imagery hence most studies in literature are based on high resolution imagery. To account for this in the study, a 30 m Landsat imagery acquired in 2005 for the study area was classified with the object-oriented technique and supplied as input land use data to calibrate a SWAT flow model matching the exact same criteria as the two main data models in the study; this model is here-to-fore referred to as the Landsat model.

It was observed during the calibration process that with the same criteria, the Landsat model was more difficult to calibrate manually. After several iterations, the best manual calibration yielded NSE of 0.41 with an approximate total stream flow over-prediction rate of 12%. The model was further subjected to the outlined auto-calibration method using GLUE as implemented in SWAT-CUP software. Due to the effect of the incorporated reservoir outflow data masking out the primary hydrologic process, more credence in our results is given to the calibrated model in the upstream gage location. However, the results from both stations are presented. At the upstream location, the auto-calibrated model produced NSE of 0.57 with a p-and r-factors of 0.28 and 0.32 respectively. This implies that the calibrated model captures 28% of the observation data with an uncertainty band of 0.32 around the best simulation which is expressed in terms of the observed data standard deviation. Results for the downstream calibration station showed NSE of 0.96 with a p- and r-factors 0.58 and 0.4 respectively. Figure 16 presents the hydrographs of the manual calibration results.

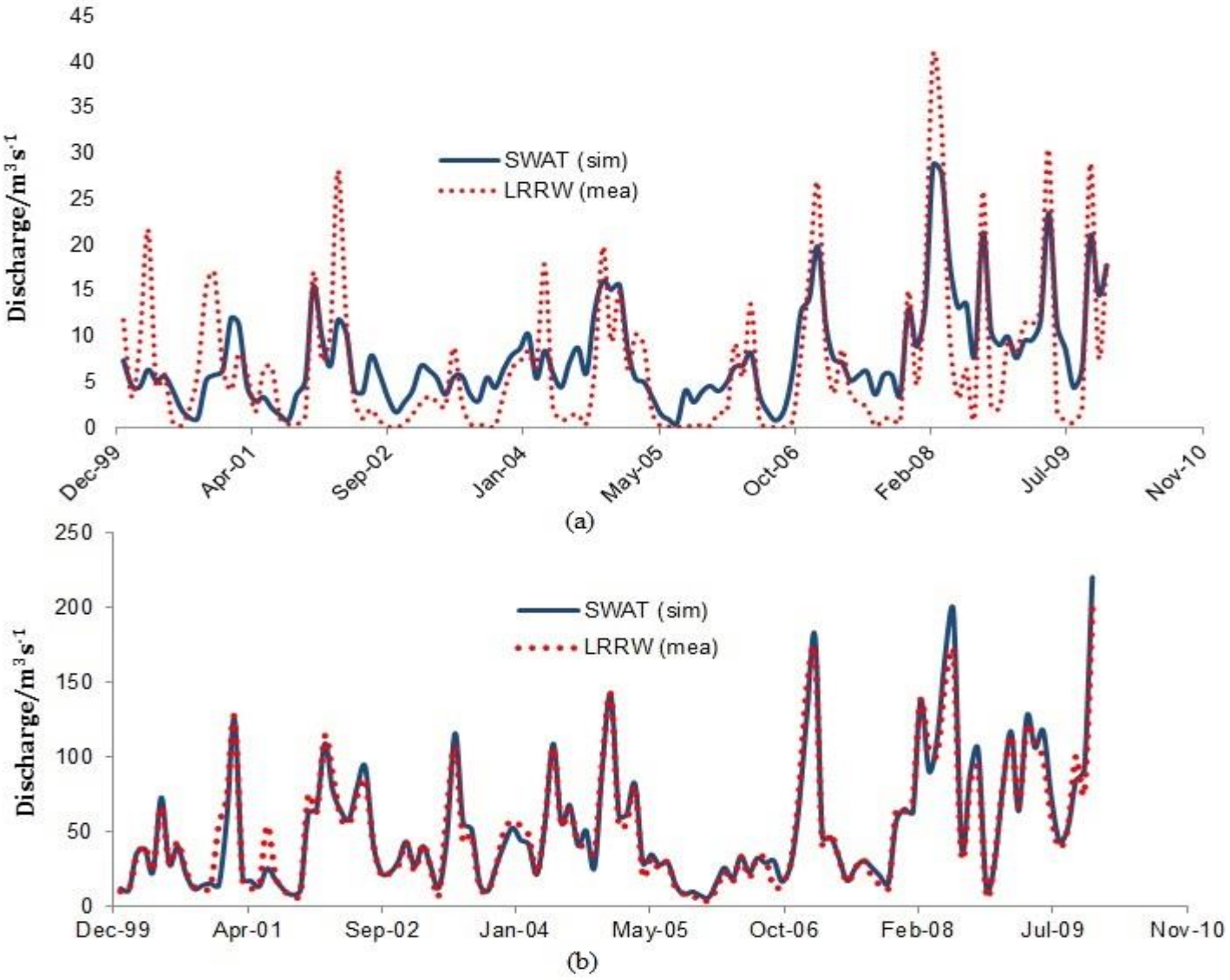

Figure 17: (a) Upstream and (b) downstream manual calibration hydrograph of Landsat model

3.5 Discussion

Examination of the low and high-resolution model results from both manual and automatic calibration procedures largely confirms the results obtained by previous researchers such as Cheng et al., (2005) and Bosch et al., (2004). Differences in model behaviour with respect to low and high resolution LULC data and the respective methods of classification on stream-flow prediction reliability, are easier to identify when periods of high and low stream-flow regimes are considered. This approach becomes necessary in this study because all the models have high NSE values and thus how the model captures system variabilities is harder to identify with manual calibration when only NSE values are considered.

The percentage bias in prediction at low and high-regimes in the watershed therefore gives a much better insight into model behavior. This information is presented in table 3. It is clear that the NLCD model over and under-predicts the stream-flow in high-flow regime with much higher bias than both low and high-resolution models. Both low and high-resolution LULC data models have similar over and under-prediction biases when compared to the NLCD data model. It is also worth noting that there was no over-prediction bias with the NLCD model in the low-flow regime.

The results from both high and low-resolution LULC data models can be explained by the fact that, much as the high-resolution model had higher HRU discretization and slightly higher NSE values, the slightly lower classification accuracy for the high-resolution LULC data could be a factor in the model's inability to account for a greater percentage of the observed discharge data over the low-resolution data model. With the results from the Landsat LULC model indicating a higher predictive reliability at the downstream gaging station, there appears to to an apparent trend in the model results. The trend is that the models with the the lower resolution LULC data

appear to offer a much higher stream flow predictive reliability. The main inference for this is that the lack of spatial heterogeneity in the low resolution imagery appear to be that the watershed is itself dominated by forest land cover therefore the main controling process are much better influenced by a cover type which is more generally categorized. By the same reasoning the introduction of spatial heterogeneity as evident in the high resolution LULC data introduces uncertainties in the model that are much less quantifiable with stream-flow as a metric of model result reliability determination.

3.6 Conclusion

The objective of this study was to determine the respective impact of high-resolution LULC data classified with the object-oriented image analysis technique and low-resolution LULC data also classified with pixel-based maximum-likelihood technique on the stream-flow predictive reliability of the SWAT model. It was shown that at the manual calibration level, model efficiency were high (NSE of over 90%) for both models. However, due to significant impact of equifinality (Beven and Binley, 1992) on the nature of the study (also with regards todifferent HRU numbers and model calibration done separately), auto-calibration with GLUE (Beven and Binley, 1992) was a necessary and integral part of the study. Out of which the predictive reliability were determined based on *p* and *r*-factors.

Both models braketed less than 40% of the observation data; 32% and 37% for high-resolution models respectively. The uncertainty band around the best estimation in each case was higher for the high-resolution model as shown by r-factors of 0.17 and 0.14 respectively. It was also clear from our results that a high-resolution imagery classified with the object-oriented method does not enhance the predictive reliability of a SWAT flow model. Furthermore, the object-oriented image analysis albeit it has been shown to provide LULC classification of significantly higher

classification accuracy than the pixel-based maximum-likelihood method (Platt and Rapoza, 2008; Yan, 2003), it is also clear from our results that in a watershed with similar characteristics, the object-oriented method has no clear advantage over a pixel-based method in producing LULC data that enhance the predictive reliability of a SWAT flow model. This conclusion is drawn from our study due to the fact that the classification accuracies of the two respective data and mothed combinations, were shown to have no statistically significant difference. Nonetheless, there were some general trends which include the fact that the monthly simulated total water yield were largely similar for both models in the calibration and validation periods. This brings the question of how the model would perform with a significantly better object-oriented classified LULC data; which ultimately requires further studies. Furthermore, a third model set-up with 30 m NLCD LULC data showed similar result to the low-resolution LULC model; with predictive reliability higher than the high-resolution LULC model. A possible limitation of this study is that, the presence of a reservoir with daily discharge data incorporated in the model makes the system a managed watershed at the chosen outlet. In such a system, natural processes take a secondary role in flow production (Abbaspour, 2011).

References

(CAST), Center for Advanced Spatial Technologies. 2006. Arkansas Watershed Information System. http://watersheds.cast.uark.edu/viewhuc.php?hucid=11010014.

CAST, 2006. "Land Use Land Cover Fall 2006 (raster). http://www.geostor.arkansas.gov/G6/Home.html?id=490250db4c86be523e551f285951f3ad.

(NOAA), National Oceanic and Atmospheric Administration. 2012. "Arkansas, Climate Division Temperature January-May 1895-2012. http://www.ncdc.noaa.gov/temp-and-precip/time-series/index.php?parameter=tmp&month=5&year=2012&filter=ytd&state=3&div=2.

(USDA-ARS), United States Department of Agriculture - Agricultural Research Service. 2012. Grassland Soil and Water Research Laboratory, Temple, Texas : US Climatic Data. http://ars.usda.gov/Research/docs.htm?docid=19388.

(USGS), U.S. Geological Survey. 2007. National Land Cover Database 2006 (NLCD2006). http://www.mrlc.gov/nlcd2006.php.

NHD, 2009. Medium Resolution: National Hydrography Dataset Line Feature (line). http://www.geostor.arkansas.gov/G6/Home.html?id=8b089ebe17516470245dd905b4965bf4.

Abbaspour K C, 2011. SWAT-CUP: SWAT Calibration and Uncertainty Programs - A User Manual.

Arnold J G, Allen P M, Muttiah R S and Bernhardt G,1995. Automated Baseflow Separation and Recession Analysis Techniques. Ground Water 33 (6): 1010–1018.

Baatz M and Schäpe A, 2000. Multiresolution Segmentation: An Optimization Approach for High Quality Multi-scale Image Segmentation. Angewandte Geographische Informationsverarbeitung. Heidelberg: Wichmann-Verlag.

Beven K and Binley A, 1992. The Future of Distributed Models: Model Calibration and Uncertainty Prediction." Hydrological Processes 6: 279–298.

Bosch D D, Sheridan J M, Batten H L and Arnold J G, 2004. Evaluation of the swat model on a coastal watershed. Transactions of the ASAE 47 (5): 1493–1506.

Bronstert A, Niehoff,D and Berger G, 2002. Effects of Climate and Land-use Change on Storm Runoff Generation: Present Knowledge and Modelling Capabilities. Hydrological Processes 16 (2) (February 15): 509–529. doi:10.1002/hyp.326. http://doi.wiley.com/10.1002/hyp.326.

Burnett, C, and T Blaschke. 2003. A Multi-scale Segmentation/object Relationship Modeling Methodology for Landscape Analysis. Ecological Modeling 168 (3): 233–249.

Carlson T N and Arthur S T, 2000. The Impact of Land Use — Land Cover Changes Due to Urbanization on Surface Microclimate and Hydrology: a Satellite Perspective." Global and Planetary Change 25 (1-2) (July): 49–65. doi:10.1016/S0921-8181(00)00021-7. http://linkinghub.elsevier.com/retrieve/pii/S0921818100000217.

Chen, Pei-yu, DiLuzio Mauro, and Jeffrey G. Arnold. 2005. "Impact of Two Land-Cover Data Sets On Stream Flow and Total Nitrogen Simulations Using a Spatially Distributed." In Pecora 16: Global Priorities in Land Remote Sensing, 23–27.

Congalton, R.G., and Green K. 1999. Assessing the Accuracy of Remotely Sensed Data: Principles and Practices. Lweis Publishers.

Curtis, John B, and Scott L Montgomery. 2002. "Recoverable Natural Gas Resource of the United States: Summary of Recent Estimates" 10 (10): 1671–1678.

Deck, Kathy, and Viktoria Riiman. 2012. Revisiting the Economic Impact of the Natural Gas Activity in the Fayetteville Shale : Vol. 1201.

Devi, Y Aruna Suhasini, and I V Murali Krishna. 2012. "Pixel-based and Object-oriented Classification of High Resolution Satellite Images." Canadian Journal on Electrical and Electronics Engineering 3 (1): 1–4.

F. Malcolm Conly, Garth van der Kamp. 2001. "Monitoring the Hydrology of Canadian Prairie Wetlands to Detect the Effects of Climate Change and Land Use Changes." Environmental Monitoring and Assessment 67 (1-2): 195–215. doi:10.1023/A:1006486607040. http://link.springer.com/article/10.1023/A:1006486607040.

Funkhouser, Jaysson E. 2012. "Personal Communication."

Gorham, Bruce. 2013. Personal Communication.

Huang, Jinliang, Pei Zhou, Zengrong Zhou, and Yaling Huang. 2013. "Assessing the Influence of Land Use and Land Cover Datasets with Different Points in Time and Levels of Detail on Watershed Modeling in the North River Watershed, China." International Journal of Environmental Research and Public Health 10 (1) (January): 144–57. doi:10.3390/ijerph10010144. http://www.pubmedcentral.nih.gov/articlerender.fcgi?artid=3564134&tool=pmcentrez&rendertype=abstract.

Laliberte, Andrea S., Albert Rango, Kris M. Havstad, Jack F. Paris, Reldon F. Beck, Rob McNeely, and Amalia L. Gonzalez. 2004. "Object-oriented Image Analysis for Mapping Shrub Encroachment from 1937 to 2003 in Southern New Mexico." Remote Sensing of Environment 93 (1-2) (October): 198–210. doi:10.1016/j.rse.2004.07.011. http://linkinghub.elsevier.com/retrieve/pii/S0034425704002147.

Lang, S, F Albrecht, and T Blaschke. 2006. OBIA Tutorial - Introduction to Object-Based Image Analysis. Salzburg, Autria.

Mauro, DiLuzio. 2013. “Personal Communication.”

Moriasi, D N, J G Arnold, M W Van Liew, R L Bingner, R D Harmel, and T L Veith. 2007. “Model Evaluation Guidelines for Systematic Quantification of Accuracy in Watershed Simulations.” Transactions of the ASABE 50 (3): 885–900.

Myint, Soe W., Patricia Gober, Anthony Brazel, Susanne Grossman-Clarke, and Qihao Weng. 2011. “Per-pixel Vs. Object-based Classification of Urban Land Cover Extraction Using High.pdf.” Remote Sensing of Environment 78 (31): 17.

NID-USACE. 2009. “National Inventory of Dams, United States Army Corps of Engineers (NID-USACE).” http://geo.usace.army.mil/pgis/f?p=397:101:1547957062223601::NO.

Peterson, L.C., G.H. Haug, K.A. Hughen, and Ursula Röhl. 2000. “Rapid Changes in the Hydrologic Cycle of the Tropical Atlantic During the Last Glacial.” Science 290 (5498) (December 8): 1947–1951. doi:10.1126/science.290.5498.1947. http://www.sciencemag.org/content/290/5498/1947.abstract.

Pham, Cu Van, Thi Hang Thuy Nguyen, and Dong Phan Nguyen. 2009. “Comparison of Pixel Based and Object Oriented Classifications in Land Cover Mapping in the Red River Delta – Example of Duy Tien District , Ha Nam Province , Vietnam Comparison of Pixel Based and Object Oriented Classifications in Land Cover Mapping in Th.” In 7th FIG Regional Conference, 1–9.

Pitman, a. J. 2004. “Impact of Land Cover Change on the Climate of Southwest Western Australia.” Journal of Geophysical Research 109 (D18): 1–12. doi:10.1029/2003JD004347. http://www.agu.org/pubs/crossref/2004/2003JD004347.shtml.

Platt, Rutherford V, and Lauren Rapoza. 2008. “An Evaluation of an Object-Oriented Paradigm for Land Use / Land Cover Classification *.” The Professional Geographer 60 (1): 87–100.

Robert C. Weih, Jr., Norman D. Riggan, Jr. 2013. “A Comparison of Pixel-based Versus Object-based Land Use/Land Cover Classification Methodologies.” http://www.featureanalyst.com/feature_analyst/publications/success/comparison.pdf.

Scanlon, Bridget R., Robert C. Reedy, David a. Stonestrom, David E. Prudic, and Kevin F. Dennehy. 2005. “Impact of Land Use and Land Cover Change on Groundwater Recharge and Quality in the Southwestern US.” Global Change Biology 11 (10) (October): 1577–1593. doi:10.1111/j.1365-2486.2005.01026.x. http://doi.wiley.com/10.1111/j.1365-2486.2005.01026.x.

Survey, Arkansas Geological. 2012. “Arkansas Physiographic Regions.” http://www.geology.ar.gov/education/physio_regions.htm.

Tang, Z, B a Engel, B C Pijanowski, and K J Lim. 2005. “Forecasting Land Use Change and Its Environmental Impact at a Watershed Scale.” Journal of Environmental Management 76 (1) (July): 35–45. doi:10.1016/j.jenvman.2005.01.006. http://www.ncbi.nlm.nih.gov/pubmed/15854735.

Texas Agricultural and Mechanical University (TAMU). 2011. “SWAT Calibration Techniques.” http://swat.tamu.edu/media/1315/swat-calibration-techniques_slides.pdf.

Trimble. 2012. “eCognition Developer 8.” http://www.ecognition.com/products/ecognition-developer.

United States Geological Survey (USGS). 2002. “Base Flow Index Grid for the Conterminous United States.” http://water.usgs.gov/GIS/metadata/usgswrd/XML/bfi48grd.xml#stdorder.

USDA-ARS. 2012. “United States Department of Agriculture’s Agricultural Research Service (USDA-ARS).” http://ars.usda.gov/Research/docs.htm?docid=19422.

Wegehenkel, M., U. Heinrich, St. Uhlemann, V. Dunger, and J. Matschullat. 2006. “The Impact of Different Spatial Land Cover Data Sets on the Outputs of a Hydrological Model – a Modelling Exercise in the Ucker Catchment, North-East Germany.” Physics and Chemistry of the Earth, Parts A/B/C 31 (17) (January): 1075–1088. doi:10.1016/j.pce.2006.07.006. http://linkinghub.elsevier.com/retrieve/pii/S1474706506001793.

White, Kati L, and Indrajeet Chaubey. 2005. “SENSITIVITY ANALYSIS , CALIBRATION , AND VALIDATIONS FOR A MULTISITE AND MULTIVARIABLE SWAT MODEL 1.” Journal of the American Water Resources Association 41 (5): 1077–1089.

White, Michael D., and Keith A. Greer. 2006. “The Effects of Watershedurbanization on the Streamhydrology and Riparian Vegetation of Los Peñasquitos Creek, California.” Landscape and Urban Planning 74: 125–138.

Winchell, M., R. Srinivasan, M. Di Luzio, and J. G. Arnold. 2009. “ArcSWAT2009 Interface for SWAT2009.”

Yan, Gao. 2003. “Pixel Based and Object Oriented Image Analysis for Coal Fire Research.”

Zampella, Robert a, Kim J Laidig, and Rex L Lowe. 2007. “Distribution of Diatoms in Relation to Land Use and pH in Blackwater Coastal Plain Streams.” Environmental Management 39 (3) (March): 369–84. doi:10.1007/s00267-006-0041-0. http://www.ncbi.nlm.nih.gov/pubmed/17219257.

Zhang, L., W.R. Dawes, and G.R. Walker. 1999. Catchment hydrology predicting the effect of vegetation changes on catchment average water balance predicting the effect of vegetation changes on.

CHAPTER 4: OBJECTIVE TWO

Abstract

No study can currently be located that is done to quantify the relative change in land-cover particularly regarding shale-gas infrastructure since active exploration and production began in the Fayetteville Shale Play in north-central Arkansas. An object-oriented land-cover change quantification paradigm developed in eCognition was applied on two sets of high-resolution imagery obtained in 2006 and 2010 of the Little Red River watershed (LRRW). The classified land-use land-cover (LULC) data was used to evaluate impact of shale-gas infrastructure change on stream-flow in the South Fork of the Little Red River (SFLRR) which is a sub-watershed of the LRRW.

Results showed that since the upsurge in shale-gas related activities in the Fayetteville Shale Play (between 2006 and 2010), shale-gas related infrastructure in the SFLRR have increase by 78%. This change in land-cover in comparison with other land-cover classes such as forest, urban, pasture, agricultural and water indicates the highest rate of change in any land-cover category for the study period. A Soil and Water Assessment Tool (SWAT) flow model of the SFLRR simulated from 2000 to 2009 showed a 10% increase in storm water runoff. A forecast scenario based on the assumption that 2010 land-cover does not see any significant change over the forecast period (2010 to 2020) also showed a 10% increase in storm water runoff. Further analyses showed that this change in the stream-flow regime for the forecast period is attributable to the increase in land-cover as introduced by the shale-gas infrastructure.

Keywords: *Shale-gas, change detection, land-use land-cover (LULC), SWAT, Storm water runoff*

4.0 Introduction and Background

Substantial reserves of natural gas are estimated to be locked up in shale formations found throughout conterminous United States. Various estimates put the total gas in place in the range of 500 tcf to over 600 tcf (tcf: trillion cubic feet); which roughly represent 102 billion barrels of crude oil (Andrews et al., 2009). Owing to their low-matrix-permeability, almost all shale-gas wells require some form of stimulation in order to produce the gas at economically viable rates (Curtis, 2002). One such well stimulation method known as hydraulic fracturing ("fracking") has in addition to technologies such as horizontal drilling has transformed this unconventional natural gas resource into an economically viable one. As a direct consequence of this technological advancement various shale formations have seen a steady increase in exploration and production activities. Among such shale plays is the Fayetteville Shale lay (FSP) located in north-central Arkansas.

Exploration and production of shale-gas in the FSP involve the clearing of vegetation for well-pad, retention ponds, access roads, drilling, etc. These have various environmental impacts including storm-water runoff and sediment loading of downstream water bodies. Environmental considerations of modern shale-gas exploration and production range from issues pertaining to water management, water availability, water handling and transportation, the release of Naturally Occurring Radioactive Materials (NORM), storm-water runoff, management of fracturing fluids, water disposal, urban drilling etc (Arthur et al, 2010). This study however investigates the specific problem of the quantification of LULC change with particular emphasis on shale-gas infrastructure and the subsequent differential effect of the increase in shale-gas related infrastructure on runoff and stream-flow generation in a sub-watershed of the Little Red River Watershed (LRRW). Currently, no study can be located to that has been done to quantify the

differential impact of shale-gas infrastructure on the relative change in LULC in the FSP. This study employs the object-oriented image analysis paradigm embedded in eCognition software to quantify the relative increase in well-pads in the LRRW from readily available and high-resolution National Agricultural Imagery Program (NAIP) aerial imagery acquired in 2006 and 2010.

Object-oriented image analysis (OOIA) is a knowledge driven digital image processing technique that mainly involves two stages; segmentation and classification. In the OOIA paradigm, segmentation is a pre-classification step that essentially aggregates pixels into image objects or divides an image into discrete objects based on homogeneity criteria determined by the spatial and spectral properties of the image (Laliberte et al., 2004; Ryherd and Woodcook, 1996). The classification stage involves the assignment of the created objects to classes based on the desired properties of the determined class (Lang et al., 2006). This is done by two main methods; nearest-neighbor based on knowledge samples and membership function based on fuzzy logic (Laliberte et al., 2004). The method has been applied in various studies involving the use of remotely sensed images. These studies bother on investigations in medicine (Baatz et al., 2006), environmental monitoring (Laliberte et al., 2004), ecology (Burnett and Blaschke, 2003), etc. The method has also been applied in change detection in nuclear monitoring studies (Niemeyer et al., 2005), pre and post-conflict damage analysis (Al-Khudhairy et al., 2005), the development of other change detection techniques (Im et al., 2008) etc. Studies have shown that OOIA offers significantly higher classification accuracy than pixel-based methods (Platt and Rapoza, 2008; Blaschke and Strobl, 2001; Yan, 2003).

This study further augments the literature by providing quantifications of change in land-cover as attributable to well-pad placement in a shale-gas watershed using the object-oriented image analysis paradigm embedded in eCognition. The detected change in the LULC data is further employed as input land-cover data to study the differential change in stream-flow in an active shale-gas exploration and production sub-watershed in the study area (LRRW). This is to help quantify shale-gas activity impact on watershed hydrology with respect to other land-cover changes as influenced by categories such as agriculture and urbanization.

The runoff or stream-flow generation and sediment loading potential of well-pad placement in natural-gas producing watersheds has been well documented (Wachal, 2008; Matherne, 2006; Sandahl et al., 2007 and Williams et al., 2007). The South Fork of the Little Red River Sub-watershed (SFLRR) is recognized by the Arkansas Department of Environmental Quality (ADEQ) to contain ecologically sensitive tributaries of the upper Little Red River that are considered Extraordinary Resource and Ecologically Sensitive water bodies (USFWS, 2009). The SFLRR is approximately 387 km^2 in area representing roughly 8% of the total LRRW watershed area. However, this sub-watershed is among the sub-watersheds that see the bulk of shale-gas exploration and production activities in the LRRW (Funkhouser, 2012). Therefore issues such as runoff and sedimentation are of prime importance in order to ensure the survival of such endangered species such as the yellow-cheek darter (which occur nowhere else in the world) (USFWS, 2012). Much as sedimentation is known to adversely impact fresh water species (Henleya et al., 2000), this study does not tackle sedimentation. Rather runoff is tackled as controlling mechanism of sedimentation (Dendy and Bolton, 1976; Easton et al., 2010). The decision to exclude sediment modeling in this study was necessitated by the lack of available long term field observed sediment data.

4.1 Study Area and Methodology

4.1.1 Study Area

The Little Red River Watershed (LRRW) encompasses the counties of Cleburne, Independence, Pope, Searcy, Stone, White and Van Buren all located in north-central Arkansas. The LRRW is one of the watersheds in the Fayetteville Shale Play that is entirely located within the Play and also sees majority of shale-gas related activities. Three main physiographic regions make up the watershed. These are the Mississippi Alluvial Valley, Arkansas Valley and Ozark Mountains. The Mississippi Alluvial Valley is found in the lower-lying portions of the watershed and is relatively level terrain with unconsolidated sediments such as sands, gravel, clay and loess. The Arkansas Valley Region encompasses a part of the mid-section of the watershed with surface rocks consisting of sandstone and relatively higher general elevation than the Mississippi Alluvial Valley. Lastly the Ozark Mountain Region is fairly mountainous with high elevations and steep rock valley walls (AGS, 2011).

The Little Red River is the major water body that flows through the watershed in a generally north-west to south-east direction. Another major water body, the Greers Ferry Lake is also located centrally within the Ozark Mountains physiographic region of the watershed. With an approximate surface area of roughly 30,000 acres (USACE, 2011), this lake plays a major role in the entire watershed hydrology. Between 65% to 70% of the watershed's 4668 km^2 area land-cover is forest land, with agricultural and urbanized land making up the rest. Located in the lower upstream portion of the LRRW is the South Fork of the Little Red River (SFLRR) sub-watershed. This is a 10-digit HUC (Hydrologic Unit Code) sub-watershed roughly 387 km^2 in area with almost 90% of its land-cover being forest land (CAST, 2006). The SFLRR is selected for the determination of the differential effect of shale-gas related infrastructure on stream-flow

due to the fact that this sub-watershed sees the majority of exploration and production activities in comparison to the other sub-watersheds within the LRRW. Also there is a USGS stream gage located at the outlet of the SFLRR sub-watershed with observation data.

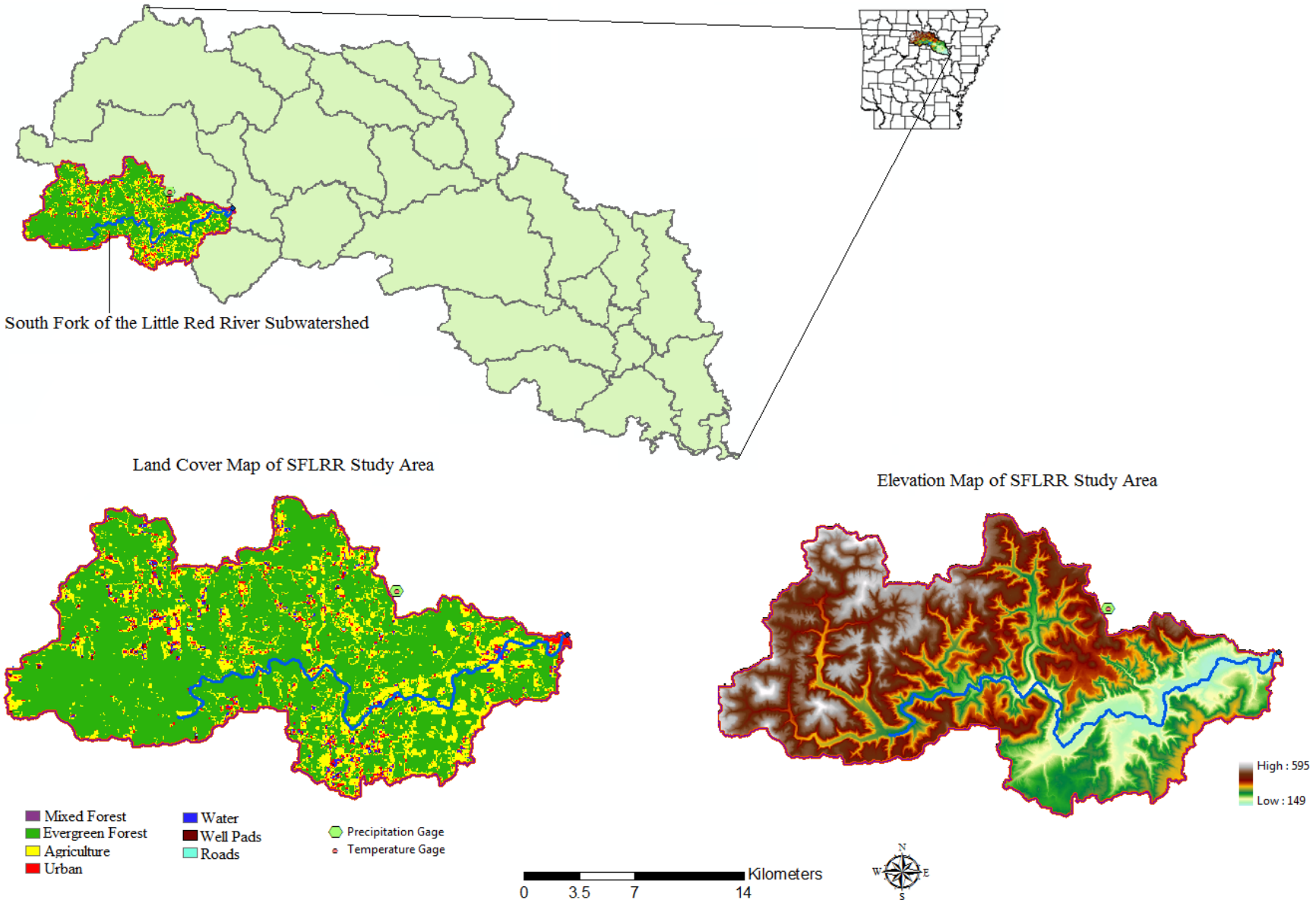

Figure 18: Land-cover and elevation characteristics of the study area: Little Red River Watershed (LRRW)

4.1.2 Object-Oriented Image Classification and Land-cover Change Quantification

The object-oriented image analysis (OOIA) method involves the two main stages of image segmentation and classification. Segmentation is the division of an image into discrete objects based on the inherent homogeneity or heterogeneity of the pixels that make up the image. The aim of this process is to optimize the correlation between the image objects and the geographical features of the real world which the objects are supposed to represent. Segmentation methodology can be categorized into histogram-based methods, which depend on the feature space, edge-based which depend on searching for edges that occur between heterogeneous objects and region-based which depends on the use of "seed pixels" from which a uniform region is aggregated (Lang et al., 2006).

National Agricultural Imagery Program data from 2006 and 2010 with 1 m resolution were resampled to 4 m in order to optimize the segmentation in eCognition, segmented and subsequently classified. Extra image layers were added comprising of infra-red bands and rasterize layer of urban areas located in the study area. Also, thematic layers for transportation network and inventory of hydrologic data (reservoirs, ponds and rivers) were incorporated. This was done to aid classification by introducing further spectral and spatial variability. In this study a fractal net evolutionary approach (FNEA) methodology of image segmentation embedded in eCognition software is used for the segmentation of the images before classification. This method of segmentation allows for the incorporation of scale in the segmentation process and is referred to as multi-resolution segmentation (MRS) (Laliberte et al., 2004). Two segmentation levels with two different scales (100 and 35 respectively) were used in this study. Objects created through the first segmentation level (level 100) were further segmented into smaller objects at the second segmentation level with a scale parameter of 35; both levels using shape and

compactness values of 0.1 and 0.5 respectively. These scales were chosen through a trial and error procedure with the goal of optimizing objects size for each classification category. The classification categories are as follows; agriculture, barren land, forest, transitional forest (forest with deciduous trees), urban, transportation (roads), water and well-pads. Classification of the segmented objects were subsequently carried out using a combination of rulesets (based on fuzzy logic) and the nearest neighbor classification method based on user-supplied object samples. This procedure was repeated for both 2006 and 2010 images to produce classified LULC data of the study area. Change detection was primarily performed based on a comparison of the calculated total percentage change in the individual land-cover class of respective areas that were correctly classified in both 2006 and 2010 datasets. This was done for the entire sub-basin in order to obtain a quantification of the well-pads in respect of the other land-cover classes in the sub-basin and also obtain a contribution of shale infrastructure to the overall sub-basin land-use change.

4.1.3 Model Description and Set-up

4.1.3.1 The Soil and Water Assessment Tool (SWAT) Model Description

SWAT is a physically based and continuous time semi-distributed parameter model that is developed to simulate the effects of land management practices on water, sediment, and agricultural chemicals in large and complex watersheds over long periods of time (Arnold et al., 1998). The version of the model that was used for this study is ArcSWAT; an ArcGIS extension that provides a graphical user interface for SWAT within a GIS environment. The model has been used to study the impact of biofuel production on water quality (Wu et al., 2012), climate change studies (Gurung and Bharati, 2012; Zhang et al., 2007). The model requires input data in

DEM, land-use data, soils and slope classes for the delineation of Hydrologic Response Units (HRUs). HRUs are created through an overlay of respective slope classes, soils and land-use data. Aggregations of overlays of the same slope class, land-use and soil type are grouped into the same HRU. Figure 2 illustrates the creation of HRUs in the ArcSWAT environment.

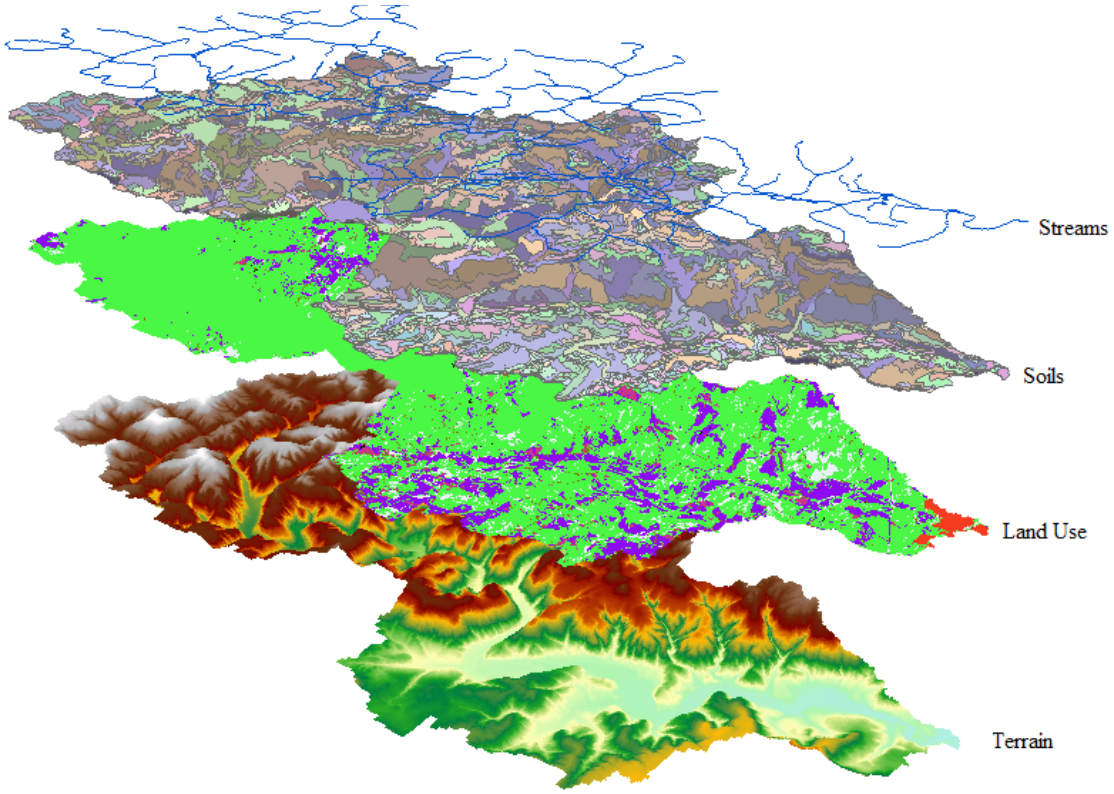

Figure 19: Illustration of Overlay in GIS for HRU Delineation in ArcSWAT

The HRU is the basic computational unit of the model and helps to ensure efficient computation. The ArcGIS interface of the 2005 version of the SWAT model (Di Luzio et al., 2001) was used to set up the model in a GIS environment in this study. This ensures a seamless integration of DEM for the delineation of the watershed, flow lines, reservoirs and basin outlets. SWAT simulates the hydrology at each HRU using the water balance equation, comprising precipitation,

runoff, evapotranspiration, percolation and base flow components as shown in equation 1. Runoff is computed with either the Soil Conservation Service Curve Number method (USDA-SCS, 1972) or the Green and Ampt infiltration method (Green and Ampt, 1911) and routed to the closest channel using the Muskingum method (Chow, 1959). Key model components include hydrology, sediment yield, nutrient fate, evapotranspiration, groundwater, etc.

4.1.3.2 Baseline and Well-Pad Impacted Scenarios

To isolate and quantify the impact of well-pads on the overall storm-water runoff volume, the following methodology was adopted. Two main scenarios were calibrated for each of the LULC data models; one with well-pads present (SFLR10W) and another with the well-pads land-cover replaced with mixed forest land-cover (SFLR10). The latter scenarios involved the representation of well-pads with the mixed forest land-cover class (FRST) in SWAT. It was assumed that this land-use class will most closely represent the hydrologic response of the hitherto undeveloped land area; these individual scenario models were then assumed to represent the baseline scenarios in 2006 and 2010 respectively. Baseline in this case is used to denote a condition where no well-pads existed as in pre-2006 and when well-pads existed as in 2010.

The second set of model scenarios involved forecast simulations performed for a 10-year projected period (duration from 2010 to 2020); this was done in order to determine the fractional impacts (in comparison to the other land-cover classes) of the current (2010) level of well-pad activity on stream-flow for the projected forecast period. The SWAT model does not have a land-use code specification for well-pads; to account for this the urban industrial land-use categorization code in the SWAT land-use database was selected. This is the land-use categorization in the SWAT land-use database that most closely has the hydrologic response of

surface such as a well-pad. The models were calibrated and validated from 2000 to 2006 and 2007 to 2009 respectively.

4.2 Results and Discussions

4.2.1 Image Classification Results

The accuracy of image classification results was assessed through the use of test and training area mask (TTA mask) created through selected samples for each class. A minimum of thirty samples were selected for each class except the Barren class which had fewer samples due to lack of ample samples that represent that class in the study area. An error matrix was then created using the TTA mask. Three measures for assessing the accuracy of the classification were used; the user's, producer's accuracy and the overall accuracy. The user's accuracy measures the probability of a classified pixel representing the category on the ground whiles the producer's accuracy measures the probability of a reference pixel being correctly classified (Congalton, 1991). For the 2006 classified data, user's accuracy was over 80 percent for all the classes except for the deciduous forest class just as was seen in the user's accuracy for the 2010 classification. Producer's accuracy was over 66 percent for all classes.

The user's accuracy for all classes for the 2010 classified data was over 68 percent with the exception of the deciduous forest and barren classes that had user's accuracies of less than 10 percent. Producer's accuracy was over 64 percent for all classes except for perennial and deciduous forest classes. Figures 2 and 3 present the respective error matrices calculated for the assessment of the individual accuracies associated with the classifications of the two datasets. Two levels of segmentation were used and subsequently followed by classification. Overall, the

two classifications were similar in accuracy as is evident from the overall accuracies of 83% and 84% for 2006 and 2010 classifications respectively.

To investigate the relative changes in percentages of the total watershed area covered by individual land-cover types from 2006 to 2010, the following generalizations were made. The respective user's accuracy measure was multiplied by the classified area for each class to obtain a theoretical accurate area as persists on the ground. A super class of the forest land-cover types was then created by the addition of the respective watershed area percentages of the mixed forest, deciduous forest and the evergreen forest; the barren class was also added to the urban class to form a super class known generally as urban. This resulted in six main classes for the percentage change analysis for the two years; these are Agricultural range land, Forest, Roads, Urban, Water and Well-pads. Results showed that the well-pad class had the most significant change (1043%) in land-cover class from 2006 to 2010, followed by agricultural range land with 4.6%. Road, forest and urban classes had negative changes indicating a reduction in total area from 2006 to 2010. However, this might be attributable to the respective lower user's accuracies obtained for these classes with the 2010 data as compared to that obtained with the 2006 data. Table 1 presents the various land-cover classes with their respective area coverage in the watershed for each year and percentage change in calculated from percentage of the total watershed area occupied by the individual land-cover from 2006 to 2010. The calculations in table 1 involve the assumption that the user's accuracy captures the true cover type as it exists on the ground and therefore this accuracy measure is taken as having the best measure of individual land-cover classification accuracy. However when the respective overall classification accuracies of 83% and 84% for 2006 and 2010 were applied, the relative percent change in well-pads was 1205% with that of agriculture being 18%.

Albeit the forest and agriculture classes had seen the highest changes in acreage, this does not present a true picture of the relative overall watershed changes since the user's accuracy associated with both classes from 2006 to 2010 had significant differences in classification accuracy. The forest cover reduced from 71% to 66%; a reductive change of 7%. This change might reasonably to attributable to an increase in agricultural land-cover much more than it might be due to well-pad construction. The reason for this being that agriculture land-cover had a significantly higher change in acreage than well-pad cover even with the high rate of change for well-pads within the period of study. The percentage change in water cover type increased slightly by 1.5%; this is well correlated with the increase in agricultural cover from the attendant construction of agricultural ponds and irrigation trenches. Figure 2 is a graph illustrating the percentage changes per class. Figures 3 and 4 also show the respective error matrices for the 2006 and 2010 classifications.

Table 10: Land-cover Classes with Respective Area Coverage and Percentage Change from 2006 to 2010 in LRRW

Land-cover Class	Area in 2006/(acres)	% of SLRR in 2006	Area in 2010/(acres)	% of SLRR in 2010	% Change (2006 - 2010)	Class Accuracy (2006)/%	Class Accuracy (2010)/%
Water	4394.53	4.60	4690.68	4.91	6.74	98.00	99.30
Road	1566.74	1.64	1060.42	1.11	-32.32	80.80	68.90
Agric	11989.41	12.55	11702.81	12.25	-2.39	88.90	77.00
Forest	76522.08	80.10	76206.82	79.77	-0.41	66.85	36.58
Well-pad	812.03	0.85	1442.55	1.51	77.65	100.00	68.90
Urban	248.39	0.26	429.90	0.45	73.08	97.00	87.99

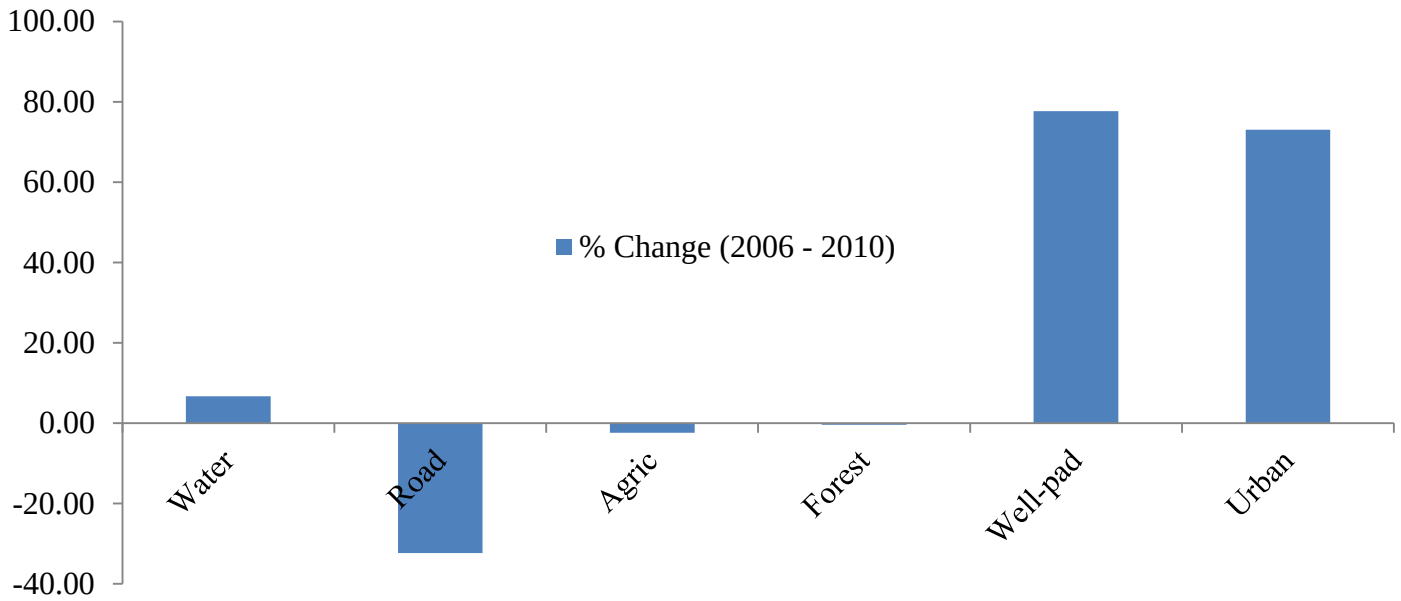

Figure 20: Graph Illustrating the Percentage Changes per Class

Table 11: Error Matrix for OOIA classification of 2006 LRRW Land-cover

User\Preference Class	Water	Road	Agriculture	Forest	Forest_Trans	Barren	Well-pads	Urban	Sum
Water	505092	0	2373	0	9381	0	0	0	516846
Road	0	28469	0	0	0	0	0	6761	35230
Agriculture	0	2706	260269	4524	19610	0	0	5631	292740
Forest	4699	0	0	502240	101202	0	0	0	608141
Forest_Trans	349	0	131029	70431	289306	0	0	0	491115
Barren	0	0	0	0	0	0	1077	0	1077
Well-pads	0	0	0	0	5703	0	0	184248	189951
Urban	0	0	0	0	0	7617	0	0	7617
Unclassified	0	0	0	0	0	0	0	0	0
Sum	510140	31175	393671	577195	42502	7617	1077	196640	

Table 12: Error Matrix for OOIA classification of 2010 LRRW Land-cover

User\Preference Class	Water	Road	Agriculture	Forest	Forest_Trans	Barren	Well-pads	Urban	Sum
Water	2433168	1346	9875	1221	2065	0	0	2818	2450493
Road	0	39571	0	0	0	0	0	17859	57430
Agriculture	0	9060	323036	82370	3167	0	1779	234	419646
Forest	1567	0	41241	222380	20504	0	0	3932	289624
Forest_Trans	4374	0	32435	230741	26970	0	0	5581	300101
Barren	0	0	0	0	0	0	831	0	831
Well-pads	0	70	6646	279	0	0	15694	103	22792
Urban	10385	641	86678	0	0	6229	0	787783	891716
Unclassified	0	0	2	41671	100126	0	0	0	141799
Sum	2449494	50688	499913	578662	152832	6229	18304	818310	

4.2.2 Model Calibration and Validation Results for the SFLRR Watershed

Simulated stream flow was calibrated against monthly measured rates by manually adjusting model parameters identified from sensitivity analysis and literature (White and Chaubey, 2005) to be sensitive to flow simulation until a best fit criterion was achieved. Model initial parameters were calculated from 1997 to 1999 (model warm-up period). Multi-criteria goodness of fit measures was employed in this study; among these measures, the most popular is the Nash-Sutcliffe Efficiency (NSE) criteria. This efficiency measure ($\boldsymbol{E_f}$) essentially measures the proportion of the total variance in the system that the model is able to account for or explain. The equation is as follows:

$$\boldsymbol{Ef} = 1 - \left[\sum_{i=1}^{n} \frac{(\widehat{Y}_i - Y_i)}{(Y_i - \overline{Y}_i)}\right] \quad (1)$$

Where n = sample size, $\widehat{Y}_i$ and Y_i predicted and measured values of dependent variable, $\overline{Y}_i$ = mean of measured values of Y. In general a stream-flow model simulation is judged satisfactory if $\boldsymbol{E_f} \geq$ 0.5 (Moriasi et al., 2007). The results of the multi-criteria measures for the calibration and validation periods for both models are presented in table 4. The calibration NSE for both models was 0.51 and 0.52 for SFLR10 and SFLR10W respectively; implying that on the average both models can account for 51.5% of the total variance in the calibration dataset. The validated model NSE was 0.9 and 0.89 respectively for SFLR10 and SFLR10W. SWAT simulates total flow as a sum of the separated baseflow and surface flow components. Graphical plots (hydrographs) of the baseflow and surface flow are presented for the calibration and validation periods in figures 3 and 4.

Table 13: Multi-criteria model efficiency measures for respective calibration and validation

	Total Flow			
Efficiency Criteria*	Calibration		Validation	
	SFLR10	SFLR10W	SFLR10	SFLR10W
NSE	0.52	0.51	0.89	0.90
R^2	0.51	0.51	0.94	0.95
PBIAS	1.57	-0.56	11.12	10.20
RSR	0.29	0.26	0.45	0.44
RMSE	0.45	0.45	3.65	3.55

*Multi-criteria measures presented in Moriasi et al., (2007),
NSE: Nash-Sutcliffe Efficiency (satisfactory if ≥ 0.5),
R^2: Coefficient of determination,
PBIAS: Percent bias (PBIAS) measures the average tendency of the simulated data to be larger or smaller than the corresponding observed data. Positive = under-prediction and vice versa (satisfactory if ± 25%),
RSR: ratio of RMSE to standard deviation of observations (satisfactory if ≤ 0.7)

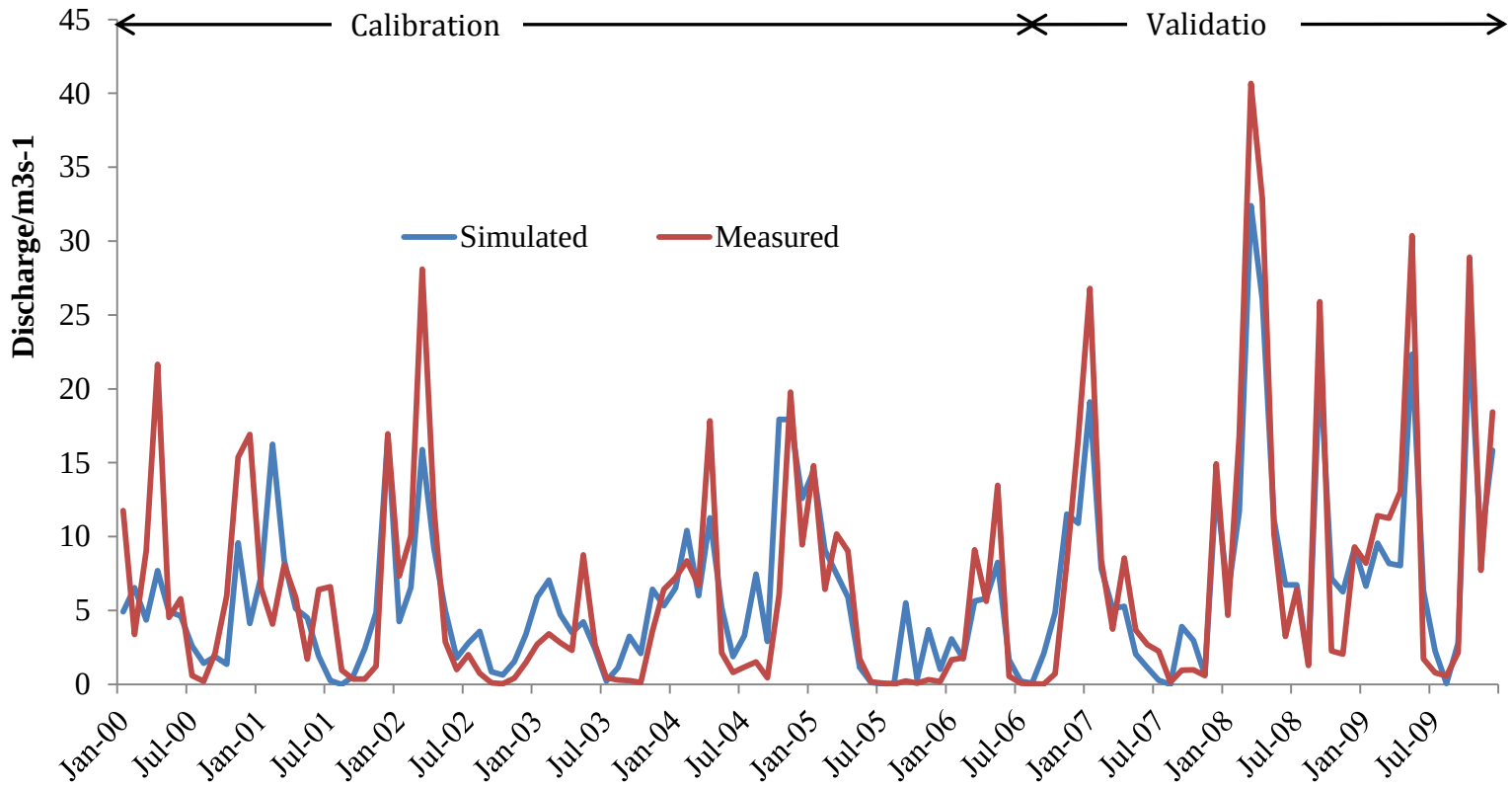

Figure 21: SFLR10 discharge hydrographs for total flow

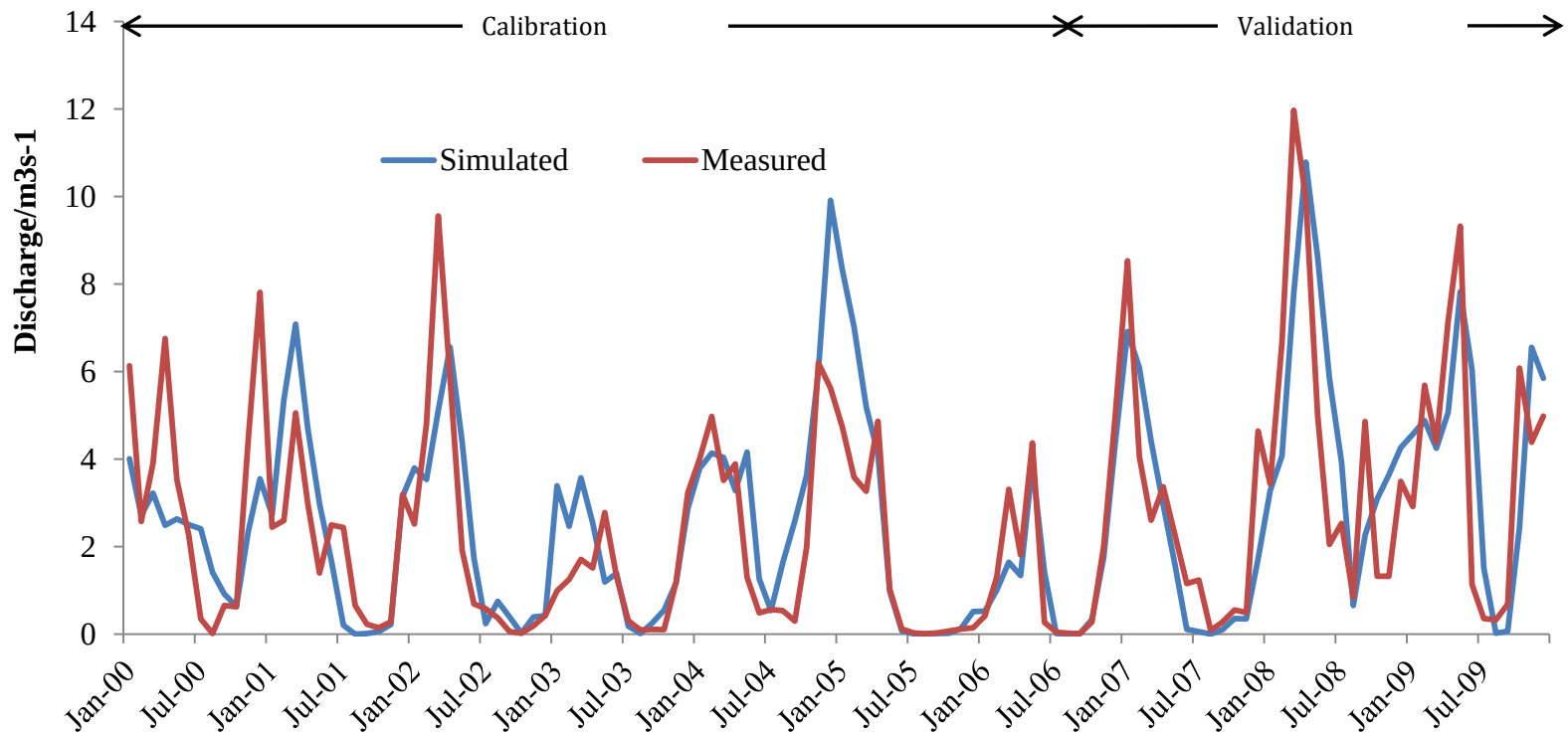

Figure 22: SFLR10 discharge hydrographs for sub-surface flow

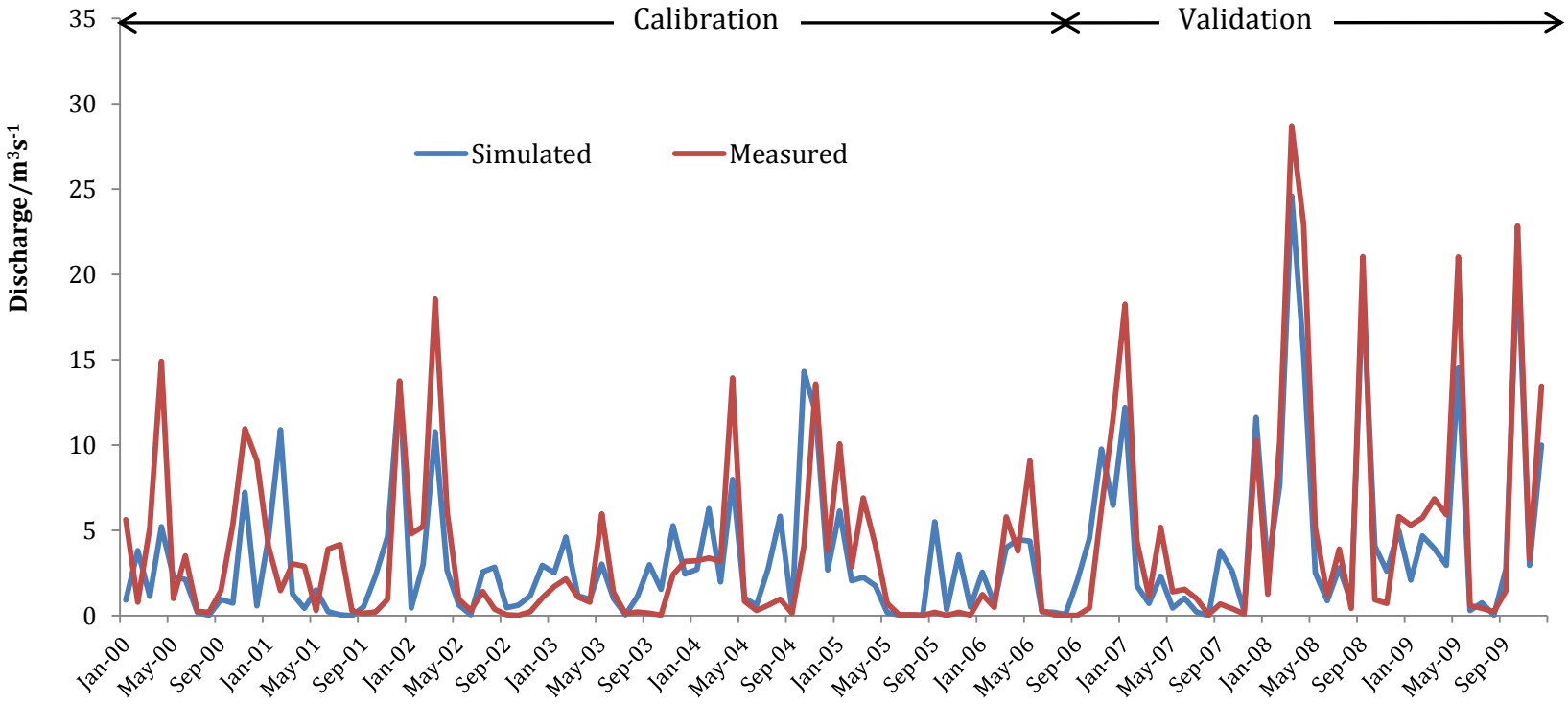

Figure 23: SFLR10 discharge hydrographs for surface flow

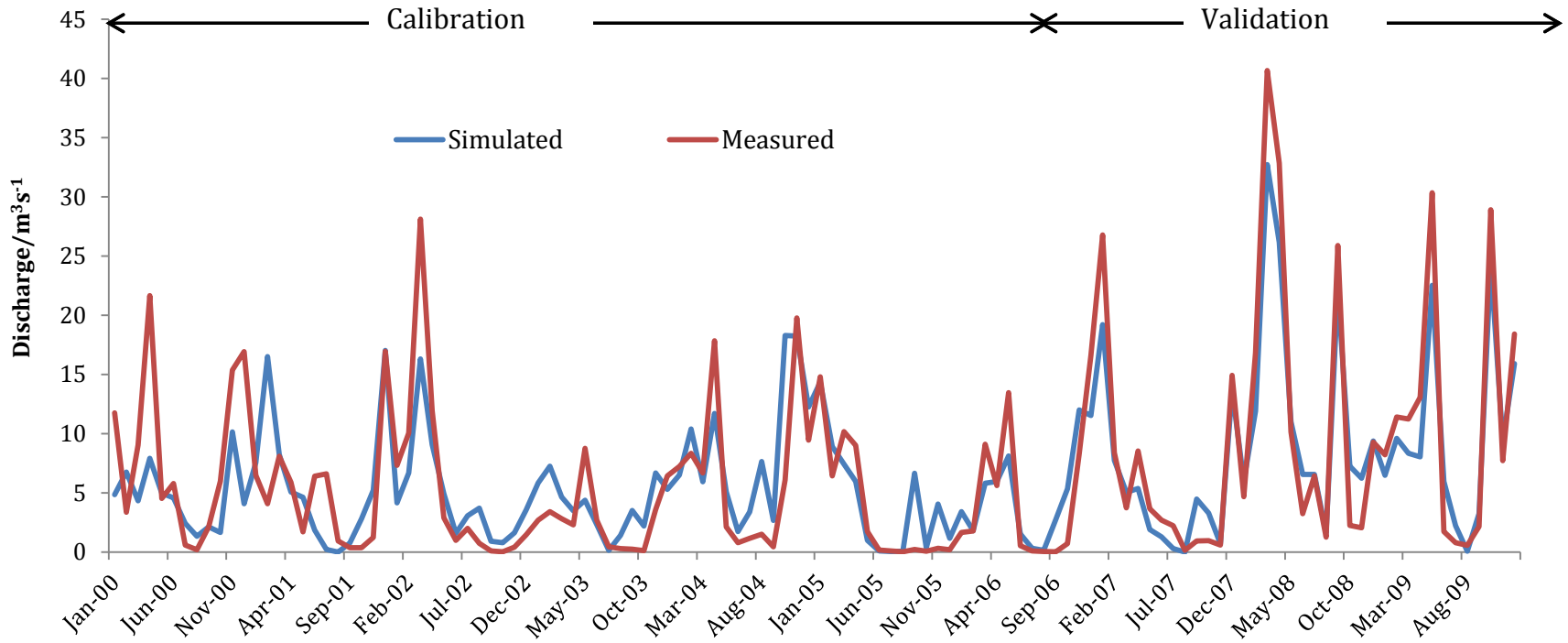

Figure 24: SFLR10W discharge hydrographs for total flow

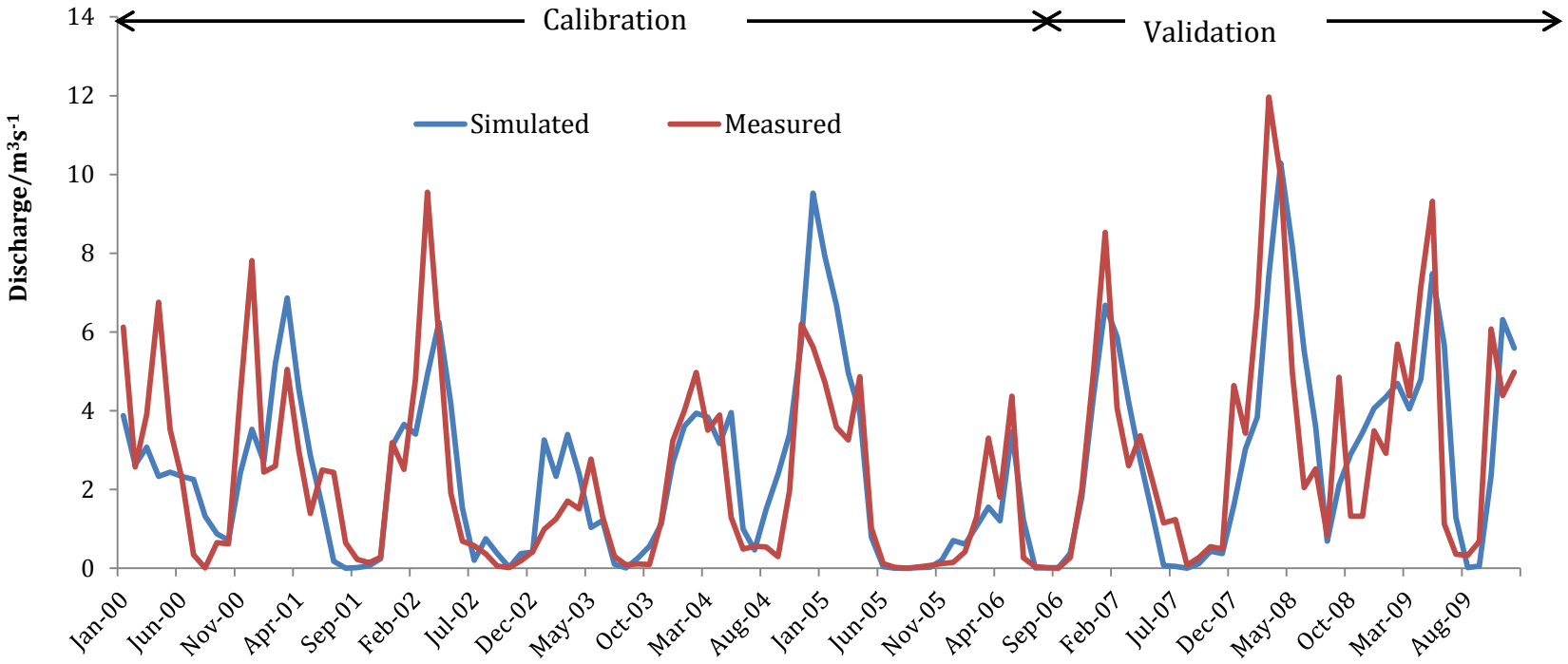

Figure 25: SFLR10W discharge hydrographs for sub-surface flow

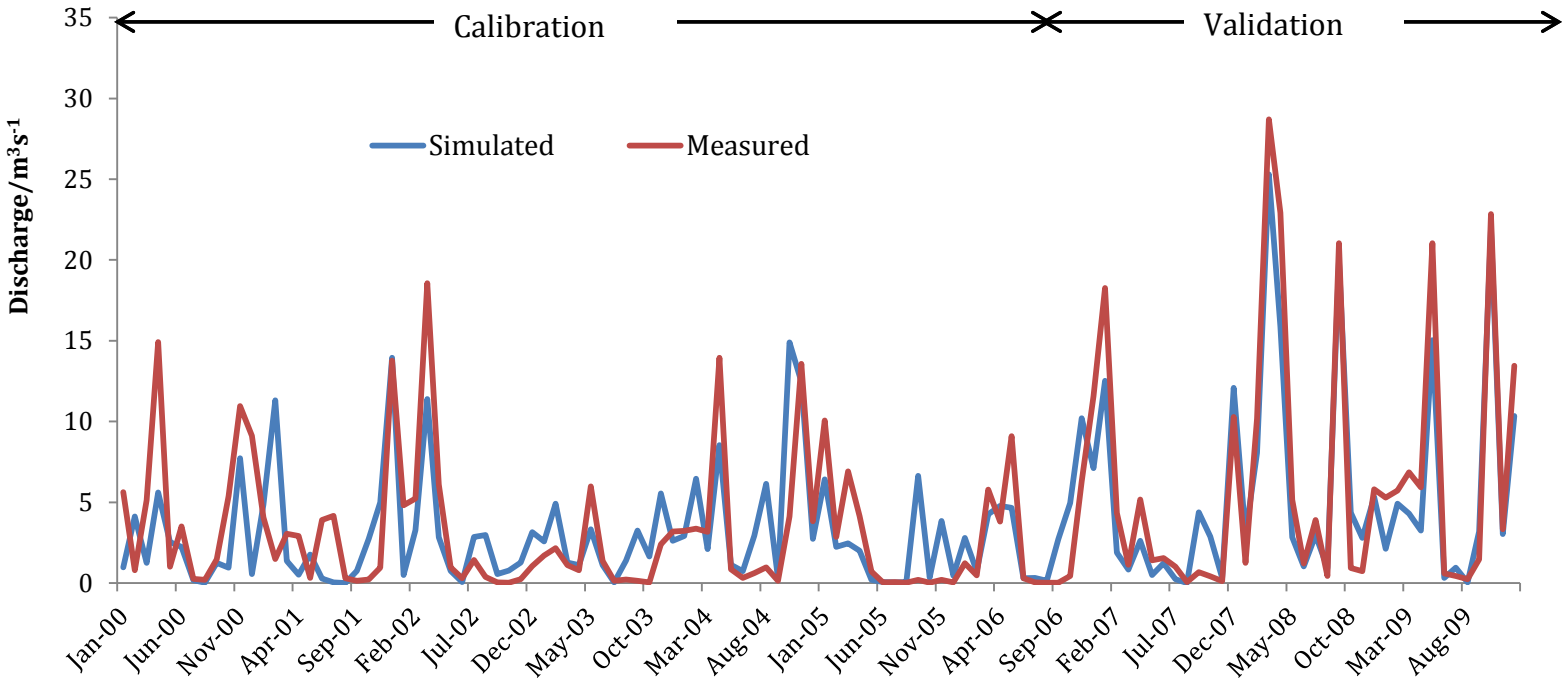

Figure 26: SFLR10W discharge hydrographs for surface flow

The validated models showed an increase in surface runoff depth for the scenarios where well-pads were present in the watershed over when the well-pads were represented by the mixed forest land-cover. Simulated average annual flow depth for the validation period for both scenarios increased from 226.33 mm to 249.61 mm (a change of ~10.3 %). Since these two scenarios representing the 2006 and 2010 land-cover scenarios, it implies that the identified 78% change from 2006 to 2010 in well-pad land-cover corresponds to a 10% increase in storm water runoff depth measured at the sub-basin outlet. The validity of the preceding statement holds only when it is considered that classification accuracies are fairly similar and equifinality is reduced to a minimum. Since the various land-cover classes had corresponding changes from 2006 to 2010, the identified 10% change in runoff depth cannot be differentially attributed to well-pads alone.

To account for this differential impact of well-pad activity on the storm water runoff depth in the sub-basin, forecast simulations were performed with the two baseline scenarios. The forecast scenarios essentially predict the projected differential impact on runoff depth if the level of well-pad activity in 2010 is maintained for a projected 10-year period (up to 2020). That is basically predicting the impact of shale-gas related infrastructure on runoff if no more of such infrastructure is constructed for the next 10-years and the general land-cover in the sub-basin remains fairly the same. For the model with well-pads present, runoff depth was predicted to marginally increase from 249.61 mm in 2010 to 249.81 mm by 2020. Considering the scenario where no well-pads or shale-gas related infrastructure existed in the sub-basin, runoff depth was predicted to also marginally increase from 226.33 mm in 2010 to 226.51 mm by 2020. From these forecast results, runoff is predicted to increase by 23.3 mm from when well-pads were introduced for the projected 10-year period (a change of ~10.3%); this change is the differential impact of the presence of shale-gas infrastructure in the sub-basin.

4.2.4 Limitations of the Flow model

There are several limitations of the model as detailed in the previous sections. First among these is the fact that the model is highly limited by the level of accuracy associated with the classified LULC image. The respective overall accuracies of 83% and 84% for 2006 and 2010 LULC classifications presented by the error matrices in tables 2 and 3. It is important to note there are other measures of classification accuracy that are of peculiar importance especially as a specific land-cover type such as well-pads is being studied. One such measure is the user's accuracy which essentially measures the certainty that a classified pixel actually represents that cover type on the ground. The distributions of 2006 and 2010 user's accuracies for all classes within their respective matrices have standard deviations of 0.13 and 0.34 with means of 0.88 and 0.61 respectively. These distributions have disparate variances indicating a lack of consistency in classifications among the individual classes across the two datasets. This is a limitation that requires further studies to assess classification accuracy impacts on model outputs.

Other sources of limitation for the model are the fact that the model was only manually calibrated and no extensive automatic calibration or uncertainty analyses were performed on the calibrated models. The lack of an uncertainty analysis in the model calibration stage introduces bias in the interpretation of model results owing to equifinality (Beven and Binley, 1992). This also limits the ability to use the model as an effective tool to analyze the inherent dynamics between the interactions human activities and the natural systems in the catchment.

4.3 Conclusion

The main objectives of the study are to: 1) quantify the land-use land-cover change in the South Fork of the Little Red River Watershed (SFLRR) with specific emphasis on natural gas related activities (well-pads) and 2) use the quantified data to examine the impact of natural gas related activities on storm water runoff generation in the South Fork of the Little Red River (SFLRR). There were generally decreases in land-cover for the forest, road and urban classes; albeit changes in the road and urban classes might be logically taken to be much more skewed by classification accuracy than in the case of the forest class. Agricultural land, water and well-pads on the other hand consistently increased in coverage from 2006 to 2010. Well-pads significantly increased in land-cover from 2006 to 2010 by 630.55 acres (representing 0.65% of the total SFLRR area). Other land-cover classes that increased in coverage were urban and water; totaling slightly over 5% of the sub-basin area. On the other hand, agriculture and forest cover types decreased by 2.39%.

The next objective of the study was to examine the impact of the identified change in land-cover attributable to well-pads on storm water runoff generation in the sub-basin. The result from calibration and validation periods is inconclusive in that the differential effect of the change in well-pads alone could not be isolated. For a 10-year forecast scenario, runoff is projected to increase by 23.3 mm which is roughly a 10% projected increase in runoff. This represents the change in runoff that is attributable the differential change in shale-gas related infrastructure. Therefore, for a 78% in well-pad land-cover, runoff is projected to increase by roughly 10% over a 10-year period assuming current conditions in the sub-basin stays fairly constant.

Acknowledgement

I would like to express my appreciation to Mr. Jaysson Funkhouser for his direction and advice on the key areas in the watershed that need model evaluation and his support with subsequent inquiries. Also I am grateful to Dr. Mansoor Leh and Dr. Naresh Pai of the Department of Biological and Agricultural Engineering of the University of Arkansas for their invaluable assistance on technical issues relating to the SWAT model. My profound appreciation goes to Mr. Bruce Gorham of Centre for Advanced Spatial Technologies of the University of Arkansas for his assistance during the image classification stage of the study.

Lastly to my very supportive and encouraging committee members: Dr. Jackson Cothren, Dr. John Brahana, Dr. Greg Thoma and Dr. Ralph Davies for their valuable, direction, advice, critique and evaluation of this study.

References

(CAST), Center for Advanced Spatial Technologies. 2006. “Arkansas Watershed Information System.” http://watersheds.cast.uark.edu/viewhuc.php?hucid=11010014.

(USFWS), U. S. Fish and Wildlife Service. 2009. “Arkansas Best Management Practices for Natural Gas Pipeline Construction and Maintenance Activities in the Fayetteville Shale Area, Upper Little Red River Watershed.” Conway, Arkansas: U. S. Fish and Wildlife Service, Arkansas Ecological Services Field Office.

Al-Khudhairy, D.H.A, I Caravaggi, and S Giada. 2005. “Structural Damage Assessments from Ikonos Data Using Change Detection , Object-Oriented Segmentation , and Classification Techniques.” Photogrammetric Engineering and Remote Sensing 71 (7): 825–837.

Andrews, A., P. Folger, M. Humphries, M., Copeland, C., Tiemann, and R. Meltz. 2009. Unconventional Gas Shales: Development , Technology , and Policy Issues. Congressional Research Service Report. http://www.fas.org/sgp/crs/misc/R40894.pdf.

Arthur, J, B Coughlin, B Bohm, and ALL Consulting. 2010. “Summary of Environmental Issues, Mitigation Strategies, and Regulatory Challenges Associated with Shale Gas Development in the United States and Applicability to Development and Operations in Canada.” In Proceedings of the Canadian Unconventional Resources and International Petroleum Conference . Society of Petroleum Engineers., 18. Calgary.

Blaschke, Thomas, and Josef Strobl. 2001. “What ’ s Wrong with Pixels ? Some Recent Developments Interfacing Remote Sensing and GIS.” GeoInformation Systems 14 (6): 12–17. http://courses.washington.edu/cfr530/GIS200106012.pdf.

Chow, V. T. 1959. Open-channel Hydraulics, McGraw-Hill, New York.

Congalton, Russell G. 1991. “A Review of Assessing the Accuracy of Classifications of Remotely Sensed Data.” Remote Sensing of Environment 46 (October 1990): 35–46.

Congalton, Russell G. 2005. “Thematic and Positional Accuracy Assessment of Digital Remotely Sensed Data.” In Proceedings of the Seventh Annual Forest Inventory and Analysis Symposium, 149–154.

Dendy, F.E, and G.C Bolton. 1976. “Sediment Yield-Runoff-Drainage Area Relationships in the United States.” Journal of Soil and Water Conservation 31 (6): 264–266.

District, United States Army Corps of Engineers (USACE) Little Rock. 2011. “Greers Ferry Lake.” http://www.swl.usace.army.mil/parks/greersferry/index.htm.

Easton, Z. M., D. R. Fuka, E. D. White, a. S. Collick, B. Biruk Asharge, M. McCartney, S. B. Awulachew, a. a. Ahmed, and T. S. Steenhuis. 2010. “A Multi Basin SWAT Model

Analysis of Runoff and Sedimentation in the Blue Nile, Ethiopia." Hydrology and Earth System Sciences Discussions 7 (3) (June 25): 3837–3878. doi:10.5194/hessd-7-3837-2010. http://www.hydrol-earth-syst-sci-discuss.net/7/3837/2010/.

Funkhouser, Jaysson E. 2012. "Personal Communication."

Green, W. H., and G. A. Ampt. 1911. "Studies on Soil Physics, J. Agric. Sci., 4(1), 1 – 24." Journal of Agricultural Science 4 (1): 1–24.

Gurung, P., and L. Bharati. 2012. "Downstream Impacts of the Melamchi Inter-Basin Water Transfer Plan (MIWTP) Under Current and Future Climate Change Projections." Hydro Nepal: Journal of Water, Energy and Environment April 2012: 23–29. http://www.iwmi.cgiar.org/offices/asia/south_asia/nepal/pdf/specia_issue_hn_bulletin_final_web.pdf.

Henleya, W. F., M. A. Pattersona, R. J. Nevesa, and A. Dennis Lemlyb. 2000. "Effects of Sedimentation and Turbidity on Lotic Food Webs: A Concise Review for Natural Resource Managers." Reviews in Fisheries Science 8 (2): 125–139.

Im, J., J. R. Jensen, and J. a. Tullis. 2008a. "Object-based Change Detection Using Correlation Image Analysis and Image Segmentation." International Journal of Remote Sensing 29 (2) (January): 399–423. doi:10.1080/01431160601075582. http://www.tandfonline.com/doi/abs/10.1080/01431160601075582.

Im J, 2008b. "Object-based Change Detection Using Correlation Image Analysis and Image Segmentation." International Journal of Remote Sensing 29 (2) (January): 399–423. doi:10.1080/01431160601075582. http://www.tandfonline.com/doi/abs/10.1080/01431160601075582.

Johansen, K, L A Arroyo, S Phinn, and C Witte. 2007. "Object-Oriented change detection Of Riparian Environments From High Spatial Resolution Multi-Spectral Images." ISPRS Journal of Photogrammetry and Remote Sensing (1).

Laliberte, Andrea S., Albert Rango, Kris M. Havstad, Jack F. Paris, Reldon F. Beck, Rob McNeely, and Amalia L. Gonzalez. 2004. "Object-oriented Image Analysis for Mapping Shrub Encroachment from 1937 to 2003 in Southern New Mexico." Remote Sensing of Environment 93 (1-2) (October): 198–210. doi:10.1016/j.rse.2004.07.011. http://linkinghub.elsevier.com/retrieve/pii/S0034425704002147.

Matherne, Anne Marie. 2006. Effects of Roads and Well-pads on Erosion in the Largo Canyon Watershed, New Mexico, 2001–02. Denver, CO. http://pubs.usgs.gov/sir/2006/5039/pdf/sir2006-5039.pdf.

Mcdermid, Gregory J, Alysha Pape, Michael S Chubey, and Steven E Franklin. 2012. "Object Oriented Analysis for Change Detection." http://www.ecognition.com/sites/default/files/354_1.pdf.

Moriasi, D N, J G Arnold, M W Van Liew, R L Bingner, R D Harmel, and T L Veith. 2007. "Model Evaluation Guidelines for Systematic Quantification of Accuracy in Watershed Simulations." Transactions of the ASABE 50 (3): 885–900.

Niemeyer, I., S. Nussbaum, and M.J. Canty. 2005. "Automation of Change Detection Procedures for Nuclear Safeguards-related Monitoring Purposes." Proceedings. 2005 IEEE International Geoscience and Remote Sensing Symposium, 2005. IGARSS '05. 3: 2133–2136. doi:10.1109/IGARSS.2005.1526439. http://ieeexplore.ieee.org/lpdocs/epic03/wrapper.htm?arnumber=1526439.

Pai, N., and D. Saraswat. 2011. "SWAT2009_LUC: A tool to activate the land-use change module in swat 2009." Transactions Of The Asabe 54 (5): 1649–1658.

Platt, Rutherford V, and Lauren Rapoza. 2008. "An Evaluation of an Object-Oriented Paradigm for Land-use / Land-cover Classification *." The Professional Geographer 60 (1): 87–100.

Ryherd, S., and C. E. Woodcock. 1996. "Combining Spectral and Texture Data in the Segmentation of Remotely Sensed Image." Photogrammetric Engineering and Remote Sensing 62 (2): 181–194.

S, Lang, F Albrecht, and T Blaschke. 2006. "Lang S, F Albrecht & T Blaschke (2006) OBIA-Tutorial – Introduction to Object-based Image Analysis, V 1.0." Salzburg, Autria.

Sandahl, J. F., D. H. Baldwin, J. J. Jenkins, and N. L. Scholz. 2007. "A Sensory System at the Interface Between Urban Storm Water Runoff and Salmon Survival." Environmental Science & Technology 41 (8): 2998–3004. http://www.ncbi.nlm.nih.gov/pubmed/17533870.

Survey, Arkansas Geological (AGS). 2011. "Arkansas Physiographic Regions." http://www.geology.ar.gov/education/physio_regions.htm.

Tang, Yuqi, Xin Huang, Kanako Muramatsu, Liangpei Zhang, Remote Sensing, and Luo Yu Road. 2010. "Object-oriented change detection for high-resolution imagery." International Archives of Photogrammetry and Remote Sensing and Spatial Information Science XXXVIII.

U.S. Department of Agriculture - Soil Conversation Service (USDA-SCS). 1972. Estimation of Direct Runoff From Storm Rainfall. U.S. Department of Agriculture, Soil Conservation Service, Washington, D.C., Pp. 10.1-10.24. SCS National Engineering Handbook, Section 4, Hydrology. Chapter 10.

Wachal, D.J. 2008. "Characterizing Storm Water Runoff from Natural Gas Well Sites in Denton County, Texas. Denton, Texas". University of North Texas. digital.library.unt.edu/ark:/67531/metadc11064/.

White, Kati L, and Indrajeet Chaubey. 2005. “Sensitivity Analysis , Calibration , And Validations For A Multisite And Multivariable Swat Model 1.” Journal of the American Water Resources Association 41 (5): 1077–1089.

Williams, H. F. L., D. L. Havens, K. E. Banks, and D. J. Wachal. 2007. “Field-based Monitoring of Sediment Runoff from Natural Gas Well Sites in Denton County, Texas, USA.” Environmental Geology 55 (7): 1463–1471. doi:10.1007/s00254-007-1096-9.

Williams, J.R., and H.D. Berndt. 1977. “Sediment Yield Prediction Based on Watershed Hydrology.” Transactions of the ASAE: 1100–1104.

Wu, M., Y. Demissie, and E. Yan. 2012. “Simulated Impact of Future Biofuel Production on Water Quality and Water Cycle Dynamics in the Upper Mississippi River Basin.” Biomass and Bioenergy 41: 44–56. doi:10.1016/j.biombioe.2012.01.030.

Yan, Gao. 2003. “Pixel Based and Object Oriented Image Analysis for Coal Fire Research.”

Zhang, X, R Srinivasan, and F Hao. 2007. “Predicting Hydrologic Response to Climate Change in the Luohe River Basin Using the SWAT Model.” American Society of Agricultural and Biological Engineers 50 (3): 901–910.

CHAPTER 5: OBJECTIVE THREE

Abstract

The United States Fish and Wildlife Services (USFWS) has in collaboration with major stakeholders in the Fayetteville Shale play developed Best Management Practices (BMPs) for implementation in the Fayetteville Shale natural gas development area in north-central Arkansas. This was mainly done to encourage energy and energy-support companies operating within the play to voluntarily adopt these BMPs in order to ensure improved environmental practices in exploration, drilling and reclamation activities. To ensure the effectiveness of the proposed BMPs there is the need to conduct evaluative studies to assess their respective effectiveness. However, no study could be located at the time of this research, which evaluates the effectiveness of the proposed BMPs on the environmental mitigation efforts in the Fayetteville Shale Play.

In this study, a modeling approach was adopted to simulate conditions and evaluate the effectiveness or efficiency of BMPs meant to control flow in the South Fork of the Little Red River sub-watershed located within the Fayetteville Shale play. Two Soil and Water Assessment Tool (SWAT) flow models calibrated and validated with and without shale-gas-related infrastructure were simulated for flow to form model baseline scenarios. Three BMPs identified to control flow were introduced and simulated for the simulation periods. The differences in the flow output at the watershed outlet for each BMP scenario were derived by comparing baseline and respective BMP scenarios. Results show that BMPs have an average effectiveness of approximately 80% in reducing shale-gas attributable flow.

Keywords: *SWAT runoff modeling, BMPs, Fayetteville Shale Play, GIS*.

5.0 Introduction

5.1 Background

Best management practices (BMPs) have been proposed and implemented in various settings where human-related activities are thought to have negative or potentially adverse effects on the natural state of the environment. The United States Environmental Protection Agency (USEPA) has various guidelines and standards for BMP implementation in various environmental mitigation efforts. Some of the areas of concern include erosion, sedimentation and storm water pollution in various industrial undertakings. BMPs, among others are part of regulatory guidelines for storm water impact mitigation that are implemented by the EPA through the National Pollutant Discharge Elimination System (NPDES) (USEPA, 2012).

Also, the U.S Fish and Wildlife Services (USFWS) in collaboration with the Arkansas Oil and Gas Commission, the Arkansas Department of Environmental Quality, members of the academic community and some energy companies have developed various BMP guidelines for exploration and production activities in the Fayetteville Shale Play. However, the activities of the oil and gas industry are exempt from NPDES regulatory provisions. Therefore the guidelines are meant to encourage voluntary implementation by the energy companies of the proposed BMPs during the exploration and drilling stages (USFWS, 2007). At the time of this study, no literature could be located that deals with the evaluation of the proposed BMPs or their potential to mitigate adverse environmental changes as a result of shale-gas activities. This study is particularly concerned with storm water generation which is known to negatively impact erosion and sedimentation (Edwards and Owen, 1991). A modeling approach is employed to evaluate the potential impact of the implementation of storm water BMPs in a shale-gas activity watershed.

The SWAT model has been employed in various studies involving BMP impact simulations. Due to its ability to simulate BMPs intended for mostly agricultural purposes and the flexibility to adapt the BMPs for other applications, the USEPA supports the use of the model for quantification requirements in watershed management planning (USEPA, 2005). Furthermore, the model is included as one of several water quality models integrated in a multi-purpose analytical software environment implemented with geographic information analysis capability (BASINS, 2012). The model has been used for specific applications such as evaluating and analyzing BMPs for reducing phosphorus levels (Lee et al., 2010) and evaluating BMPs for storm water control (Kaini et al., 2007; Hunt et al., 2009).

In the case of the shale-gas activities the major environmental concerns include the potential impacts on climate change due to climate forcing effects of the released methane gas (Wood et al., 2011; Schrag, 2012). In addition to the climate change impacts, it is also known that the clearing of vegetation and the use of heavy exploratory equipment contribute to changes in runoff generation and sediment yield (Seguis et al., 2004; Entrekin et al., 2011). These ultimately have negative impacts on the runoff generation, aquatic life and the overall water quality of the subject watersheds (Harney and Hubert, 1984; Hogg and Norris, 1991; Deletic and Maksimovic, 1998). It is therefore imperative that the storm water BMPs intended for implementation in the Fayetteville Shale Play region be evaluated to determine their effectiveness in mitigating the negative environmental impacts.

5.2 Methods and Materials

5.2.1 Study Area

The South Fork Little Red River (SFLRR) is a 386km^2 sub-basin of the Little Red River Watershed with a 10-digit Hydrologic Unit Code of 1101001402. The sub-basin is located within Van Buren County in north-central Arkansas. This study area was selected due to fact that it is the only sub-basin within the Little Red River Watershed that sees major shale-gas activities and also has reliable gage station data at the sub-basin outlet. The average annual precipitation in the region is approximately 1270 – 1320 mm with winter and summer average temperatures of 2^{o}C and 30^{o}C respectively. Precipitation normally occurs less frequently during the months of June, July and August; summers are hot and humid while winters are relatively mild and short. Mean annual high and low temperatures are 5^{o}C and 17^{o}C respectively (NOAA, 2012).

The land-cover distribution is approximately 80% forest land, 12% agricultural land, 1% Urbanized, 5% water and 2% shale-gas infrastructure. There two main population centers within the sub-basin; namely the cities of Scotland and Clinton with population density of 5 persons per square kilometer (CAST, 2007). Elevation in the sub-basin ranges between 149 and 595 m above mean sea level. The major soils are Steprock-Mountainburg complex which are loamy skeletal, red clayey loam (Udults) and some fine-silty and loamy soils (USDA-NRCS, 2013) with depths ranging between 0.5 and 2 m. With the combination of available stream flow observation data and the presence of a significant shale-gas infrastructure, the sub-basin presents a unique opportunity to evaluate the potential impact of BMPs meant to control runoff possibly attributable to shale-gas activities.

5.2.2 SWAT model Description

SWAT is a physically based and continuous time semi-distributed parameter model that is developed to simulate the effects of land management practices on water, sediment, and agricultural chemicals in large and complex watersheds over long periods of time (Arnold et al., 1998). The version of the model that was used for this study is ArcSWAT; an ArcGIS extension that provides a graphical user interface for SWAT within a GIS environment. The model requires input data in DEM, land use data, soils and slope classes for the delineation of Hydrologic Response Units (HRUs). HRUs are created through an overlay of respective slope classes, soils and land-use data. Aggregations of overlays of the same slope class, land-use and soil type are grouped into the same HRU.

The HRU is the basic computational unit of the model and helps to ensure efficient computation. SWAT simulates the hydrology at each HRU using the water balance equation, comprising precipitation, runoff, evapotranspiration, percolation and base flow components. Runoff, stream-flow and groundwater flow is simulated within the watershed and at the watershed outlet (Gitau et al., 2006). Runoff is computed with either the Soil Conservation Service Curve Number method (USDA-SCS, 1972) or the Green and Ampt infiltration method (Green and Ampt, 1911) and routed to the closest channel using the Muskingum method (Chow, 1959). BMPs are implemented in SWAT by specifying or modifying parameter values that are meant to represent the desired BMP in a sub-basin. Specific BMPs such as filter strips are represented in SWAT by modifying the FILTERW parameter while other BMPs such as grassed waterways is simulated by modifying the parameter CH_N(1) (manning's 'n' value for the main channel).

5.2.3 SWAT model setup

The modeling framework was established in ArcSWAT version 2009 (SWAT2009) in ArcGIS 9.3.1. The watershed was delineated based on an input 10 m digital elevation model (DEM) with threshold specifications in flow accumulation and direction. Land-cover data derived from 4 m aerial imagery by object-oriented image classification was overlaid with soil data and slope class were subsequently divided into hydrologic response units (HRUs) with specific threshold values based on soils, slope and land-use. A trial and error procedure was adopted to pick the optimum values for the data categories. This was to ensure the inclusion of significant areas of land-use and soils while reducing computation overhead by the exclusion of insignificant areas. A total of 214 HRUs were derived from the overlay of soil, slope, land-use and slope class at their respective thresholds. SWAT formatted observed daily rainfall and temperature data from 1950 to 2010 were obtained from the United States Department of Agriculture's Agricultural Research Service (USDA-ARS) climate database (USDA-ARS, 2012) for the weather stations shown in figure 2. The model was calibrated from 1997 to 2006 and validated from 2007 to 2009 with the data from January-1997 to December-1999 serving as the period for computation of model initial (warm-up period) parameters.

5.2.4 BMP Simulation

Three BMPs intended to reduce storm water flow were simulated. These BMPs were selected based on recommendations in USFWS (2007) and USEPA (2005). The selected BMPs were grassed waterways, wetlands and check dams. After selecting the appropriate BMPs, the calibrated (2000 to 2006) and validated (2007 to 2009) flow model was set as the baseline while successive runs with the various BMPs were set as separate BMP scenarios. Grassed waterways are implemented in either natural or constructed channels that are graded to specific dimensions

and lined with suitable vegetation (SWAT, 2005). The purpose of this BMP is to reduce storm water runoff velocity by conveying water from concentrated waterways without causing erosion thus helping to improve water quality. Grassed waterways were implemented in this study in the main channel of the sub-basin to reduce the storm water flow velocity thus reducing the erosive power. This BMP was simulated in SWAT by changing the Manning's "n" (roughness coefficient) value for the main channel (CH_N(1)) assuming a dense grass cover condition. From the SWAT manual a recommended value for Manning's "n" for the selected cover type was determined to be 0.3. The model-calculated main channel length of 45 km, depth and width of 1.4 and 45 m respectively were used thus leading to a channel width-to-depth ratio of 32. Based on an assumption of a fairly uniform main channel soil composition (red clayey loam), an effective hydraulic conductivity of 2.5 mm/hr was determined from recommended values as in (ArcSWAT Manual, 2009).

Next, wetlands were simulated as a BMP to control storm water flow. This BMP was selected for this study in particular since there are no natural wetlands in the study area sub-basin. Wetlands basically serve as impoundments and receive runoff thus effectively allowing loadings from the land area to settle. Wetlands data from the USGS National Hydrographic Dataset (NHD) database for the state of Arkansas was not available at the time of the study to help in possible estimation of wetland parameter based on available data. Therefore wetland simulation parameters were determined as follows. The minimum contributing area for the measured data at the watershed outlet was determined from a method developed by Dickenson and Whiteley (1962) to be 0.74. By proportion the fraction of the basin area that drains into the wetland (WET_FR) was subsequently determined. From HRU analysis, HRUs that had slopes of 3% or less were selected as suitable response unit types for implementation of the wetland BMP

(USFWS, 2007). Through this procedure, a total of approximately 10 km^2 was derived to be the area of the sub-basin that drains into the wetlands. Adopting the method of Wang et al., (2010) in the calculation of WET_FR and applying proportionality as defined earlier, this procedure resulted in a WET_FR value of 0.019 for wetlands. The remaining wetland simulation parameters which account for surface area and volume at principal and emergency spillways were also determined as follows. Assuming that wetlands are constructed such that the surface area does not vary with depth, the volume at principal and emergency spillways could be obtained as a product of wetland depth and surface area. Furthermore, the principal spillway area and volume were constrained to be smaller than the emergency spillway area and volume. With a uniform depth of 0.1 m for the principal spillway surface area and volume were calculated to be 802 X 10^4 m^2 and 80.2 X 10^4 m^3 respectively as emergency spillway surface area and volume were also adjusted for in order to satisfy the model constraints stated earlier.

Finally, impact of introducing check dams to control storm water flow was simulated. Check dams are implemented on areas with concentrated flow and essentially serve to pond water thereby reducing storm water runoff during periods of high flow (ArcSWAT manual, 2005). In this study check dams were simulated as ponds in SWAT and parameters determined as in wetlands BMP. Pond simulation parameters were determined as in wetlands scenarios with the exception that ponds total sub-basin area occupied by ponds was estimated to be 61 X 10 m^2 from shapefile data obtained from CAST(2010).

To quantify the effectiveness of the BMPs at reducing storm water flow that can be differentially attributable to shale-gas infrastructure, the difference in simulated flow rates for model runs with and without well-pad cover types was determined. This value was divided by the difference in baselines simulated flow rates of the two models and expressed as a percentage to obtain the

BMP effectiveness at reducing flow that is caused by the presence of well-pads in the sub-basin. This value is termed well-pad-flow in table 2. The model calibrated without well-pad land cover type was set-up with the exact parameters as in the previous model to achieve the similar efficiency criteria measures. The only difference was that well-pads were simulated as normal vegetated forest land. The difference in the simulated surface flows between the two models is the storm water flow attributable to the impact well-pads have on flow in the sub-basin. This analysis was done in order to isolate and quantify the effectiveness of the BMPs on storm water flow as impacted by shale-gas infrastructure.

Table 14: Implemented BMPs and how they were modeled in SWAT

Scenario Name	Description	SWAT parameter	SWAT file to be modified
Baseline	Baseline scenario		
Scenario 1	Grassed Waterways	Manning's "n" (roughness coefficient) value for the main channel (CH_N(1))	Sub-basin (.sub)and routing (.rte)
Scenario 2	Wetlands	All wetland parameters that apply to flow	Pond component in sub-basin (.pnd)
Scenario 3	Check dams	Simulated as ponds. All pond parameters that apply to flow	Wetland in pond component (.pnd)

5.2.5 BMP Impact

BMP impact on flow was evaluated with baseline and the various BMP scenarios calibrated and validated against monthly observation data. The effectiveness of a BMP in reducing or controlling storm water flow was calculated by subtracting the simulated surface flow components of each BMP scenario from that of the baseline. The result was then divided by the baseline simulated surface flow and expressed as a percentage. The obtained value is the measure of the BMP effectiveness at reducing flow in the sub-basin.

5.3 Results and Discussion

The baseline scenario was simulated from 2000 to 2009 from the calibrated (2000 to 2006) and validated (2007 to 2009) models with a warm-up period set from 1997 to 1999. Calibration and validation Nash-Sutcliffe efficiencies (NSE) were 51% and 90% respectively. The calibrated model had a slight over prediction bias of 0.48% as the validated model was under-predicted by 10.2% with RMSE values of 0.45 and 3.6 respectively. Simulated average surface flow rate for the baseline scenario as determined at the sub-basin outlet was 3.83 m^3s^{-1}. Figure 1 shows the hydrographs for the total-flow, base-flow and surface-flow components.

The study examined flow reductions between baseline and BMP scenarios. With the introduction of grassed waterways, simulated surface flow (storm water flow) reduced from the baseline scenario value of 3.83 m^3s^{-1} to 3.47 m^3s^{-1}. This represents a grassed waterways BMP effectiveness of 9% for storm water flow during the study period (2000 to 2009). This simulation result was obtained by modifying the manning's "n" value for the main channel from a baseline value of 0.014 to 0.3 in order to represent the effect of introducing a dense cover grassed waterways. However the generated storm water flow is the flow contributed by all the other land cover categories (agriculture, forest, transportation, well pads, etc). Table 2 shows the baseline and adjusted scenario values of parameters used for the simulation of the respective BMPs.

To account for the change in flow rate impacted by the presence of well-pads, a separate model was calibrated and validated with well-pads cover type replaced with mixed forest cover. This was done with the assumption that the natural undisturbed land area occupied by well-pads was hitherto most likely occupied by mixed forest land-cover. The model evaluation or efficiency criteria values for both the calibration and validation periods are presented in table 3 for both

models. Also table 4 shows the baseline flow rates and the respective BMP effectiveness for each scenario.

Table 15: Model Efficiency criteria for calibration and validation simulation

Calibration		
Criteria	**Model with Well-Pads**	**Model without Well-Pads**
NSE	0.51	0.52
PBIAS	-0.48	1.57
RMSE	0.45	0.45
R2	0.51	0.51
RSR	0.26	0.29
Validation		
NSE	0.90	0.89
PBIAS	10.20	11.12
RMSE	3.55	3.65
R2	0.95	0.94
RSR	0.44	0.45

Table 16: Model effectiveness for the respective BMP

Scenario	Model with Well-Pad[a]	Model without Well-Pad[a]	BMP Effectiveness[b]	BMP Effectiveness on Well-Pad[c]
Baseline	3.83	3.6		
Grassed Waterways	3.47	3.26	9	91
Check Dams	3.67	3.44	16	100
Wetlands	2.7	2.59	30	48

[a] Flow rate measured in m^3s^{-1} at sub-basin outlet, **[b]** BMP effectiveness measured with all land-cover types expressed as percentage
[c] Effectiveness of respective BMPs at reducing flow attributable to well-pads expressed as a percentage

Table 17: Default and adjusted values of BMP parameters for respective BMP scenarios

Parameter*	BMP						
	Grassed Waterways		Check Dams		Wetlands		Units
	Default	Adjusted Value	Default	Adjusted Value	Default	Adjusted Value	
CH_N(1)	0.014	0.3					
PND_FR			0	0.026			
PND_PSA			0	1000			ha
PND_PVOL			0	100			10^4 m^3
PND_ESA			0	200			ha
PND_EVOL			0	200			10^4 m^3
PND_VOL			0	0			10^4 m^3
WET_FR					0	0.26	
WET_NSA					0	1000	ha
WET_NVOL					0	100	10^4 m^3
WET_MXSA					0	200	ha
WET_MXVOL					0	200	10^4 m^3
WET_VOL					0	0	10^4 m^3

*CH_N(1) Manning's 'n' value for main channel; PDN_FR fraction of sub-basin that drains into ponds; PND_PSA principal spillway pond surface area; PND_PVOL principal spillway pond volume; PND_ESA emergency spillway pond surface area; PND_EVOL emergency spillway pond volume; PND_VOL initial volume of water in pond; WET_FR fraction of sub-basin that drains into wetlands; WET_NSA normal level wetland surface area; WET_NVOL normal level wetland volume; WET_MXSA maximum water level wetlands surface area; WET_MXVOL maximum water level wetlands volume; WET_VOL initial volume of water in wetlands.

The curve number for the second model (without well-pad) was adjusted for mixed forest land cover which ultimately decreased the average curve number for the entire sub-basin. This resulted in a reduction in the average flow rate and slightly better fit to the observation data as in shown in NSE of 0.52. The difference in flow rates between both models was determined to be 0.23 m^3s^{-1} (heretofore referred to as well-pad surface flow). Much as this value seem insignificant in comparison to the respective flow rate values as seen in table 3 it is important to note that this is the increase in flow rate that is attributable to the presence of well-pads in the sub-basin. Subsequently the effectiveness of the various BMPs at reducing this increase in flow rate was evaluated.

Wetlands were most effective at reducing the general sub-basin flow rate; reducing it by 30%. To achieve this, 26% of the generated sub-basin surface flow has to be intercepted by the wetlands. The previous computations for the idealized (based on wetlands draining 10 km^2 of sub-basin) essentially means that by using a slope threshold of 3% or less for wetland suitable HRUs, only 1.9% of the generated sub-basin surface flow will be intercepted by the wetlands. Check dams were also suitable for reducing general sub-basin flow; effectively reducing surface flow rate by 16%. Grassed waterways were least effective at reducing general sub-basin surface flow. On the contrary, the implementation of grassed waterways reduced 91% of the well-pad surface flow whiles wetlands reduced almost half (48%) of the well-pad flow. Albeit least effective at reducing the general sub-basin flow rate, check dams were most effective (100%) at mitigating well-pad flow.

This study is however limited by the fact that the derived effectiveness values for the various BMPs are dependent on the simulation period (2000 to 2009) and can vary when evaluated over different periods. Another limitation is that model parameter sets obtained are subject to

equifinality (Beven and Binley, 1992). Also, no specific BMPs implementation are stated in USFWS (2007) so the most closely related SWAT BMPs were selected from the SWAT BMP manual to meet the measures meant to control storm water flow as presented in USFWS (2007).

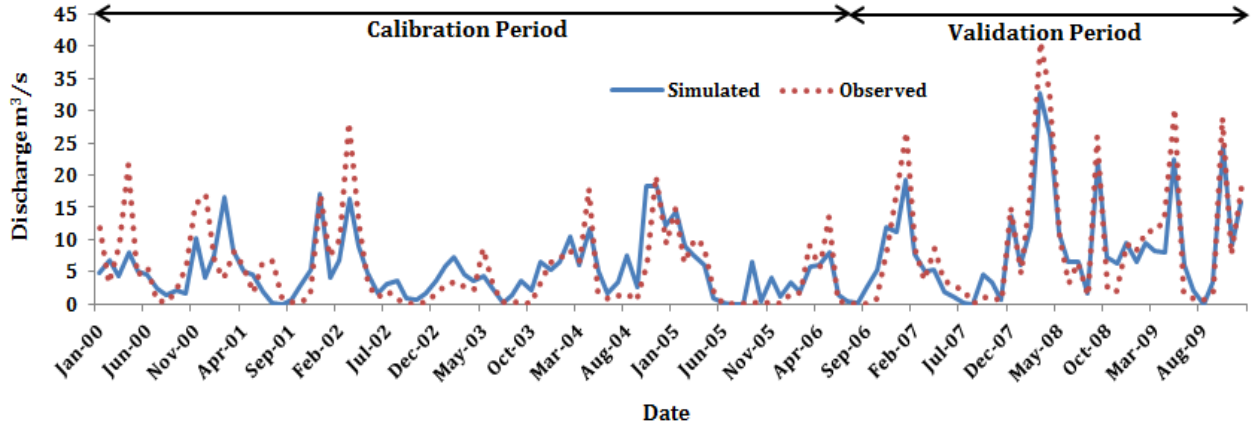

(a)

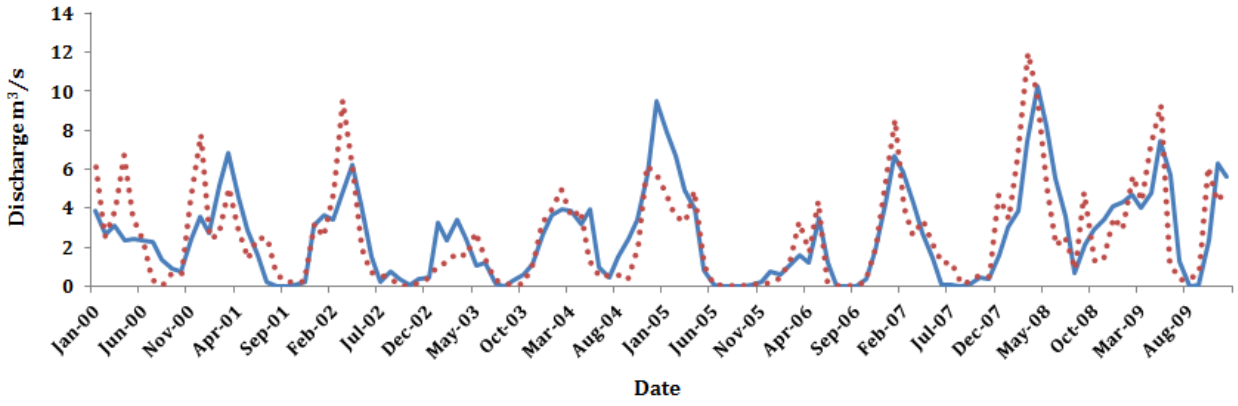

(b)

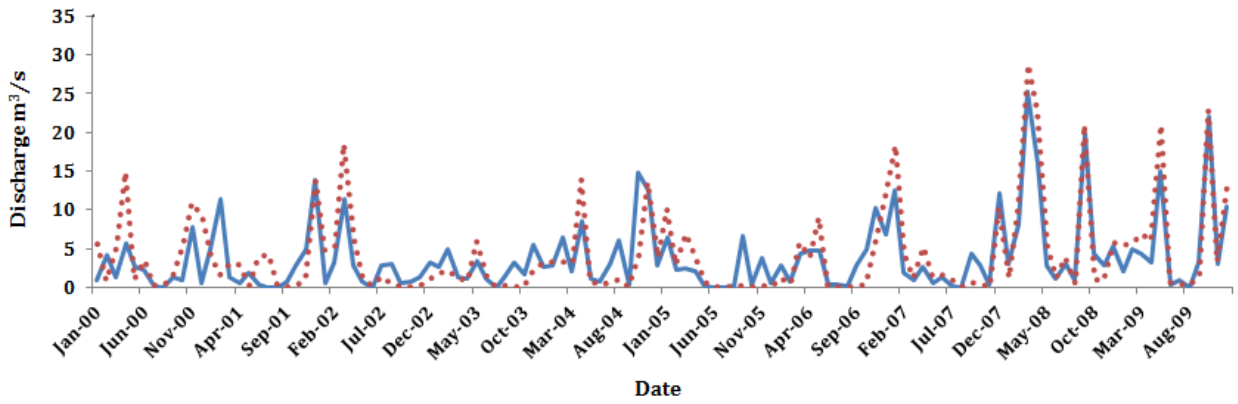

(c)

Figure 27: Total-flow (a), Base-flow (b) and Surface-flow (c) hydrographs for the baseline Scenario with well-pads

5.4 Conclusion

The United States Environmental Protection Agency (USEPA) under the Clean Water Act regulates the discharge of storm water from industrial activities through the issuance of permits under the National Pollutant Discharge Elimination System (NPDES). The oil and gas industry is however exempt from this regulatory provision. Nonetheless, oil and gas activities do impact storm water flow generation and this has prompted agencies such as the United States Fish and Wildlife Services (USFWS) to develop guidelines and encourage operators to voluntarily implement. This study applied a modeling approach to evaluate the effectiveness of storm water control Best Management Practices in a sub-watershed with predominant shale-gas activities. Using the Soil and Water Assessment Tool (SWAT) model, three storm water control BMPs were evaluated in the South Fork of the Red River sub-watershed of the Little Red River Watershed (a sub-basin that sees a majority of shale-gas activities in the Fayetteville Shale Play (Funkhouser, 2012)).

This study found that SWAT model could adequately be employed to represent baseline and various scenarios involving the implementation of BMPs in the sub-basin and evaluate their respective storm water control impacts at the sub-basin outlet. Based on the model simulations the BMPs were estimated to reduce storm water flow in the sub-basin by an average of 18%. An even higher average BMP effectiveness of 80% was achieved on the differential storm water flow attributable to well-pads alone. Among the BMPs, grassed waterways was least effective with the general sub-basin flow rates but was very effective (91%) with flow rates attributable to well-pad land-cover.

Perhaps the most important finding of this study is that much as a BMP might appear less effective at controlling flow from the overall land-cover of the sub-basin, it is highly likely that it will certain have a significant effectiveness on flow generated as a result of the presence of well-pads. This leads to the implication that the implementing appropriate BMPs will most likely have effective impacts on the flow generating components. With awareness of the stated limitation of the model in this study, it is the conclusion of this study that the suggested BMPs do have positive impacts on flow mitigation measures. When implemented along with well-pad construction activities as suggested by USFWS (2007), significant changes can be made on the negative effects of storm water generation attributable to shale-gas activities.

References

(CAST), Center for Advanced Spatial Technologies. 2006. “Arkansas Watershed Information System - 10-Digit: 1101001402.” http://watersheds.cast.uark.edu/viewhuc.php?hucid=1101001402.

CAST, 2007. “Land Use Land Cover Fall 2006 (raster).” http://www.geostor.arkansas.gov/G6/Home.html?id=490250db4c86be523e551f285951f3ad.

(NOAA), National Oceanic and Atmospheric Administration. 2012. “Arkansas, Climate Division Temperature January-May 1895-2012.” http://www.ncdc.noaa.gov/temp-and-precip/time-series/index.php?parameter=tmp&month=5&year=2012&filter=ytd&state=3&div=2.

(SWAT)Balckland Research and Extension Center, Texas A&M AgriLIFE. 2005. Soil and Water Assessment Tool Advanced Manual.

(USDA-ARS), United States Department of Agriculture - Agricultural Research Service. 2012. “Grassland Soil and Water Research Laboratory, Temple, Texas : US Climatic Data.” http://ars.usda.gov/Research/docs.htm?docid=19388.

(USDA-NRCS), United States Department of Agriculture - Natural Resource Conservation Service. 2013. “Web Soil Survey.” http://websoilsurvey.nrcs.usda.gov/app/WebSoilSurvey.aspx.

(USFWS), United States Fish and Wildlife Service. 2007. “Best Management Practices for Fayetteville Shale Natural Gas Activities.” U.S. Fish and Wildlife Service: 30.

Anon. “The Basics: SHIP - Shale Gas Information Plattform.” http://www.shale-gas-information-platform.org/categories/operations/the-basics.html.

Beven, Keith, and Andrew Binley. 1992. “The Future of Distributed Models: Model Calibration and Uncertainty Prediction.” Hydrological Processes 6: 279–298.

Chow, V. T. 1959. Open-channel Hydraulics, McGraw-Hill, New York.

Deletic, Ana B., and C. T. Maksimovic. 1998. “Evaluation of Water Quality Factors in Storm Runoff from Paved Areas.” Journal of Environmental Engineering 124 (9) (September 16): 869–879. doi:10.1061/(ASCE)0733-9372(1998)124:9(869). http://ascelibrary.org/doi/abs/10.1061/(ASCE)0733-9372(1998)124:9(869).

Dickinson, T. 1962. “Watershed Areas Contributing to Runoff” (1951).

Edwards, W. M., and L. B. Owens. 1991. “Large Storm Effects on Total Soil Erosion.” Journal of Soil and Water Conservation 46 (1): 75–78.

Entrekin, S., M. Evans-White, and E. Johnson, B. Hagenbuch. 2011. “Rapid Expansion of Natural Gas Development Poses a Threat to Surface Waters.” Frontiers in Ecology and Environment 9 (9): 503 – 511.

Funkhouser, Jaysson E. 2012. “Personal Communication.”

Gitau, M W, W J Gburek, and P L Bishop. 2008. “Use of the SWAT Model to Quantify Water Quality Effects of Agricultural BMPs at the Farm-Scale Level.” Transactions Of The Asabe 51 (2003): 1925–1936.

Gitau, Margaret W., Tamie L. Veith, William J. Gburek, and Albert R. Jarrett. 2006. “Watershed Level Best Management Practice Selection And Placement In The Town Brook Watershed, New York 1.” Journal of the American Water Resources Association 42 (6) (December): 1565–1581. doi:10.1111/j.1752-1688.2006.tb06021.x. http://doi.wiley.com/10.1111/j.1752-1688.2006.tb06021.x.

Green, W. H., and G. A. Ampt. 1911. “Studies on Soil Physics, J. Agric. Sci., 4(1), 1 – 24.” Journal of Agricultural Science 4 (1): 1–24.

Heaney, James P., and Wayne C. Huber. 1984. “Nationwide Assessment Of Urban Runoff Impact On Receiving Water Quality.” Journal of the American Water Resources Association 20 (1) (February): 35–42. doi:10.1111/j.1752-1688.1984.tb04639.x. http://doi.wiley.com/10.1111/j.1752-1688.1984.tb04639.x.

Hogg, ID, and RH Norris. 1991. “Effects of Runoff from Land Clearing and Urban Development on the Distribution and Abundance of Macroinvertebrates in Pool Areas of a River.” Marine and Freshwater Research 42 (5): 507. doi:10.1071/MF9910507. http://www.publish.csiro.au/view/journals/dsp_journal_fulltext.cfm?nid=126&f=MF9910507.

Hunt, W. F., N. Kannan, J. Jeong, and P. W. Gassman. 2009. “Stormwater Best Management Practices: Review of Current Practices and Potential Incorporation in SWAT.” International Agricultural Engineering Journal 18(1-2): 78 – 89.

Kaini, P., K. Artita, and W.K. Nicklow. 2007. “Evaluating Optimal Detention Pond Locations at a Watershed Scale.” In World Environmental and Water Resources Congress. Tampa, Florida.

Kieser and Associates. 2008. Modeling of Agricultural BMP Scenarios in the Paw Paw River Watershed Using the Soil and Water Assessment Tool (SWAT).

Kirsch, K, A Kirsch, and J G Arnold. 2002. “P s p l r r b u Swat” 45 (6): 1757–1769.

Lee, T., M. E. Rister, B. Narashimhan, R. Srinivasan, D. Andrew, and M. R. Ernst. 2010. “Evaluation and s partially distributed.” Transactions of the ASABE 53 (5): 1619–1627.

Macholl, Jacob A., Katherine A. Clancy, and Paul M. McGinley. 2011. "Using a GIS Model to Identify Internally Drained Areas and Runoff Contribution in a Glaciated Watershed1." JAWRA Journal of the American Water Resources Association 47 (1) (February 3): 114–125. doi:10.1111/j.1752-1688.2010.00495.x. http://doi.wiley.com/10.1111/j.1752-1688.2010.00495.x.

Schrag, Daniel P. 2012. "Is Shale Gas Good for Climate Change?" Daedalus 141 (2) (April): 72–80. doi:10.1162/DAED_a_00147. http://www.mitpressjournals.org/doi/abs/10.1162/DAED_a_00147.

Séguis, L., B. Cappelaere, G. Milési, C. Peugeot, S. Massuel, and G. Favreau. 2004. "Simulated Impacts of Climate Change and Land-clearing on Runoff from a Small Sahelian Catchment." Hydrological Processes 18 (17): 3401 – 3413.

U.S. Department of Agriculture - Soil Conversation Service (USDA-SCS). 1972. Estimation of Direct Runoff From Storm Rainfall. U.S. Department of Agriculture, Soil Conservation Service, Washington, D.C., Pp. 10.1-10.24. SCS National Engineering Handbook, Section 4, Hydrology. Chapter 10.

United States Environmental Protection Agency (USEPA). 2012a. "National Menu of Stormwater Best Management Practices." http://cfpub.epa.gov/npdes/stormwater/menuofbmps/.

United States Environmental Protection Agency (USEPA), 2012b. "BASINS (Better Assessment Science Integrating Point & Non-point Sources)." http://water.epa.gov/scitech/datait/models/basins/index.cfm.

USEPA)., U.S. Environmental Protection Agency (U.S. 2005. "Handbook for Developing Watershed Plans to Restore and Protect Our Waters. Office of Water, Nonpoint Source Control Branch, Washington." (EPA 841-B-05-005).

Wang, Xixi, Shiyou Shang, Zhongyi Qu, Tingxi Liu, Assefa M Melesse, and Wanhong Yang. 2010. "Simulated Wetland Conservation-restoration Effects on Water Quantity and Quality at Watershed Scale." Journal of Environmental Management 91 (7) (July): 1511–25. doi:10.1016/j.jenvman.2010.02.023. http://www.ncbi.nlm.nih.gov/pubmed/20236754.

Wood, R., P. Gilbert, M. Shamima, and K. Anderson. 2011. Shale Gas : a Provisional Assessment of Climate Change and Environmental Impacts Tyndall Centre Manchester Shale Gas : a Provisional Assessment of Climate Change and Environmental Impacts. Vol. 2011.

CHAPTER 6: SUMMARY, CONCLUSIONS AND RECOMMENDATIONS

6.0 Summary

Unconventional energy resources have in recent years been the focus of various discussions and initiatives aimed at exploring alternative sources of energy in response to climate change challenges. In the United States, perhaps the most popular energy resource that has received significant attention and subsequent increase in exploration and production is natural gas from unconventional sources; particularly shale formations. The overall goal of this study was to investigate the complex dynamics that exist between human interactions with the environment specifically with regards to shale gas exploration and production.

In this study, human interactions were defined in terms of changes in land-cover as a result of increase exploration activities and the attendant potential impacts on runoff and stream-flow generation. A key component of the study is the evaluation of the predictive reliability of the modeling paradigm on stream-flow; primarily based on choice of land-cover data and method of classification in determining the suitability of the chosen hydrologic model for the study. Suggested methods of Best Management Practices (BMPs) aimed at mitigating the identified potential impacts are also evaluated using a modeling approach. The study used methods in hydrologic modeling, geographic information science and remote sensing to address specific objectives.

This dissertation comprises three main objectives. The first objective was to evaluate and determine the stream-flow predictive reliability of the ubiquitous Soil and Water Assessment Tool (SWAT) based on input land-use land-cover (LULC) method of classification and data

spatial resolution. Essentially the goal was to determine if the high-resolution land-cover data classified with the object-oriented image analysis technique presents any advantage in terms of model flow predictive reliability over low-resolution land-cover data classified with the pixel-based maximum likelihood method.

The second objective was to develop a classification rule-set based on the object-oriented image analysis technique to quantify land-cover changes with particular attention to shale-gas related infrastructure in a watershed which has seen increased activities related to shale-gas exploration and production. The classified land-use change data was then used as input LULC data to determine effect of shale-gas activities on stream-flow generation in the watershed. The third and final objective was to use hydrologic modeling to evaluate the effectiveness of suggested BMPs in mitigating the identified runoff and stream-flow impacts on the watershed.

The study area for the first objective was the Little Red River Watershed (LRRW) with an approximate area of close to 4700km^2 and located in the north-central portion of Arkansas within the Fayetteville Shale Play.

6.1 Objective 1

To evaluate the predictive reliability of a calibrated SWAT stream-flow model set-up with high-resolution (1 m) NAIP LULC data classified with object-oriented image analysis technique and low-resolution (28.5 m) LULC data classified with pixel-based maximum likelihood method.

Two main land-cover data were used. A high-resolution land-use land-cover data classified with objective oriented image analysis with an overall classification accuracy of 83% and a low-resolution LULC data classified with maximum-likelihood method also with an overall

classification accuracy of 85%. The two LULC datasets were used to set-up two stream-flow models respectively. The calibration and validation periods were from 2000 to 2006 and 2007 to 2009 respectively with a three-year model warm-up period from 1997 to 2000. Nash-Sutcliffe efficiency values after manual calibration and validation simulations were over 90% in both models. In general both low and high-resolution models under simulated total stream-flow by 10.83% and 9.76% respectively.

Due to the effect of equifinality in this study, the manual calibration stage was followed by auto-calibration with the GLUE method. From this method, the p and r-factors (Abbaspour, 2011) were determined which were used to evaluate the predictive reliability of the models. The high-resolution data model was able to bracket or capture 32% of the observation data as the low-resolution data model accounted for 37% of the observed data out of seven thousand simulations.

6.2 Objective 2

To quantify the overall LULC change relative to shale-gas related infrastructure from 2006 and 2010 using NAIP aerial imagery classified with Object-oriented image analysis and assess their contribution to the generation of the storm-water runoff and stream-flow in the most active (in terms of shale gas activities) 10-digit HUC sub-watershed of the Little Red River watershed.

The object-oriented image analysis method was used to classify the data since the method is optimized for high resolution data (Baatz and Schape, 2000). The classified 1 m NAIP 2006 and 2010 LULC datasets had overall accuracies of 83% and 84% respectively. Results showed that between 2006 and 2010, well-pads land-cover increased by approximately 78%. Albeit, land-cover types such as agriculture and forest change were smaller, they still occupied a much higher

land area than the well-pads. Two SWAT stream-flow models were simulated to quantify the differential impact the increase in well-pads alone affected runoff and total stream-flow generation. With the effects of equifinality assumed to be at a minimum, the identified 78% change from 2006 to 2010 in well-pad land-cover was found to correspond to a 10% increase in storm water runoff depth. A 10-year (2010 to 2020) forecast simulation was also performed to determine the potential impact of well-pads alone on change in runoff depth (assuming all other land-cover changes are minimal); it was determined that for the forecast period and with all assumptions holding, runoff depth will increase by 10.3%.

6.3 Objective 3

Employ a modeling approach to evaluate the effectiveness of the implementation of storm-water BMPs in mitigating runoff generation identified in a high shale-gas activity watershed.

Proposed runoff mitigation Best Management Practices (BMPs) were implemented in a SWAT runoff model calibrated for the South Fork Little Red River watershed (SFLRR). Three BMPs implementations were evaluated against an established baseline scenario; these BMPs were grassed waterways, wetlands and check dams. Results of BMP impact on the simulated runoff were divided by the baseline simulated runoff and expressed as a percentage. The evaluated BMP effectives were 9%, 16% and 30% for grassed waterways, wetlands and check dams respectively. However these figures were the evaluated effectiveness for the combined runoff generation of all the land-cover classes. The effectiveness of the BMPs in mitigating runoff determined to be generated as a result of the presence of well-pads alone, were 91%, 100% and 48% respectively.

6.4 Further Studies

1. This study did not account for the predictive reliability of the SWAT flow model calibrated with a high resolution LULC data with significantly higher classification accuracy. Several studies (Platt and Rapoza, 2008; Gao, 2003; Baatz and Schape, 2000) have reported significantly higher classification accuracy for high-resolution land-use data classified with the object-oriented image analysis technique. However, no study could be located that investigates whether the object-oriented image classified with its superior classification algorithm can be translated into similar gains for the reliability of hydrologic models. Further work is thus important to fill this gap in literature as remote sensing techniques hold significant potential for hydrologic modeling.

2. There is also the need to replicate the methodology in this study in other shale-gas activity-intensive watersheds throughout the United States to determine the respective outcomes. As economically viable and producing shale formations are being discovered on a rapid basis in the country, there is the need to develop predictive environmental technologies particularly with hydrologic resources so as to ensure a harmonized approach to exploration and production. The development of accurate and reliable hydrologic models could serve as back-end data source for the development of front-end decision support system based on geographic information science. Again, it is important to produce and maintain region-specific and accurate hydrologic models as the variations in the underlying input data, have been shown (White and Chaubey, 2005) to affect model output as well.

References

Abbaspour, Karim C. 2011. SWAT-CUP: SWAT Calibration and Uncertainty Programs - A User Manual.

Baatz, M., and A. Schäpe. 2000. Multiresolution Segmentation: An Optimization Approach for High Quality Multi-scale Image Segmentation. Angewandte Geographische Informationsverarbeitung. Heidelberg: Wichmann-Verlag.

White, Kati L, and Indrajeet Chaubey. 2005. Sensitivity analysis , calibration , and validations for a multisite and multivariable SWAT model. Journal of the American Water Resources Association 41 (5): 1077–1089.